Master's thesis

NTNU
Norwegian University of Science and Technology
Faculty of Natural Sciences
Department of Biotechnology and Food Science

Anne Helene Sandsmark

The impact of unsuccessful *Yersinia ruckeri* invasions on planktonic bacterial community characteristics

Master's thesis in Biotechnology
Supervisor: Olav Vadstein
Co-supervisor: Madeleine Gundersen
May 2022

NTNU
Kunnskap for en bedre verden

Anne Helene Sandsmark

The impact of unsuccessful *Yersinia ruckeri* invasions on planktonic bacterial community characteristics

Master's thesis in Biotechnology
Supervisor: Olav Vadstein
Co-supervisor: Madeleine Gundersen
May 2022

Norwegian University of Science and Technology
Faculty of Natural Sciences
Department of Biotechnology and Food Science

NTNU
Kunnskap for en bedre verden

Abstract

A microbial invasion is a process in which a microorganism enters a new community where that specific microbial type is not present at that time. In order for an invasion to succeed the invader must establish in the resident community by maintaining an active population for a significant period of time. Microbial invasions play a role as a useful tool and positive force in many important contexts such as the food industry, agriculture, waste treatment, and are important for human and animal health. Invasions can also be harmful. For example, the invader can be a disease carrier for the microbiome host, lead to the destruction of food, change the ecosystem function and reduce biological diversity. Most studies of microbial invasions focus either on the characteristics of the invader or aspects of the community that facilitate invasion. Few studies have examined the impact of invasion on the community, and even fewer have looked at cases where the invader does not establish.

This study set out to investigate the impact of repeated bacterial invasions attempts by the same single model invader on a planktonic bacterial community in a flow-through system. When invasions were unsuccessful the effect on the diversity and composition of the bacterial communities, and invasion resistance at following invasion attempts, were investigated. To address this, several invasion attempts were conducted with two different propagule pressures. The experiment was carried out over 22 days in 15 lab-scale bioreactors. The invader's establishment in the communities was monitored through quantification by qPCR and the bacterial community characteristics were examined using Illumina sequencing and flow cytometry.

The intruder was unable to establish in any of the invasion attempts, meaning that all the invasion attempts were unsuccessful. A temporal change in the diversity and composition of the communities was observed, but these changes could not be linked to the invasion attempts. The unsuccessful invasion attempts did not impact the bacterial composition or diversity of the resident communities. Invasion resistance remained unchanged in subsequent invasion attempts. All communities experienced a period of low pH. The drop in pH led to lower diversity and a change in bacterial community composition. In addition, the rate of change of the invader was higher during the period of low pH. The rate of change of the invader in the communities was lower than the minimum expected value in the majority of the invasion attempts even at low pH. Methodological errors, lysis of the invader, and predation were ruled out as possible causes. The reason why the intruder disappeared faster than expected is still unclear. Although no connection was found between failed invasions and the changes in the communities, I suggest, on the basis of previous findings, that the impact on the communities, or absence thereof, may be related to how competitive the invader is. In further research, the questions posted in this study should be re-examined with a more competitive intruder. An investigation of the connection between the rate of change of the invader and the impact on the community from a failed invasion may also be of interest.

Sammendrag

En mikrobiell invasjon er en prosess hvor en mikroorganisme kommer inn i et nytt samfunn der den spesifikke mikrobielle typen ikke er til stede på dette tidspunktet. For at en invasjon skal lykkes, må inntrengeren etablere seg i samfunnet ved å opprettholde en aktiv populasjon over en betydelig periode. Mikrobielle invasjoner har en rolle som et nyttig verktøy og en positiv kraft i mange viktige sammenhenger som matindustri, landbruk, avfallsbehandling, og er viktig for menneskers og dyrs helse. Invasjoner kan også være skadelige, inntrengeren kan være sykdomsbærer for mikrobiomverten og kan ødelegge matvarer, endre økosystemfunksjonen og redusere biologisk mangfold. De fleste studier av mikrobielle invasjoner fokuserer enten på egenskaper hos inntrengeren eller aspekter ved samfunnet som legger til rette for invasjon. Få studier har undersøkt hvilken innvirkning invasjon har på samfunnet, og enda færre har sett på tilfeller hvor inntrengeren ikke er i stand til å etablere seg.

I denne studien ble det sett på effekten av gjentagende bakterielle invasjonsforsøk med den samme inntrengeren på et planktonisk bakteriesamfunn i et gjennomstrømningssystem. Ved mislykkede invasjoner ble effekten på diversiteten og sammensetningen av bakteriesamfunnet undersøkt, samt invasjonsresistensen til samfunnet ved påfølgende invasjonsforsøk. Flere invasjonsforsøk ble utførte hvor andelen inntrengere ved invasjon utgjorde enten 1 eller 10% av samfunnene. Forsøket ble gjennomført i løpet av 22 dager i 15 bioreaktorer. Inntrengerens etablering i samfunnene ble overvåket gjennom kvantifisering med qPCR og, bakteriesamfunnets karakteristikker ble undersøkte ved bruk av Illumina-sekvensering og flowcytometri.

Inntrengeren var ikke i stand til å etablere seg ved noen av invasjonsforsøkene. En endring i diversitet og sammensetning av samfunnene over tid ble observert, men disse endringene kunne ikke kobles til invasjonsforsøkene. Det ble ikke funnet endring i diversiteten eller sammensetningen av bakteriesamfunnene som resultat av de mislykkede invasjonsforsøkene. Invasjonsresistens ble heller ikke endret ved etterfølgende invasjonsforsøk. Alle samfunnene opplevde en forstyrelse i form av en periode med lav pH. Fallet i pH førte til lavere diversitet og endring i bakteriell sammensetning. I tillegg var endringsraten til inntrengeren høyere i perioden med lav pH. Endringsraten til inntrengeren i samfunnet var lavere enn minste forventede verdi i hovedandelen av invasjonsforsøkene selv ved lav pH. Metodiske feil, lysing av inntrengeren og predasjon ble utelukket som mulige årsaker. Årsaken til at inntrengeren forsvant raskere enn forventet er fortsatt uklar. Selv om det ikke ble funnet en sammenheng mellom mislykkede invasjoner og endringer i samfunnet foreslår jeg på bakgrunn av tidligere funn at påvirkning på samfunnet, eller uteblivelse av endring, kan ha sammenheng med hvor konkurransedyktig inntrengeren er. Ved videre forskning bør spørsmålene i denne studien undersøkes på nytt med en mer konkurransedyktig inntrenger. En undersøkelse av sammenhengen mellom endringsraten av inntrengeren og påvirkningen på samfunnet ved mislykket invasjon kan også være av interesse.

Acknowledgements

This project was performed as a collaboration with the PhD candidate Madeleine Gundersen at the Department of Biotechnology and Food Science (IBT) at the Norwegian University of Science and Technology (NTNU) in Trondheim.

First of all, I would give my deepest gratitude to my supervisor Olav Vadstein and co-supervisor Madeleine Gundersen for all their help and support. Thank you both for all your kindness, and for providing guidance and support throughout this thesis. I have really appreciated the opportunity to collaborate with Madeleine in and outside of the lab, and the valuable feedback from Olav throughout the whole process. I am so grateful that you both shared your knowledge and compassion with me, and for pushing me through some hard months. I can't imagine having better supervisors then you two.

I would also like to thank Ingrid Bakke for guidance with experimental and analytical methods, and Amalie Johanne H. Mathisen for always helping me in the lab when I needed it. Thank you to Alexander Willi Fiedler and Martha Kristine Rindarøy Drågen for showing me the ropes in the lab, and to the whole research group, Analysis and Control of Microbial Systems (ACMS), for welcoming me and inspiring me throughout my master's program.

To all my friends who have let me have conversations with myself in the group chat in order for me to figure out my questions, you are really appreciated. Thank you for rooting for me, and for only judging me through kindness when I forget the words for completely normal things. To Vilde Frydenlund, I admire you and appreciate your ability to always have my back and cheer me on. Lastly, I would like to thank my parents for encouraging me and believing that I can figure it out even when they had no idea what I was talking about.

Trondheim, May 2022

Anne Helene Sandsmark

Table of Contents

1 Introduction

Microorganisms are found everywhere and represent by far the largest fraction of biodiversity, as well as possessing vast metabolic and physiological versatility (Curtis & Sloan, 2005; Prosser et al., 2007). They play key roles in all ecosystems, performing essential functions such as organic matter decomposition, contributing to almost half of global primary productivity, and driving major biogeochemical cycles (Litchman, 2010; Renes et al., 2020). Microorganisms also have an important role in industrial biotechnology, human and animal health, the food industry, and agriculture (Kinnunen et al., 2016; Stecher et al., 2010; Verstraete et al., 2007).

1.1 Microbial community ecology and microbial communities

In microbial ecology general ecological principles are investigated and applied to microbial systems (Litchman, 2010). The word ecology comes from the Greek oikos 'house' and the suffix -logy from lógos "study of" and was coined by Ernst Haeckel (Schwarz & Jax, 2011). Ecology can be defined as the scientific study of interactions that determine the distribution and abundance of organisms (Krebs, 1985). Microbial ecology is the scientific study of interactions that determine the distribution and abundance of microorganisms. Microbial community ecology focuses on microbial communities, groups of potentially interacting microbes cooccurring in space and time (Nemergut et al., 2013). This field seeks to analyze microbial communities' structure and the mechanisms of their assembly, what their functional interactions are, how community structure changes in space and time, and which processes are driving the formation of these patterns (Konopka, 2009; Nemergut et al., 2013). It's worth noting that community definitions, concerning geography, are often arbitrary. Communities are not discrete and their boundaries may vary both spatially and temporally (Nemergut et al., 2013). In terms of phylogeny, what we refer to as microbial communities are often restricted by the use of certain molecular probes such as universal bacterial primers to the study of just bacterial communities (Nemergut et al., 2013).

Patterns in diversity, abundance, and composition of microbes in microbial communities can be described by four processes as underlined by Vellend (Vellend, 2010). These four processes are selection, drift, dispersal, and speciation. Selection and drift both contribute to the loss of organisms from communities and the shaping of their relative abundances. Selection is a deterministic process in which the organisms with the highest fitness will increase in abundance, while drift is the random changes in organism abundances. Dispersal and speciation, on the other hand, contribute to the acquisition of new organisms. Dispersal is the movement of organisms across space and between communities and speciation is the creation of new species (Nemergut et al., 2013; Vellend, 2010).

1.2 Microbial invasions and their effect on resident communities

Microbial invasions are special cases of dispersal, i.e. movement of organisms between communities, where the type of organism coming into the community is not present in the community at that particular time (Kinnunen et al., 2016; Mallon et al., 2015). The microbial type entering the resident community, that it was not a part of prior, is referred to as the invader. The resident community is the specific community considered. For an invasion to succeed the invader must enter, and establish in the resident community by maintaining an active population for a significant period of time. A successful invader will impact the environment or community and eventually spread (Kinnunen et al., 2016; Mallon et al., 2015).

A better understanding of microbial invasion could generate significant payoffs across many domains, as microbial invasions play a role in many important contexts (Kinnunen et al., 2016). Microbial invasions are utilized in the food industry, agriculture, waste treatment, and are important for human and animal health (Albright et al., 2021; Kinnunen et al., 2016; Stecher et al., 2010; Verstraete et al., 2007). Invasions can have both positive and negative effects on the resident community. We may thus want to understand more of the mechanisms behind invasion so that we can prevent or improve the chances of a successful invasion. The invader can be a disease carrier for the microbiome host, lead to spoilage of foodstuff, alter the ecosystem function, and reduce biodiversity (Pearson et al., 2018; Vitousek et al., 1996). This emphasizes the importance of understanding the mechanism of invasion such that action can be taken to reduce the risk of invasion. However, the impact of invasion can also be positive, when the invader is perceived as a beneficial bacteria or when it will improve the functionality of an ecosystem by manipulating the composition of microbes (Albright et al., 2021). Facilitating for invasion of beneficial invaders can be used for fermentation of both food and waste, development of plant growth-promoting inoculum, soli improvement, bioaugmentation, waste water treatment, and possibly for human and animal health befits by for example pro-, and prebiotic use (Albright et al., 2021; Kinnunen et al., 2016; Stecher et al., 2010; Verstraete et al., 2007).

In the past two decades, there has been an explosion of research interest in human-mediated invasions. This explosion has, in turn, resulted in a substantial development in the understanding of the invasion process. However, despite bacteria being the most diverse group of organisms we still know little about the processes behind microbial invasions (Acosta et al., 2015; Blackburn et al., 2011). One of the reasons why microbial invasions have been such a poorly studied phenomenon is because of the Baas-Becking hypothesis. The hypothesis was a previous leading principle in microbial community ecology, "Everything is everywhere, but the environment selects". This consideration of ubiquity rendered any exploration of invasion behavior moot, because an invader could not invade a region where it already existed. However, the idea that 'everything is everywhere' has been challenged. Recent research efforts have revealed that microbes do, in many cases, exhibit biogeographic patterns. Microbial communities and ecosystems alike are mosaics of genetically and phenotypically distinct organisms that are susceptible to invasion by fitter forms. In light of this revelation, there has been a surge of literature examining and documenting microbial invasions of a variety of environments and the mechanisms that control this process (Mallon et al., 2015; Martiny et al., 2006).

Most studies on microbial communities either focus on the invader-specific traits that facilitate the invasion process (e.g. (Eisenhauer et al., 2013; Gao et al., 2019; Jones et al., 2017; Ma et al., 2015)) or properties of the resident community that aid invasion (e.g. (Acosta et al., 2015; Mallon et al., 2015; van Elsas et al., 2012)). We know that resource availability is related to invasibility. For an invader to succeed it must be able to take over a niche. Thus, relative fitness differences between intruders and the resident community are important (Vila et al., 2019). In addition, the more available niches the greater the likelihood of success (Eisenhauer et al., 2013; Li et al., 2019; Lourenco et al., 2018; Mallon et al., 2015). The diversity of the resident community is also an important factor. This is assumed to be because communities with lower diversity are more likely to have unoccupied niches that can be occupied by invaders. The higher the diversity of the community, the more niches are used, and the lower the probability of invasion success due to competition (Acosta et al., 2015; Litchman, 2010; Stecher et al., 2010; van Elsas et al., 2012). If the invader must compete for niche space the propagule pressure, the initial concentration of the invader, will influence the success rate. Propagule pressure of

the invader has been investigated as a determinant of invasion success in many studies (Acosta et al., 2015; Jones et al., 2017).

Until recently, few studies had investigated the impact invasion has on the resident community both regarding community diversity and functionality, and we, therefore, lack insight into these effects (Buchberger & Stockenreiter, 2018; Mallon et al., 2018a). What we do know is that invasions can lead to changes in the community diversity, in the form of increased Shannon diversity and evenness (Buchberger & Stockenreiter, 2018), increased richness, and a tendency for increased evenness. It can also lead to changes in functional properties such as increased niche breath (Mallon et al., 2018b). It has also been shown that the impact of invasion may be dependent on the initial propagule pressure of the invader (Acosta et al., 2015; Jones et al., 2017).

1.1.1. Unsuccessful microbial invasions

Changes in microbial communities have also been observed when the invasions are transient and the invader does not establish in the community, ie. an unsuccessful invasion (Buchberger & Stockenreiter, 2018; Mallon et al., 2018b; Weithoff et al., 2017). Mallon et al 2018 observed that an unsuccessful invasion caused changes in community composition and increased both the diversity and the average number of carbon sources used by a resident soil community (Mallon et al., 2018b). Lasting effects of unsuccessful invasions on resident communities have also been observed in phytoplankton communities (Buchberger & Stockenreiter, 2018; Weithoff et al., 2017). Buchberger & Stockenreiter observed maintained diversity in unsuccessfully invaded communities in contrast to a fall in diversity in control communities (Buchberger & Stockenreiter, 2018). Mallon et. all (2018) suggested a conceptual explanation of the observed impact of unsuccessful invasions in their experiment. In short, the explanation was that the invader upon initial introduction outcompeted the other taxa that relied heavily on the same C-substrates as the invader. This resulted in rare taxa better utilizing niches not used by the invader via competitive release (Mallon et al., 2018b).

Mallon et al 2018 observed that although transient and unsuccessful, the invader created a legacy effect. The invader rearranged the structure of the soil microbial community by altering the community composition and shifting the niche structure of the community away from the invader's resources. This raised the question of whether this legacy effect would increase the rate of invasion success for subsequent invasion attempts by the same invader because the nice of the invader would be freed resulting in less competition at a secondary invasion attempt (Mallon et al., 2018b). A new research gap was consequently identified. Does an unsuccessful invasion increase the chance of invasion success during a secondary invasion?

1.3 Aim of study and research questions

This study aimed to investigate the impact of multiple bacterial invasions attempts by a single model invader at two different propagule pressures on a planktonic bacterial community in a flow-through system. Based on prior research and knowledge gaps outlined above the following questions and accompanied hypotheses will be addressed.

Research question 1: What is the impact of unsuccessful invasions on a planktonic bacterial community in a flow-through system?

Hypothesis: In accordance with observations of Mallon et. all 2018, I hypothesized that a failed bacterial invasion would cause changes in community composition and increased the bacterial community diversity. However, this change would be temporary as the resources were supplied continuously in the flow-through system. The original community composition and diversity would be restored after the invader was removed from the community through washout.

Research question 2: Does an unsuccessful invasion increase the rate of invasion success for subsequent invasion attempts by the same invader?

Hypothesis: In accordance with my hypothesis that the effect of unsuccessful invasions will not have a lasting impact on the resident community, I hypothesized that the rate of invasion success would not increase with subsequent invasions in a flow-through system.

2 Materials and Methods

2.1 Experimental design and invasion regime

The aim of this study was to investigate the impact of multiple invasions attempts on the characteristics and invasibility of a planktonic bacterial community in a flow-through system. We cultivated freshwater bacterial communities in 15 lab-scale continuous bioreactors over 22 days. The reactors were divided into 3 treatment groups of 5 rectors each, treatment A and B, invaded at 1 and 10% propagule pressure with *Yersinia ruckeri* respectively, and a control group (C) (Figure 1). The first invasion was carried out after the communities had been adapting to the lab conditions for 18 days total. The subsequent invasion attempts were carried out when there were less than 15000 cells/ml of the invader present in the reactors. The communities in treatment group A were exposed to five invasion attempts on days 0, 3, 6, 12, and 17, and B were exposed to four attempts on days 0, 6, 12, and 17.

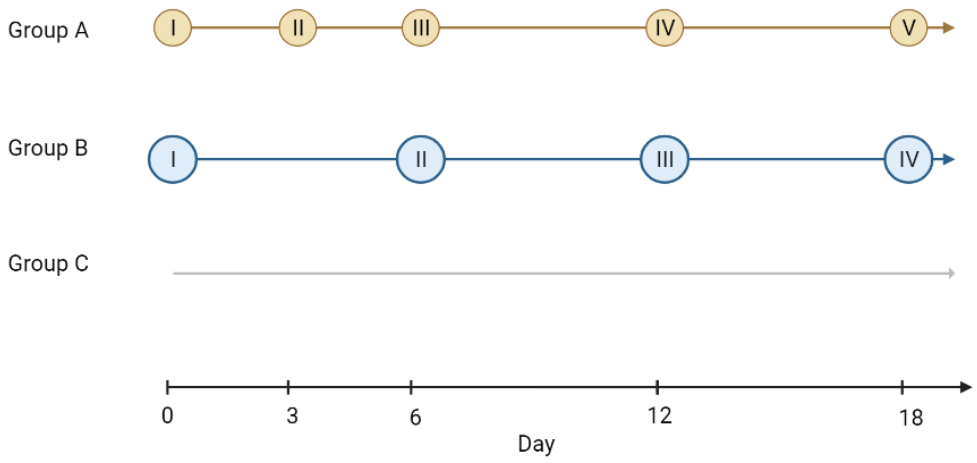

Figure 1: Timeline of invasion attempts with *Yersinia ruckeri* for each treatment group of reactors. The numbered circles mark invasion attempts. Created with BioRender.com

Three bioreactors were inoculated with 300 mL each of a *Y. ruckeri*-free freshwater community. The communities were initially cultivated in the bioreactors for 14 days until the bacterial density had stabilized, indicating that the community had adapted to the new environment. After the 14 days the communities were mixed and split into 15 new reactors (Figure 2). They were then cultivated for four more days until the bacterial density had stabilized again. The first invasion was executed after the adaptation period of 18 days in total.

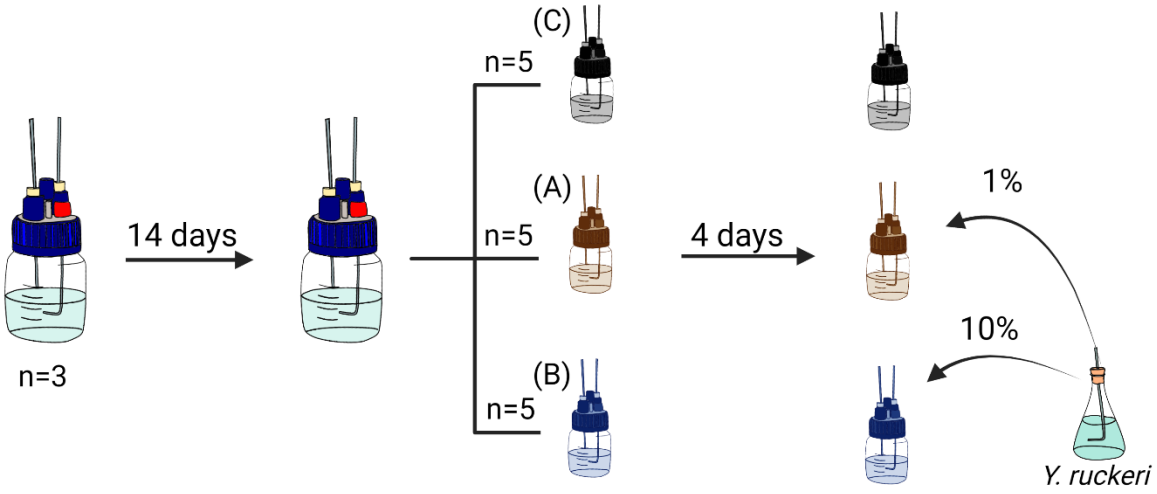

Figure 2: Schematic representation of adaptation of the planktonic bacterial community to the media and lab conditions for a total of 18 days (14 + 4 days), and the first invasion attempt. Treatment groups A and B were invaded at 1 and 10% propagule pressure with *Yersinia ruckeri* respectively, and group C was the control. Created with BioRender.com

2.1.1 Bioreactor setup

The experimental setup consisted of 15 bioreactors, a media reservoir, two digital peristaltic pumps (Ismatec MCP and IPC), aeration with hydrated air, and an outlet to a waste tank (Figure 3). Cultivating bacterial communities in continuous-flow bioreactors gives higher control compared to a natural setting, the opportunity to observe the same community over time, and makes it possible to have many biological replicates. Each bioreactor (Figure 4), a 500 mL wide neck Duran bottle, contained 300 mL of a freshwater bacterial community and a magnet. The reactors were placed on a magnetic stirrer to keep the communities homogeneous. The community received medium at a flowrate of 0.208 mL/min by a peristaltic pump. To avoid contamination of the medium reservoir, due to backflow or upstream swimming bacteria, the medium was supplied through the same port as the hydrated air in the five-port connection lid (Duran). The cultures were aerated to secure aerobic growth and to avoid the growth of anaerobic bacteria. The air was hydrated to minimize evaporation of the culture, and filtered through a 0.2 µm filter to avoid contamination. Positive air pressure was established inside the bioreactors by the air being pumped in, leading to excess culture being pushed out true the outlet. The outlet tubing was placed so that there was always 300 mL of a freshwater bacterial community in the reactors. One port in the five-port connection lid (Duran) was also accessible through a screw cap for sampling. The experimental setup was in a climate-controlled room, holding the temperature of the cultures at 13.4±0.2°C.

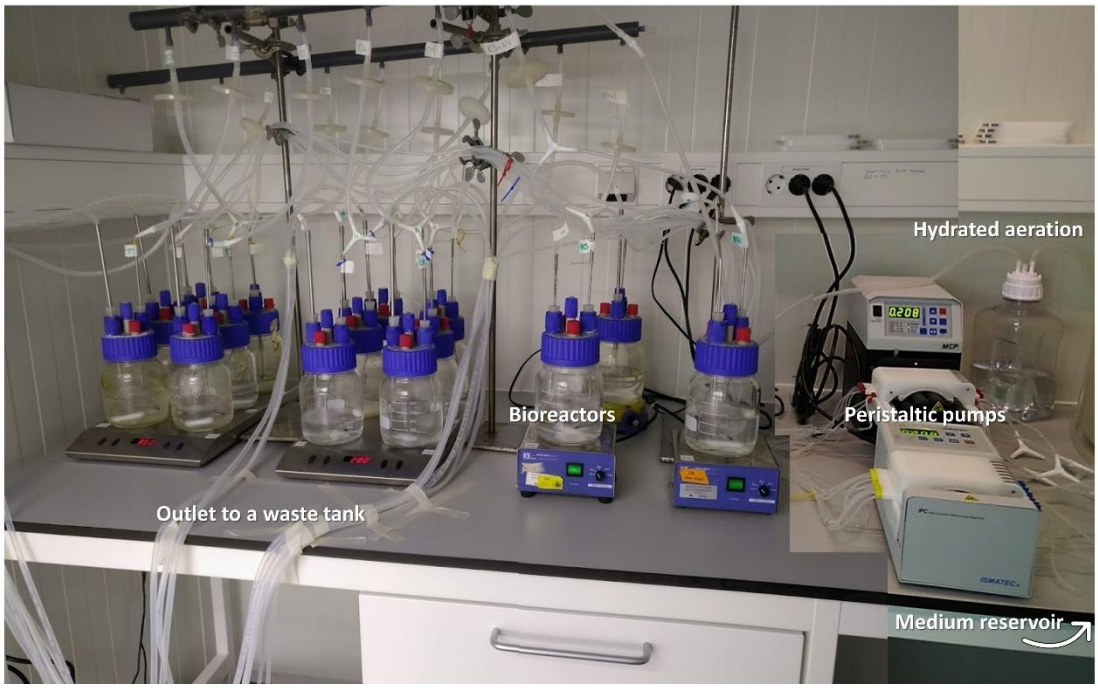

Figure 5: The experimental setup. Bioreactors were supplied with media from a media reservoir by two peristaltic pumps. The medium was mixed with hydrated air and delivered through the silicone tubes.

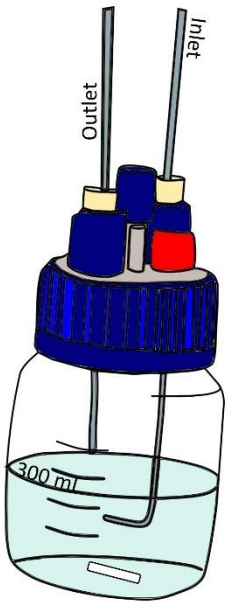

Figure 6: Illustration of bioreactor. Wide neck Duran bottle containing 300 mL of a freshwater bacterial community and a magnet.

2.1.2 Invader

As a model organism of an invading bacteria, we chose *Yersinia ruckeri. Y. ruckeri* is part of the *Enterobacteriaceae* family in the class *Gammaproteobacteria* (Kumar et al., 2015). Eighteen different species have been described so far (Wrobel et al., 2018). *Y. ruckeri* is rod-shaped, approximately 0.75 µm in diameter and 1-3 µm in length. It's a gram-negative, facultative anaerobe, glucose-fermentative bacteria with a 3.7 Mb genome. *Y. ruckeri* is a freshwater species and some strains are pathogenic to salmonoid fish species as the causative agent of enteric redmouth disease, *yersiniosis* (Kumar et al., 2015). In infected fish farms, *yersiniosis* can lead to as much as 70% mortality (Wrobel et al., 2018), resulting in significant economic losses to the aquaculture industry (Kumar et al., 2015). Its main replication is within the fish host, however, it has been observed to survive over 4 months outside the host (Kumar et al., 2015). The bacteria can be released into new aquatic environments through the shedding of the bacterium in the feces of infected fish, and through shedding from the lower intestine of carrier fish when they become stressed (Kumar et al., 2015).

2.1.3 Resident community

As a model system of a resident community, a complex planktonic bacterial community was cultivated in the lab. The bacterial community originated from a freshwater salmon tank at the RAS facility of Lerøy in Lensvik (Trøndelag), an environment in which *Y. ruckeri* could be found. A 1L water sample was collected from the tank. To remove particles and predators such as grazers I filtered the community through 3.0 µm filters before adding it to the bioreactors. We collected samples of the community and measured the bacterial density of the community with flow cytometry and checked for the presence of the invader by *Y. ruckeri* specific qPCR.

2.1.4 Medium preparation

We developed a specific growth medium (CDM-10) to cultivate freshwater bacterial communities in a carbon limited environment. The medium was designed to sustain a relatively high diversity in the context of lab cultivation. To facilitate for a high bacterial community diversity 28 different carbon sources were chosen (see the full list in Appendix A). Each C-source was adjusted to be of equal molarity with regards to their C-atoms (1,12 µM carbon per component). The medium sustained carbon limited growth with a density of around 10 000 cells/µl. The phosphate source was also used as pH buffer. On day 15 the pH- buffer was increased from 0.2 to 0.6 mM P-atoms/L in the medium. This was done by filling a syringe with phosphate buffer (K_2HPO_4 and Na_2HPO_4) and injecting it into the media tank using a sterile needle. The tank was gently stirred to mix the additional phosphate into the medium. Complete media composition can be found in Appendix A.

2.1.5 Contamination

We experienced four instances of contamination of the system. We discovered microbial growth in the tubing and/or media tank on days 4, 8, 16, and 24 of the experiment. When the contamination was discovered, feeding to the communities was temporarily stopped and the media reservoir was changed. Tubing was sterilized by rinsing with 70% EtOH followed by dH_20 before autoclavation.

2.2 Sampling

The reactors were sampled 16 times throughout the experiment on days -1, 0, 1, 2, 3, 4, 5, 6, 8, 10, 12, 14, 16, 18, 20, and 22 where day 0 is the day of the first invasion attempt. This time series gave us a good time resolution so that it was possible to quantify the rate of change for the invader, and samples were taken more frequently in the initial phase to monitor the impact of the first invasion. Every sampling day 14 to 24 mL of culture was collected from each bioreactor. 4 mL of each sample was transferred to 4.5 mL cryotubes and directly fixated with Glutaraldehyde (0.1% final concentration) for analysis with flow cytometry. We used up to 1 mL of the fixated samples for analysis with flow cytometry. The remaining fixated sample volume was flash-frozen with liquid nitrogen and stored at negative 20°C for later analysis. The remaining 10 to 20 mL of the initial sample was filtered true 0.2 µm polycarbonate filters using a vacuum-filtration device. The bacteria collected on the filters were stored at -20 °C until DNA extraction.

2.3 Analytical methods

2.3.1 Flow cytometry - determination of bacterial density

2.3.1.1 The principle of flow cytometry

Flow cytometry is a type of cytometry, which is a process of measuring the physical and chemical characteristics of biological cells (Shapiro, 2003). The word cytometry is derived from the Greek "kytos" meaning "hollow vessel", as a cell, and "metron" meaning measure (Bonnevier et al., 2018). In flow cytometry, single cells such as microorganisms, cellular components, or other particles are suspended in a fluid phase and their light scattering and fluorescence properties are measured as they move in a liquid stream through a laser beam. From their light-scattering properties their structural and morphological properties, such as size and granularity, can be derived. While the fluorescent emission is proportional to the number of fluorescent molecules bound or found on or in the particle (Adan et al., 2017).

The main components of a flow cytometer are fluidics, excitation and collection optics, detectors, and a computer. The fluidic system directs the particles from the original sample solution through the instrument, and aligning's the cells such that they pass vertically through a laser beam one by one. The light source, commonly a laser, is part of the excitation optics which, with the help of lenses, focuses the light source on the particles. When the laser light hits one of the moving particles, light is deflected around the edges of the particle and the light is scattered. The collection optics collects the light scatter and fluorescent light emitted from the particle and transmits it to the detectors (Adan et al., 2017). The detectors detect the light scatter or fluorescent light and convert it to digital data that is proportional to the incoming light intensity. The digital data is transferred to a computer for analysis (Adan et al., 2017).

As mentioned, the particles can be differentiated and analyzed based on their light-scattering properties and fluorescence emission (Adan et al., 2017). When the laser light hits one of the moving particles two types of light scatter are collected, forward scatter (FSC) and side scatters (SSC). FSC light is scattered along the same axis as the laser beam in the forward direction. While SSC light is scattered at approximately 90 degrees to the laser beam. From the particles' light scattering properties, their structural and morphological properties can be derived (Adan et al., 2017). FSC light tells us about the size or surface area of the particle as it is proportional to the square of the radius of a sphere (Adan et al., 2017; Macey, 2007). SSC on the other hand is considered proportional

to cell granularity or internal complexity as light may enter the cell and be reflected and refracted by the nucleus and other contents of the cell (Adan et al., 2017; Macey, 2007). Fluorescence emission from the particle is measured at the same angle as the SSC light. The fluorescent light can be derived from fluorescent-labeled antibodies, fluorescent membrane, cytoplasmic, or nuclear dyes (Adan et al., 2017; Macey, 2007) or autofluorescence of photosynthetic pigments such as Chlorophyll a (Davey & Kell, 1996).

Flow cytometry has many applications such as identification and quantification of specific cell groups in a mixed population, investigation of cell viability, detection of specific proteins, assessment of DNA and RNA (Adan et al., 2017), and characterization of phenotypic attributes for first-line assessments of microbial diversity dynamics (Props et al., 2016). Most relevant for our application, flow cytometry allows for speedy and accurate counting of bacterial cells, analyzing thousands of cells per second improving statistical data compared to traditional cell counting methods (Jachimowicz, 2017).

Bacteria are small in comparison to other particles measured by flow cytometry such as human cells. Therefore, data collection of bacterial cells is more dependent on staining and electronic thresholds. In contrast to bigger particles, the intensity of scattered light of bacteria is close to the detection limit of most flow cytometers. The use of nucleic acid-specific stains, such as SYBRGreenI, is therefore required. Electronic thresholds minimize the recording of background noise by setting a level that a signal must exceed to be recorded. In addition, electronic gates may be set around an area in a histogram or scatterplot defining a population of interest to filter out data not fulfilling this parameter and displaying data reflecting only the population of interest (Davey & Kell, 1996; *Quantification of Bacteria by Flow Cytometry*).

2.3.1.2 Determining the bacterial density of planktonic bacterial communities and invader

To achieve invasion at different propagule pressures, 1 and 10%, the bacterial densities of the communities and invader culture had to be quantified. The quantification of bacterial density was done by flow cytometry. Measurements of bacterial density were also used to monitor potential changes in the community density through the experiment. Quantification of the bacterial densities was carried out by flow cytometry, with the BD Accuri C6 instrument. This instrument has two lasers (blue 488 nm and red 635 nm), and four filters (FL1 533/30 nm, FL2 585/40 nm, FL3 >670 nm, and FL4 675/25 nm) (*BD Accuri™ C6 Plus System User's Guide*, 2016). The flow cytometer was routinely validated before use with 8-and 6-peak beads validation (3 mm, BD Accuri Cytometers), to ensure correct data collection. Community and invader samples were diluted to a concentration of 200-1000 events/µL with 0.2 µm filtered 1x PBS (AccuGENE) if the samples had a higher count than 1000 events/µL. The C6 flow cytometer gives the most accurate count in this range. The bacteria in the diluted samples were stained with 2x SYBR Green II RNA Gel Stain (ThermoFisher Scientific) a nucleic acid stain that exhibits the highest quantum yield when bound to RNA forming a SYBR Green II/RNA complex. The stain is maximally excited at 497 nm and can thereby be excited by the 488 nm blue lasers of the flow cytometer. Following excitation, the SYBR Green II/RNA complex emits fluorescence between 497 to 520 nm which is within the FL1 detector range (*BD Accuri™ C6 Plus System User's Guide*, 2016; *SYBR® Green II RNA Gel Stain*, 2001). The working solution of SYBR Green II RNA Gel stain (200x) was a 1:50 dilution of SYBR Green II stock solution (10 000x concentrated in DMSO) diluted in 0.2 µm filtered 1x PBS. The samples were incubated at 37℃ in the

dark for approximately 20 minutes after staining. To ensure homogeneity samples were briefly shaken before analysis. We ran each sample for 3.5 minutes (or until 10^5 events were recorded) at medium fluidics (35 mL/minute, 16 µm core size). Signal thresholds were applied on the green fluorescence at FL1-H = 5000 and on the forward scatter at FSC-H = 10. The FSC signal threshold was applied because the flow cytometer instrument we used created false events with FSC-H < 10 mimicking the patterns of the other events collected. Every second sample was followed by 0.2 mm filtered dH_2O water which ran for 2 minutes at fast fluidics (66 mL/minute, 22 µm core size) to minimize carry-over between samples.

The data acquired were analyzed using the BD Accuri C6 Software. The first step was the exclusion of false events with FSC-H < 15, as the FSC-H = 10 signal thresholds had not been applied to all samples. Next, events assumed to represent the bacterial population was defined by gating via FL1/FL3 scatterplot. Events with FL1-A signals below $10^{4.6}$ and FL3-A signals below $10^{2.6}$ were excluded. This was based on experience in the ACMS group (NTNU) and preliminary tests showing that events with signals below these thresholds typically were the results of noise from the cultivation media and smaller particles. The cell density of each sample was determined, taking dilution into account.

2.3.2 DNA extraction

DNA was extracted from bacterial cells collected on the 0.2 µm polycarbonate filters. The filters were cut into small pieces with a scalpel in a petri dish and transferred to a PowerBead tube (DNAeasy). DNA was extracted with a PowerSoil DNeasy kit according to the manufacturer's protocol (Appendix B). 5µL of each DNA extract was used to quantify the presence of *Y. ruckeri* in the reactors by qPCR. The remaining DNA extracts were stored at -20°C until library preparation for Illumina sequencing.

2.3.3 Quantitative PCR for quantifying the abundance of the invader in the communities

2.3.3.1 The principle of quantitative PCR

Quantitative PCR (qPCR) is a molecular biological technique that allows for the quantification of a targeted DNA sequence (Pabinger et al., 2014). The method is widely used in microbial ecology for the quantification of taxonomic gene markers within different environments (Smith & Osborn, 2009). Quantification happens simultaneously with the amplification of the targeted DNA molecules through PCR. Quantification is made possible by the detection of a fluorescent reporter, which indicates the accumulation of DNA molecules. As the number of targeted DNA molecules increases exponentially for every cycle the fluorescent reporter is recorded in 'real-time'. There are two commonly used reporter systems, the SYBR Green I and the TaqMan probe system. SYBR Green I binds to all double-stranded DNA, intercalating between adjacent base pairs. Only when bound to DNA will SYBR green emit a fluorescent signal following light excitation. As the number of double-stranded DNA molecules accumulates with each cycle of PCR, there is a corresponding increase in fluorescence. A threshold is set for where the fluorescent signal is significantly greater than the background level, called the cycle threshold (Ct). When the Ct is reached the Ct-value is reported as the number of PCR cycles needed to reach this point. The Ct-value is directly proportional to the initial concentration of the target DNA. The higher the initial concentration of target DNA, the earlier the Ct will be reached, and the lower the Ct-value will be (Heid et al., 1996; Smith & Osborn, 2009).

From the Ct-values the number of initial target molecules in samples with an unknown concentration can be determined either in relative (Smith & Osborn, 2009), by The Pfaffl Method, or in absolute terms, by the standard curve method or digital PCR method. In the standard curve method, a standard curve is generated by amplification of the target molecule present at a range of initial template concentrations (Smith & Osborn, 2009). Ct-values for each concentration in the range are plotted against the log copy number ($\log(N_0)$). A linear regression of $\log(N_0)$ versus Ct gives the standard curves (Brankatschk et al., 2012), from which the number of initial target molecules in samples can be determined.

2.3.3.2 Quantification of invader

qPCR was conducted to quantify the amount of our invader *Y. ruckeri* in samples from the bacterial communities by amplifying and quantifying a *Y. ruckeri*-specific gene region of the Hom7 gene. Absolute quantification was done by the standard curve method. Whole genome DNA extracted from *Y. ruckeri* isolate NVI-10705 DNA was used to make the standard curve. The amount of DNA in the extract was determined using Qbit (Invitrogen), and the standards consisted of three replicas of five dilutions ranging from 53 to 66 500 Hom7 copies/µl.

qPCR reactions were carried out with the Power SYBR Green Master Mix (Applied Biosystems) (12.5 µl), the Hom7-685F and the Hom7-685 primer pair (1.25 µL of each, 10µM) (primer sequences are presented in Table 1), sample (5µl) pre-diluted 1:5 and DNA-free water (5 µL). The reactions were performed in triplicates with a total volume of 25 µl per reaction in MicroAmp AnduraPlate Optical 96-Well Clear Reaction Plate (Applied Biosystems) covered with MicroAmp Optical Adhesive Film (Applied Biosystems). All equipment was treated for 30 minutes with UV to minimize the risk of contamination.

Standard samples and non-template controls were included for each qPCR run to ensure that reagents were not contaminated. The qPCRs were run in the qPCR thermocycler QuantStudio5 (Applied Biosystems) with the cycling conditions as followed: pre-incubation at 50℃ (2 min) and 95°C (10 min), 40 cycles of denaturation at 95°C (15 sec) and annealing and extension at 60 °C (1 min) with fluorescence measuring. A post-PCR melting curve analysis was performed (95 °C for 15 sec., 60 °C for 1 min., and 95°C for 1 sec. with fluorescence measuring) to confirm that the generated fluorescence signal was only stemming from the target templates. All samples with target amplification should have uniform peaks with a Tm of ~80.5℃ and Melt Peak Hight at ~150 00- 200 000.

Tabell 1: qPCR primer sequence designed for quantification of *Y. ruckeri* by targeting the Hom7-gene.

Primer ID	**Sequence (5'-3')**	**Product length**
Hom7-685F	5'-CCTCGGCGTCTATACGGAAGT-3'	63 bp
Hom7-685R	5'-CAGGGTGAGCGTGAAATCCT-3'	

Data obtained by QuantStudio5 was processed in QuantStudio Design and Analysis Software v1.5.0 (AppliedBiosystems) and exported to Microsoft Excel. Ct values from standard curve samples were plotted agents log(template start concentration). A linear regression provided the standard curve. The standard curve was validated by calculating the correlation coefficient ($R^2 \geq 0.99$), and the efficiency ($95\% > E < 105\%$) of the standard curve was calculated by using equation 1.1. The standard curve was used to calculate the starting template, Hom7, concentration (N_0) in the experimental samples from the Ct values, and the intercept (a) and slope (b) of the standard curve by using equation 1.2.

$$E = 10^{(-\frac{1}{b})} \quad \text{Eq. 1}$$

$$C_{T\ sample} = a + b * \log\left(N_{0\ sample}\right) \quad \text{Eq. 2}$$

The relative rate of change (r) of *Y. ruckeri* in the community was calculated by plotting the quantity of our invader *Y. ruckeri*, equivalent to Hom7, in the bioreactors versus time. The plot is semi-logarithmic, as we assumed logarithmic growth. I made a linear regression for each community, and the slope equals r of *Y. ruckeri* in the community in question. The Shapiro-Wilk test of normality was performed in R-studio using the function shapiro.test() from the package stats (version 3.6.2) to test whether r were normally distributed. Statistical significance between groups was determined with a one-way analysis of variance (ANOVA) and a two-samples t-test.

2.3.4 Illumina sequencing of bacterial communities

2.3.4.1 The principles of Illumina sequencing

Illumina sequencing consists of two main steps, clonal amplification, and sequencing by synthesis (Hu et al., 2021) (Figure 5). During clonal amplification the DNA strands to be sequenced are subjected to repeated rounds of amplification, creating clusters of about 1000 copies of each DNA strand (Slatko et al., 2018). The goal is to be able to produce strong, detectable signals during sequencing. This happens through what is known as "bridge amplification" on a solid phase called a flow cell (Hu et al., 2021). The DNA templates were tagged before amplification with an adaptor on each end. The adapters have a sequence that is complementary to oligonucleotides coating the surface of the flow cell (Slatko et al., 2018). The oligonucleotides on the slide are spaced such that clusters are created in a way where all the DNA strands in one cluster are copies of a single forward DNA strand (Slatko et al., 2018).

Sequencing happens through what is known as sequencing by synthesis. This involves the incorporation of modified deoxynucleotides (dNTPs) by DNA-polymerase (Hu et al., 2021). The dNTPs are labeled with base-specific, cleavable fluorophores and coupled to a reversible terminator. The terminator blocks the ribose 3'-OH group thus preventing elongation of the complementary strand (Goodwin et al., 2016). Depending on the read length the reactions are repeated for 300 or more cycles (Slatko et al., 2018). During each cycle, a mixture of all four modified dNTPs, primers, and DNA polymerase is added. A single dNTP is incorporated into each strand and the rest is removed. The surface is then imaged, and the fluorescent signal identifies which dNTP was incorporated at each cluster. The fluorophores and terminators are removed, and a new cycle of nucleotide addition, elongation, and cleavage can begin (Goodwin et al., 2016). Once the DNA strand is fully sequenced the generated sequence read is removed and the index codes are sequenced. Indexes are attached to the DNA during sample preparation and are used to tag the DNA so that they can be traced to their origin. This allows multiple samples to be run at the same time on the same flow cell. After the forward strand has been sequenced the revers-strand is then sequenced, this is called paired-end sequencing (*Illumina Sequencing Technology*, 2010).

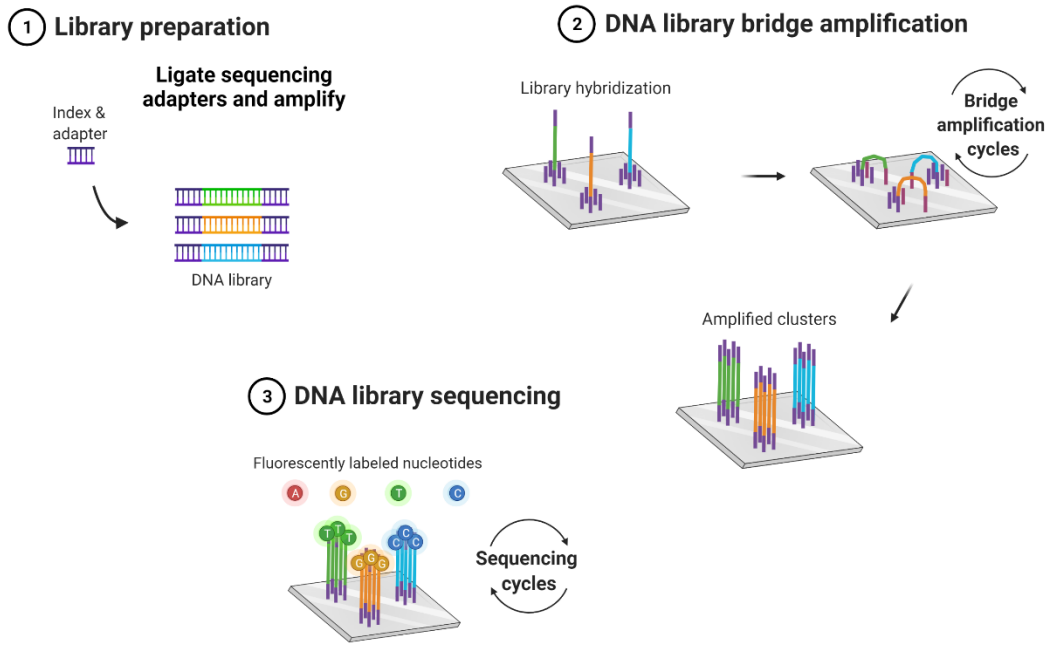

Figure 7: Illustration of main steps of Illumina sequencing. Created with BioRender.com

2.3.4.2 Investigating bacterial community characteristics through 16S rRNA gene sequencing

To assess the impact of unsuccessful invasions on the bacterial composition of the resident communities we needed to determine the bacterial composition prior, at point of, and after the attempted invasions. For analysis of bacterial community compositions, we used Illumina MiSeq amplicon sequencing of the V3 and V4 regions of the 16S ribosomal RNA gene.

In amplicon sequencing, a gene, gene fragment, or sequence is specifically amplified with the help of specific primers that target the region of interest, here the V3 and V4 regions of the 16S ribosomal RNA gene. The sequence is then determined by high throughput next-generation sequencing such as Illumina (Di Bella et al., 2013). The 16S rRNA gene codes for the RNA component of the small subunit of a prokaryotic ribosome witch functionality is highly conserved among procaryotes prokaryotes (Ames et al., 2017; Poretsky et al., 2014). However, 16S rRNA gene sequencing is limited to the bacterial and archaea domains (Rausch et al., 2019). The gene both contain highly conserved and variable regions altering each other. The conserved regions can be utilized for the development of universal primers that bind to conserved sequences that are shared among all bacteria. Given that the function of the 16S rRNA gene has not changed over time, the genetic differences in the hypervariable regions have been considered to reflect time and genome divergence. This allows for the use of the 16S sequence to obtain a trustworthy level of taxonomic information by comparing the resulting 16S gene amplicons sequences against existing databases (Ames et al., 2017; Janda & Abbott, 2007; Rosselli et al., 2016). However, bias can be introduced into microbiota studies at all methodological stages. Only a part of the 16S gene can be sequenced, which can lead to adverse effects on the reported diversity of the analyzed communities mainly as an effect of inconsistent taxonomic coverage. In

addition to inconsistent taxonomic coverage, it can be challenging to assess diversity in 16s amplicon analysis due to many bacteria having multiple copies of the 16S rRNA gene (Ames et al., 2017; Barb et al., 2016; Di Bella et al., 2013; Poretsky et al., 2014). The use of the 16S ribosomal RNA gene as a phylogenetic marker has however proven to be an efficient and affordable tool for the analysis of bacterial communities and is to date the technique that most studies of bacterial communities have depended on. There are well-developed databases not seen for any other sequencing methods, and it is well suited for analyses of large numbers of samples while still being cost-efficient (Di Bella et al., 2013).

2.3.4.3 Library preparation

Targeted PCR

To prepare the amplicon library for Illumina sequencing we first amplified the V3 and V4 region of the 16S ribosomal RNA gene adding Illumina adapters to the amplicons. This was done with targeted PCR of the DNA extracts as templates and using the specific primers Ill341F_KI and ill805R (Eurofinss) which have Illumina adapters. Primer sequences are presented in Table 2. The PCR reactions were run for 35 cycles (98 °C 15 sec., 55 °C 20 sec., 72 °C 20 sec.) in the thermocycler (Bio-Rad t100 Thermal cycler) with 0.3 µM of each primer, 0.2 mM of each dNTP (VWR), 1.5 mM of MgCl2 (Thermo Fisher), 1x Phusion buffer HF (Thermo Fisher), 0.02 units/µL of Phusion Hot Start II DNA polymerase (Thermo Fisher), 1 µL of DNA template and dH_20 (Rouche) to a total volume of 25 µL. For samples with low PCR amplification yield, the number of cycles was increased to 37. PCR workstation (VWR) and equipment that was UV treated for 30 before use. A non-template control was included for each PCR run to ensure that reagents were not contaminated. After PCR amplification the PCR products were examined by gel electrophoresis (110V, 20w, 1h) on a 1% agarose gel in 1x TAE buffer to ensure that the products were of the correct size (approx. 540 nt).

Tabell 2: Nucleotide sequence of primers Ill341F_KI and ill805R. A = adenine, T = thymine, C = cytosine, G = guanine, N = A, T, C or G, W= A or T, K = G or T and V = G, C or A. Underlined sequences represent the Illumina adapters.

Primer	*Nucleotide sequence*
Ill341F_KI	5'-TCG TCG GCA GCG TCA GAT GTG TAT AAG AGA CAG NNNN CCT ACG GGW GGC AGC AG-3'
ill805R	5'- GTC TCG TGG GCT CGG AGA TGT GTA TAA GAG ACA G NNNN GAC TAC NVG GGT ATC TAA KCC-3'

Normalization and purification of PCR product

Normalization and purification of the PCR products were performed using the SequalPrep Normalization Plate Kit for 96-well plates (Thermo Fisher) according to supplier protocol in Appendix C to ensure that all samples contained the same amount of DNA. The kit requires a minimum of 250 ng DNA per well and yields 25 ng DNA per amplicon after normalization.

Indexing by PCR and pooling of samples

All PCR amplicons were indexed with a unique combination of forward and reverse oligonucleotides. The oligonucleotides had known sequences so that the sequence could be tracked to the correct sample. This was done with PCR using the Index 1 (N-series) and Index 2 (S-series) (Illumina) as primers and the PCR amplicons from the previous PCR as templates. The PCR reactions ran for 12 cycles (98 °C 15 sec., 50 °C 20 sec., 72 °C 20 sec.) in the thermocycler (Bio-Rad t100 Thermal cycler) with 2.5µl of each primer, 0.2 mM of each dNTP (VWR), 1.5 mM of MgCl2 (Thermo Fisher), 1x Phusion buffer HF (Thermo Fisher), 0.0152 units/µL of Phusion Hot Start II DNA polymerase (Thermo Fisher), 2.5 µL of DNA template and dH_20 (Rouche) to a total volume of 25 µL. After PCR amplification the PCR products were examined by gel electrophoresis (110V, 20w, 1h) on a 1% agarose gel in 1x TAE buffer to ensure that the products were indexed. Indexed amplicons were normalized as described above.

All samples were then pooled in one tube and concentrated using the AmiconUltra 0.5 centrifugal filter devices (30K membrane, Merck Millipore). The concentrations of the pooled amplicons were determined to be 18.5 ng/µl using NanoDrop (ThermoFisher). The amplicon library was sequenced on a MiSeq Illumina lane at the Norwegian Sequencing Centre (NSC).

2.3.4.4 Processing and analysis of sequence data

The sequencing data was processed using the Usearch pipeline (https://www.drive5.com/usearch/). First paired ends were merged, and primers and reads shorter than 400 base pairs were removed. Then, the merged reads were quality filtered to an error rate of 1% and converted to fasta files with the addition of sample labels. Next, the fasta files were pooled together and unique sequences (singletons) were disregarded. After this, zOTUs were generated using Unoise3 at the same time as chimeras were removed. When generating zOTU no clustering is involved, meaning that sequences with as little as one nucleotide's difference will be distinct zOTUs. Lastly, a zOTU table was made and zOTUs were assigned taxonomy by comparing their sequences to the RDP reference data set (version 18) at an 80% confidence threshold. The output of the pipeline used for downstream analysis was a zOTU table containing the number of sequence reads per zOTU for each sample and a sintax file containing the taxonomic assignment of each zOTU. The datasets were further processed and analyzed in Microsoft Excel.

In Microsoft Excel, the sintax file and zOTU table was merged into a table containing the number of sequence reads per zOTU for each sample and the taxonomic assignment of each zOTU. zOTUs with low abundance (total abundance < 8) were sorted out. Samples from reactor A2 day 1 and B2 day 16 were excluded from further analysis due to an indexing mix-up. Samples from reactor B5 days 5, 6, and 12 were also excluded due to weary low total number of reads (2, 7, and 5 respectively). 31 zOTUs were excluded from further analysis, three due to being classified as Chloroplast and 28 that were only present in negative controls. After removing control samples, a total of 159 samples remained all from bioreactor samples. The datasets were further processed and analyzed in R studio.

Construction of a phylogenetic tree

A phylogenetic tree was constructed using the phangorn R package (version 2.5.5). A neighbor-joining tree was first constructed, and then fit a GTR+G+I (Generalized time-reversible with Gamma rate variation) maximum likelihood tree using the neighbor-joining tree as a starting point (Callahan et al., 2017).

The normalization of sequence depth and estimation of coverage

The sequencing effort was determined with the function rarecurve() in the vegan package (version 2.5.7). It describes the increase in the number of zOTUs as a function of sequencing depth. Samples were normalized to 45 434 sequences per sample by scaling to the 25 quantile. Chao1 was calculate with the function estimate_richness()in the phyloseq package (version 1.34.0).

Taxonomic composition of samples

To inspect the development in the communities the taxonomic composition was plotted for each selection regime over time. Composition was investigated on all taxonomic levels: phylum, class, order, family, genus, and zOTU.

Diversity analysis

Alpha diversity of order 0 (richness) and 1 (exponential Shannon) was calculated with the the renyi() function from the vegan package (version 2.5.7), and the evenness was calculated as diversity of order 1 over diversity of order 0. The Shapiro-Wilk test of normality was performed using the function shapiro.test() from the package stats (version 3.6.2) to test whether the diversity numbers were normally distributed. The null hypothesis is that the data is normally distributed and a p-value < 0.1 indicates a rejection of the null hypothesis. Statistical significance between several groups was determined with Kruskal-Wallis as the data was not normally distributed. The output from Kruskal-Wallis test tells us whether there is a significant difference between the groups but not which pairs of treatments are different. The pairwise Wilcox rank sum test was used to calculate pairwise comparisons between group levels with corrections for multiple testing.

Beta diversity was assessed by calculating the Bray-Curtis dissimilarity with the phyloseq package (version 1.34.0). Bray-Curtis is a dissimilarity matrix that calculates how dissimilar two communities (samples) are with regards to OTU abundance. Two identical communities will have the value of 0, while two completely different communities have the value of 1. All the samples were then ordinated with PCoA plots that maximize the variation between all samples. Statistical significance between groups was determined with a permutational ANOVA (PERMANOVA) analysis.

3 Preliminary experiments

3.1 Optimization of the medium

We aimed to develop a medium that would support the growth of *Y. ruckeri* and the residents of freshwater bacterial communities in a flowthrough system. The medium was designed to be carbon-limited and sustain a high diversity community with a density of around 10 000 cells/ul. To facilitate for high diversity 28 different carbon sources were chosen. Each C-source was adjusted to be of equal molarity with regards to their C-atoms (1,12 µM carbon per component). The complete medium composition of the carbon-limited defined (CDM-10) medium can be found in Appendix A.

3.2 Growth in carbon-defined medium

To investigate whether the medium would support the growth of *Y. ruckeri* and freshwater bacterial residents, pure strain *Y. ruckeri*, as well as freshwater community from zebrafish tanks, were inoculated in the original CD-medium. The cultures were cultivated in batches and cell density was measured every day using flow cytometry (Figure 8).

Pure strain *Y. ruckeri* (Figure 8a) and the freshwater community from zebrafish tanks (Figure 8b) were successfully cultivated in batches. *Y. ruckeri* cultures went straight into exponential growth, with some reaching the stationary phase within the three days. The freshwater community had a lag period before entering exponential growth.

a)

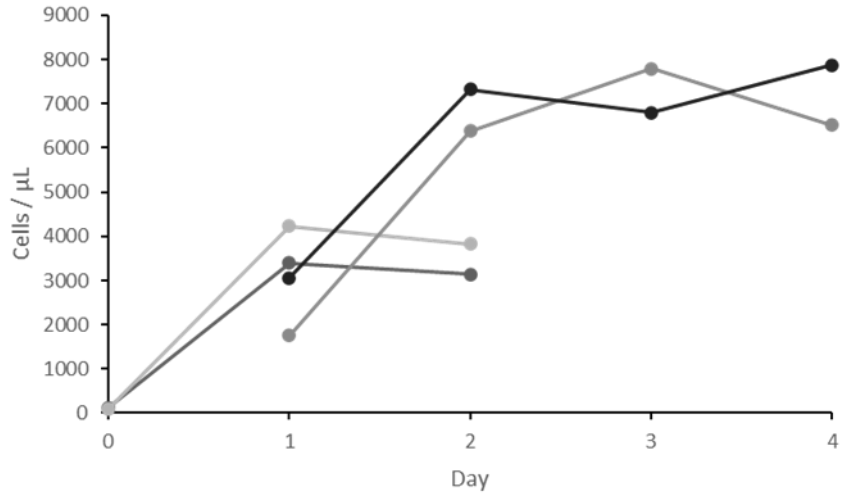

b)

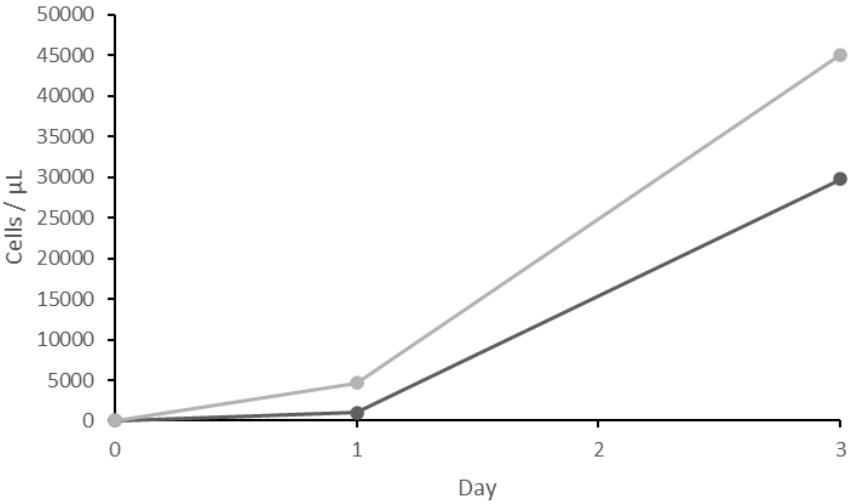

Figure 8:Growth curves for a) *Yersinia ruckeri* and b) freshwater microbial community from a zebrafish tank in CD-medium measured over three days. Cell concentration measured as cells per µl by flow cytometry is plotted against time (days). (A) Growth curves of four *Yersinia ruckeri* cultures, consisting of two groups of two biological replicas. (B) Growth curves of two (biological replicas) cultures from the freshwater microbial community from a zebrafish tank.

The freshwater community from the zebrafish tank was also cultivated with a continuous flow of the CD-medium of 0.99 day^{-1}. The culture was sampled every day for cell density measurements by flow cytometry (Figure 9). The freshwater community from zebrafish tanks was successfully cultivated in the bioreactor. The community had a short lag period before entering exponential growth after one day. After 3 days the culture entered the stationary phase with an average cell density of 48 140 cells/µl ± 4 259. The cell density decreased on day 7 before restabilizing at 49 120 cells/µl on day 9. In summary, the medium supported growth of both *Y. ruckeri* and freshwater bacterial residents.

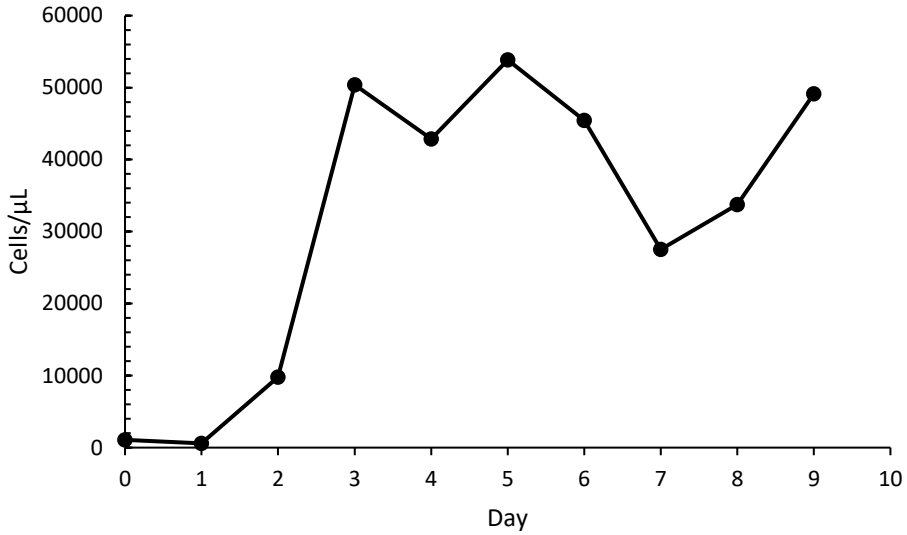

Figure 9: Growth curves for a freshwater microbial community from a zebrafish tank in CD-medium measured over nine days in a bioreactor with a 0,99 day-1 dilution rate. Cell concentration measured as cells per µl by flow cytometry is plotted against time (days).

3.3 Bacterial diversity of communities cultivated in carbon-defined medium

To determine the diversity the CD-medium sustained, two samples from the bioreactor from the previous reactor tests were sequenced on the Illumina MiSeq platform. Bioinformatic processing performed by Alexander Fiedler found 79 and 78 OTUs in the two samples. Three OTUs were dominating (25% Flavobacterium, 25% av Pseudomonas, 15% Zooglea), however, the diversity was deemed satisfactory for the experimental design.

3.3.1 Affirmation of carbon limitation

To investigate whether the medium was carbon limiting *Y. ruckeri*, pre-cultivated in media with 50 times nutrient concentration compared to the original medium for 7 days, was inoculated in the original CD-medium and divided into nine different 50 mL batch cultures. To eight of the flasks, a 5x concentration spike of one medium component was added, while one flask was left as control. The cultures were cultivated at 140RPM and 24℃ in the dark for three days. The cultures were sampled each day, and cell density was measured by flow cytometry (Figure 10).

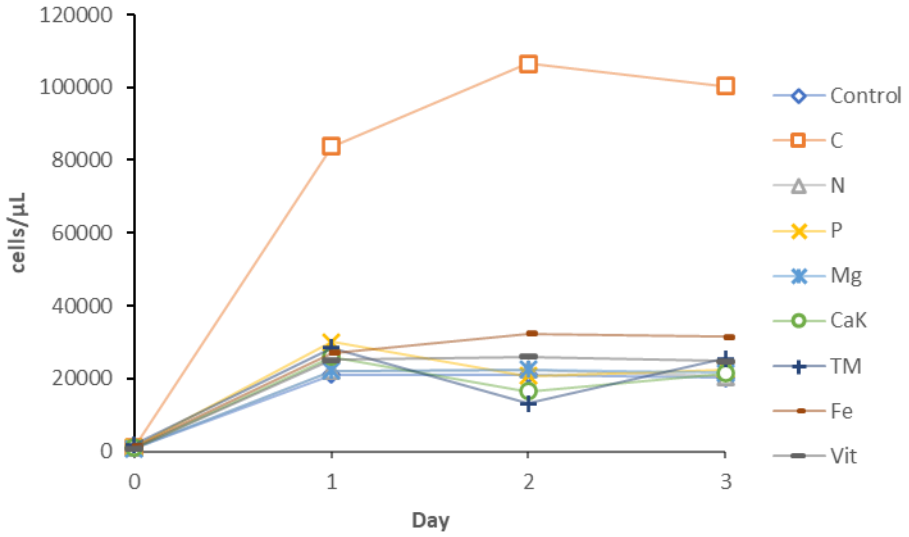

Figure 10: Growth curves for *Yersinia ruckeri* in eight different modified CD-mediums with five times the original carbon (C), nitrogen (N), phosphorus (P), magnesium (Mg), Potassium + Calcium (CaK), trace metals (TM), iron (Fe), and vitamin (Vit) concentration and non-modified medium (control) measured as cells per µl by flow cytometry.

All cultures, except the carbon spiked (C), showed approximately equal response entering stationary phase after one day at a maximum average cell density of 25238 cells/µl ± 3048. The culture growing in the carbon spiked medium displayed a longer exponential phase and entered stationary phase after two days with a maximum cell density of 106480 cells/µl, more than four times higher than the maximum average cell density of the rest of the cultures including the control. From this, we concluded that the CD-medium was carbon limited, at least for the growth of our invader *Y. ruckeri*.

3.3.2 Adjustments of carbon-defined carrying capacity

In freshwater environments the total microbial cell numbers are typically around 10 000/µl (Madigan et al., 2015). From the previous reactor test we found the average carrying capacity of the CD-medium to be 48 336 ± 3 829 cells/µl (Figure 9). In an effort to mimic a natural environment we lowered the carbon concentration by a factor of ten (from 326 µM to 32.6 µM C-atoms total). *Y. ruckeri* was then inoculated in the new media (CDM-10) and batch-cultivated at 122RPM, 20℃ in the dark for two days. The cultures were sampled on days 0, 1, and 5, and cell density was measured by flow cytometry (Figure 11). Both cultures entered stationary phase after one day with a maximum average cell density of 6 460 cells/µl ± 160. From this we concluded that the new carbon-defined-medium-10 (CDM-10) had a sufficiently lowered carrying capacity.

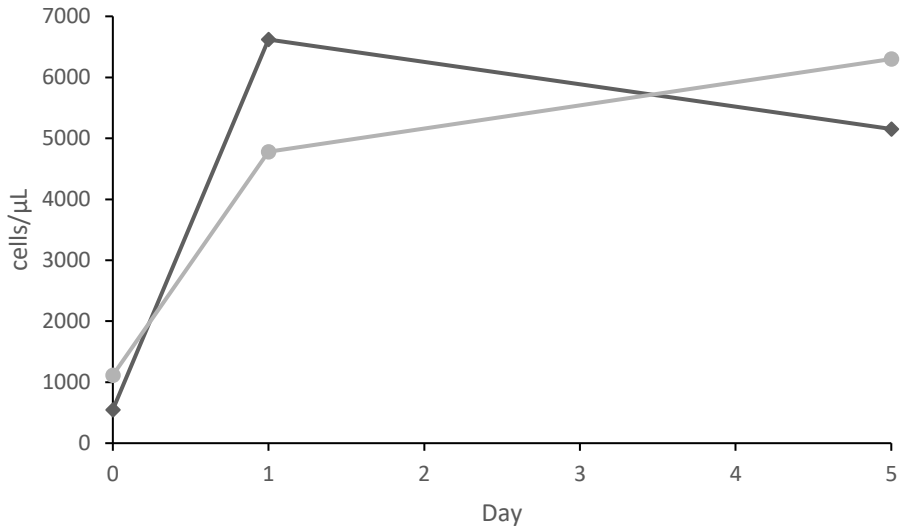

Figure 11: Growth curves for *Yersinia ruckeri* in modified CD-medium with tenfold reduction in carbon concentration (CDM-10) measured over five days. Cell concentration of the two biological replicates was measured as cells per µl by flow cytometry and is plotted against time (days).

3.4 Optimizing the flow cytometry protocol

We aimed to develop a flow cytometry protocol where the choice of sample fixation method, SYBR green solvent, and incubation temperature for staining with the SYBR green dye was well documented. For the optimization four different sample types were investigated: a freshwater microbial community (F), a saltwater microbial community (S), the gram-positive bacteria Arthrobacter (P), and the gram-negative bacteria *Yersinia ruckeri* strain B (G).

First, we wanted to determine if sample-fixation was necessary and whether the fixation should be done with glutaraldehyde alone or in combination with flash freezing with liquid nitrogen. The samples were either fixated with glutaraldehyde 0.1% (G01) or glutaraldehyde 1% (G1), and some were in addition flash frozen (G01S and G1S). The fixated samples were stored for 92 hours either at room temperature (G01, G1) or at -20°C (G01S and G1S). Samples taken after 0, 2, 20, and 92 hours were diluted in 0.2 µm filtered PBS (1x) and stained with SYBR green I diluted in DMSO.

Cell density and signal intensity was determined by flow cytometry focusing on plot: FL1 vs FL3, FL1 density overlap, and cell densities. We found that to maintain samples most similar to the sample at time 0h one should fixate the samples with 0.1% Glutaraldehyde followed by snap freezing. With this treatment the samples appear to be consistent over time although there is some variation between replicates.

Second, we wanted to determine if the solvent used to dilute the stain SYBR green I affect the signal intensity and cell density determined by flow cytometry. Three of the different sample types, F, S, and G were stained with SYBR green I diluted in either DMSO (unfiltered) or 0.2µm filtered 1/10 TE-buffer. All samples were incubated for 20 minutes. It appeared like the solvent used to dilute SYBR green 1 did not affect the FL1, FL3 or FSC signal. The signals for the FL1-H vs FL3-H scatterplots were consistent regardless of

solvent, and the FL1-H density plot indicated that the technical replicates were overlapping regardless of solvent.

Lastly, we wanted to determine whether the incubation temperature for staining with SYBR green I should be 25 or 37°. This was determined by comparing the signal intensity of F and G samples incubated at these temperatures in the dark. We found that incubating the samples at 37℃ produced the best results when comparing the FL1 vs FL3 scatterplots and the density distributions.

The FL1-FL3 signals were more defined after incubation at 37°C. For the freshwater community samples one could clearly distinguish two main populations at 37°C in contrast to one diffuse at 25°C. There were no major differences between the cell densities based on the incubation temperature of SYBR green I.

For the remainder of our experiments samples to by analyzed by flow cytometry were fixated with 0.1% glutaraldehyde followed by snap freezing, the SYBR green I stain was dissolved in 0.2µm filtered 1/10 TE-buffer, and stained samples were incubated at 37℃.

3.5 *Y. ruckeri* as the invader

Yersinia ruckeri was chosen as the invading bacteria. We have established that *Y. ruckeri* could grow in the CD-medium. Further, I wanted to investigate whether *Y. ruckeri* could grow under the planned experimental conditions of continious cultivation with a flow rate of 0,208 ml/min at 14°C. This was determined by inoculating *Y. ruckeri*, pre-cultivated in batch with CD-medium-10 for 2 days, in four reactors. Two of the reactors (Y1 and Y2) were inoculated with 250 ml of the culture while the two other reactors were inoculated with 20 ml culture and 280 ml CD-medium-10 (Y2 and Y3). The bioreactors were operated for four days with sampling every day. Cell density was measured by flow cytometry (Figure 12).

Y. ruckeri did grow ($\mu>0$) under the planed experimental conditions (Figure 12). However, the growth rate was lower than the dilution rate for most of the observed growth period. Y3 and Y4 reach steady state after two days, Y1 after three days, while Y2 had a negative net growth for the whole observed growth period. This could indicate that *Y. ruckeri* is more likely to establish with lower density inoculations and higher resource availability. Even though *Y. ruckeri* showed negative net growth for most of the observed growth period, with the likelihood of wash out, there still seemed to be potential for establishment. We therefore consider *Y. ruckeri* to be a good candidate to for observation of the effect of failed invasions under these conditions.

a)

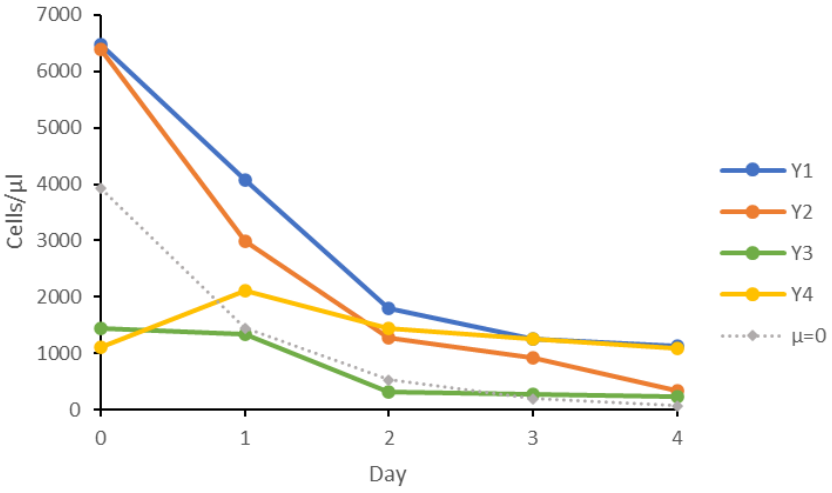

b)

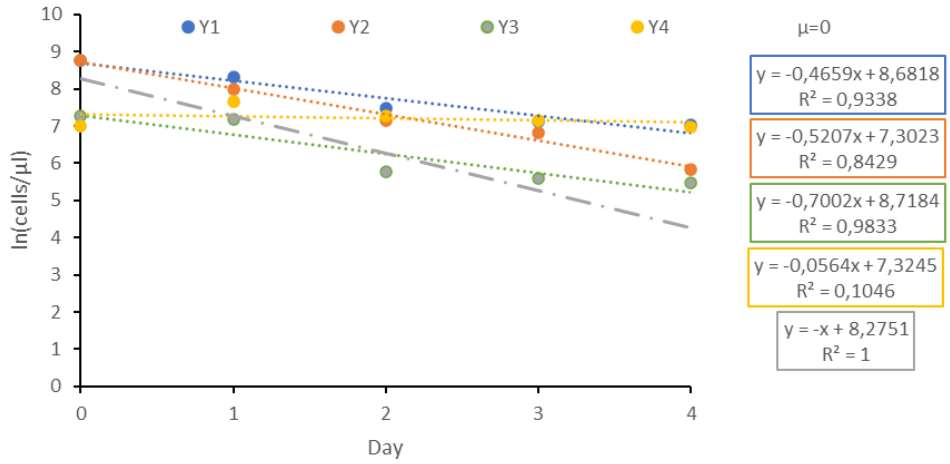

Figure 12: Growth curves for *Y. ruckeri* in CD-medium-10 measured over a four-day period in bioreactor with a 0,99 day-1 dilution rate. Trendline µl=0 illustrates a theoretical growth curve where the growth rate is 0. Y1 and Y2 are reactors initially inoculated with 250 ml culture while the Y3 and Y4 were inoculated with 20 ml culture and 280 ml CD-medium-10. a) Cell concentration measured as cells per µl by flow cytometry is plotted against time (days). b) Cell concentration on a semi logarithmic scale, ln(cells/µl) plotted against time (days). Trendlines are linear regressions.

3.6 Developing a qPCR protocol for quantification of *Y. ruckeri*

To be able to track the quantity of *Y. ruckeri* in bacterial communities we developed a qPCR protocol for quantification of *Y. ruckeri*.

3.6.1 Primer design

The first step in this process was to design qPCR-primers that target a *Y. ruckeri*-specific gene. The Hom7 gene of *Y. ruckeri*, encoding a non-ribosomal peptide synthetase involved in Holomycin synthase (Qin, Baker, et al., 2013; Qin, Huang, et al., 2013), has previously been identified as unique for *Y. ruckeri* and pointed out as a good targets for qPCR-primers (source Marthas master thesis).

Hom7 gene sequences originating from ten different *Yersinia* strains were aligned using the muscle algoritm from mega7. Of these *Yersinia* strains six were retrieved from the JGI microbial database (Table S1) and the four remaining had previously been sequenced in the AKMS group (Drågen, 2020).

Three qPCR primers were designed based on the conserved regions. Primer design was performed in Primer Express 3.0.1 with default settings, based on the Hom7 conserved sequence of strain NVI/10705. The primers identified in Primer Express were tested for unique specificity with primer-BLAST, eliminating primers with products on potentially unintended templates. From the remaining candidates three primer pairs at unique genomic locations were chosen based on lowest penalty.

The primers were tested with PCR using genomic DNA extracted from *Y. ruckeri*-strain NVI-10705. This was done to verify that all primer pairs were able to bind and amplify DNA producing a single product with the correct length (~60bp). Agarose gel electrophoresis confirmed that all reactions resulted in product with the correct length (see Figure 13).

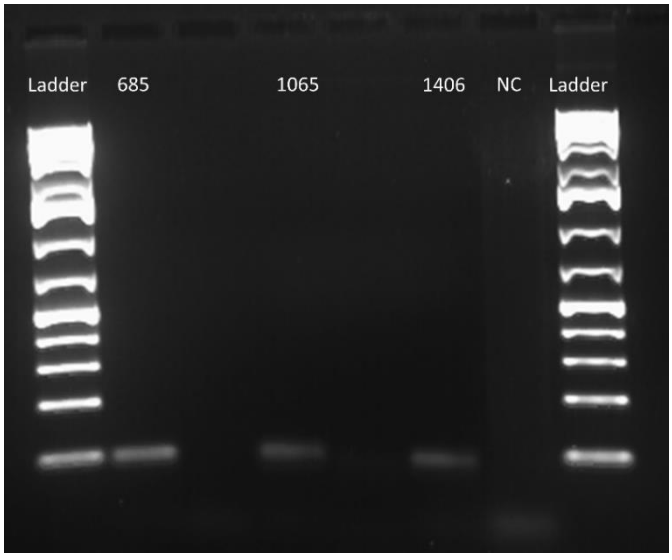

Figure 13: 1,5% agarose gel showing PCR products obtained with qPCR primer pares Home7-685, -1065, and -1406 targeting the gene hom7, from DNA extracted from *Y. ruckeri*-strain NVI-10705, Non-template control (NC) and GeneRuler 1 kb Plus DNA Ladder (Ladder).

The Home7-685 primer pair resulted in the highest product concentration measured with Qubit after purification with the QIAquick PCR purification kit and was chosen for further testing. Primer sequences are presented in Table 3.

Tabell 3: qPCR primer sequence designed for quantification of *Y. ruckeri* in microbial communities by targeting the Hom7-gene.

Primer ID	Sequence (5'-3')	Product length
Hom7-685F	5'-CCTCGGCGTCTATACGGAAGT-3'	63 bp
Hom7-685R	5'-CAGGGTGAGCGTGAAATCCT-3'	

3.6.2 Absolute quantification of Y.*ruckeri* using the standard-curve method

The standard-curve method is a commonly used method for absolute quantification with qPCR. The standard-curve is used to calculate concentration of target genes of experimental samples and consists of a dilution series of known template concentrations.

A critical aspect of the standard-curve method is to have reliable and accurate standards that reflect the samples well. Thus, we produced two standard-curves either based on genomic *Y. ruckeri* DNA or the Hom7-685 PCR product. First, DNA from *Y. ruckeri* isolate NVI-10705 DNA was extracted with the PowerSoil DNEasy kit according to protocol. Then, the Hom7-685 PCR product was amplified from the genomic DNA extract using PCR with the Hom7-685 primer pair. The PCR product was purified with the QIAquick PCR purification kit (Qiagen) following the manufactures protocol (Appendix E) using a microcentrifuge.

Since absolute quantification was an aim for the qPCR approach, we needed to estimate the concentration of *Y. ruckeri* cells in each standard. One can estimate the concentration of target-genes in a PCR product using equation 3.

$$c_{target}[\frac{molecules}{\mu l}] = n_{target}[molecules] \times \frac{c_{DNA}[\frac{ng}{\mu l}] \times N_A[\frac{bp}{mol}]}{l_{DNA}[bp] \times M_{bp}[\frac{ng}{mol}]} \quad \text{Eq. 3}$$

Where C_{target} is the concentration of the target (Hom7), C_{DNA} the DNA concentration, l_{DNA} the length of the DNA fragments, n_{target} the number of targets per DNA fragment, N_A Avogadro constant (6.022×10^{23} bp/mol), and M_{bp} the average weight of a double-stranded base pair (6.6×10^{11} ng/mol) (Brankatschk et al., 2012).

For the Hom7-685 PCR product based approach there was 1 targets per DNA fragment and the DNA fragment was 63bp. The concentration of PCR product was measured with Qubit 4 Fluorometer (Invitrogen) (protocol in Appendix F) to 2.14 ng/µL, corresponding to 3.1×10^{10} copies Hom7/µl according to equation 3. For the genomic DNA based approach we assumed that each *Y. ruckeri* cell only contained one copy of the Hom7 gene (Drågen, 2020) and the genome size was 3.87×10^6 bp (diCenzo George & Finan Turlough). The concentration of DNA in the genomic standard was measured to 48.01 ng/µL corresponding to 1.13×10^7 Hom7 copies/µl according to equation 3. Estimating the Hom7 concentration using the cell-density of the *Y. ruckeri* culture gave a slightly different estimate. Prior to DNA extraction, the cell-density of the *Y. ruckeri* culture was quantified to 1.13×10^6 cells/µl. The theoretical number of *Y. ruckeri* genomes, and thus Hom7 genes, in the DNA extracts was thus calculated to be 3.4×10^7 Hom7 genes/µL DNA extract.

Dilution series were made according to Table S2 and S3 from the amplified Hom7 PCR product and genomic DNA of *Y. ruckeri* isolate NVI-10705. The standards consisted of three replicas of six dilutions ranging from 16 000 to 1×10^8 Hom7 copies /µl for the PCR product

standard, and of three replicas of nine dilutions ranging from 1.6 to 1 × 10^7 Hom7 copies/µl for the genomic standard measured by cell density. The standards were tested by qPCR using Power SYBR Green as reporter and the Hom7-685 primer pair as described in section 2.3.3.2. Using each serial dilution in separate qPCR reactions their cycle threshold values (C_t) were determined. C_t values for each concentration in the two dilution series were plotted against log copy number (log(N_0). A linear regression of log(N_0) versus C_T gave the standard curves (Figure 14) (Brankatschk et al., 2012). The linear regression gives the intersection point (a) and the slope (b). The slope number is used to estimate amplification efficiency (E), according to Equation 1. An acceptable E should be between 90 and 110%.

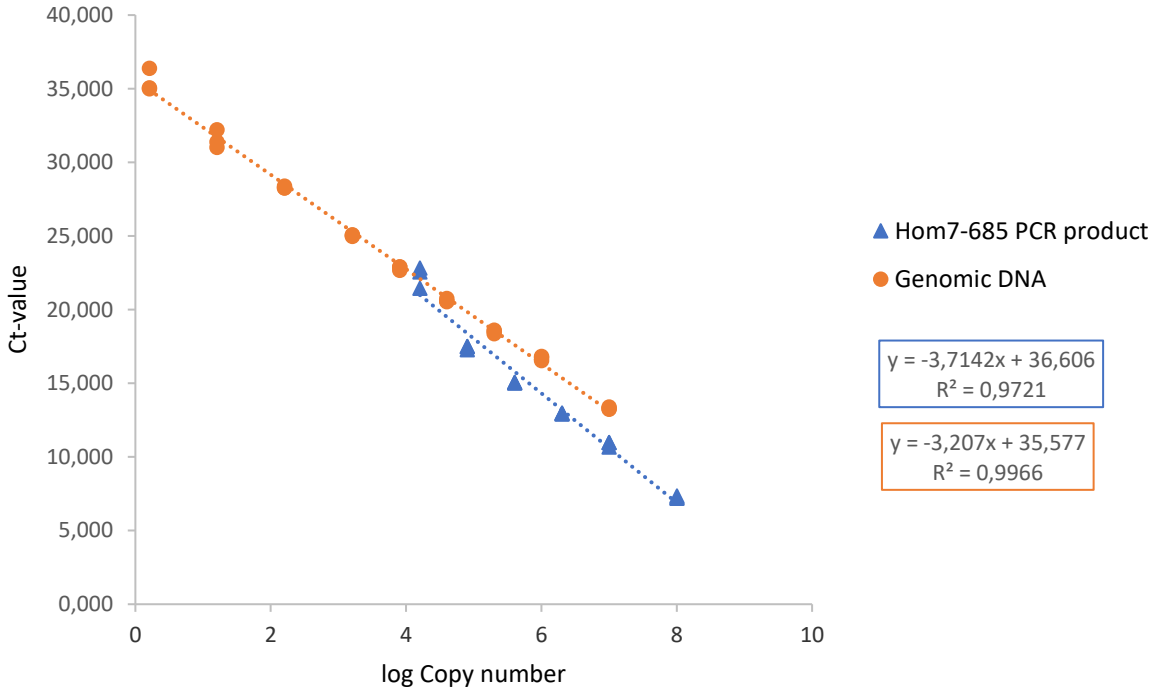

Figure 14: qPCR standard curves. Standard samples are dilutions of the amplified Hom7 PCR product (blue) and genomic DNA of *Y. ruckeri* isolate NVI-10705 (orange).

The Hom7-685 PCR product standard curve had an E of 85% and the genomic DNA standard curve 105%. The correlation coefficient (R^2) of the linear regressions were above 0.99 for the genomic DNA standard curve, which indicates a strong linear correlation, but not for the Hom7-685 PCR product. For the higher concentrations the Ct-values were lower than expected for both standard curves, possibly due to inhibition caused by too high template concentrations. For the lower concentrations there was low precision between replicates, possibly due to the concentration being lower than limit of quantification. Thus, in further optimization the lowest and highest concentrated samples from the Hom7-685 PCR product and the two lowest and highest concentrated samples from the genomic DNA standard curve were excluded.

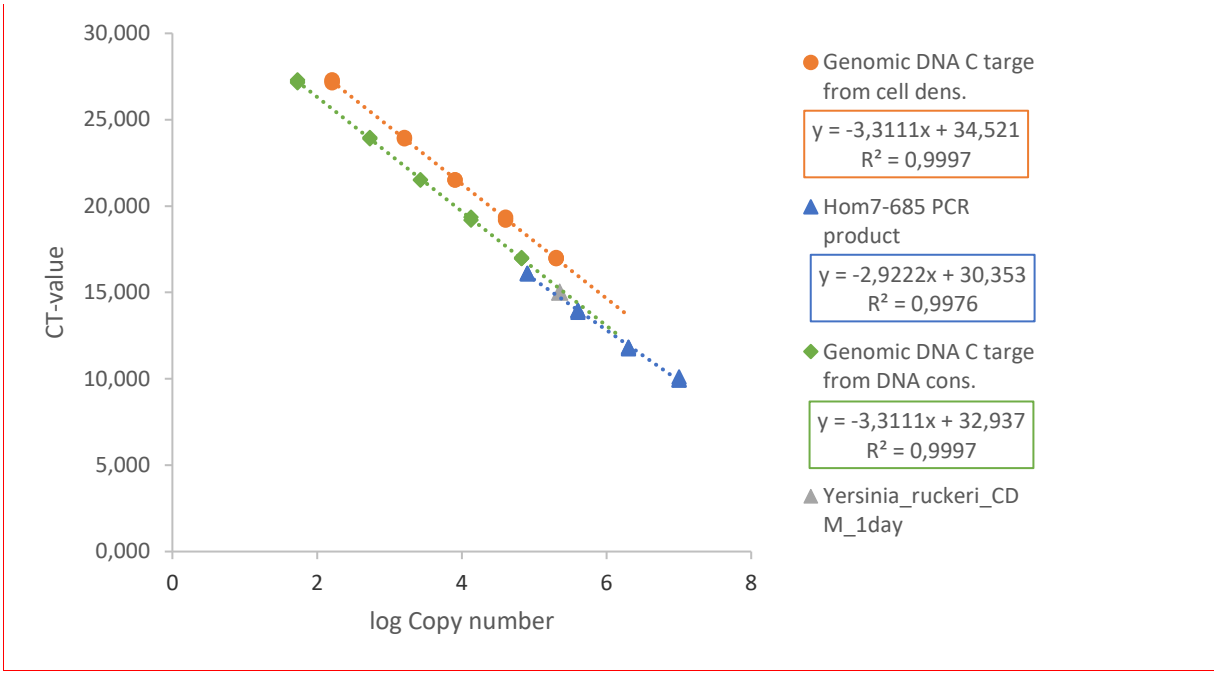

Figure 15: qPCR standard curves. Standard samples are dilutions of the amplified Hom7 PCR product (blue) and genomic DNA of *Y. ruckeri* isolate NVI-10705 with copy number calculated from cell density before DNA extraction (orange) and from DNA concentration in extract (green). Also included a sample of *Y. ruckeri* with known density (grey).

To assess the accuracy of the two candidate qPCR standards we set up a new qPCR reaction and included a sample of *Y. ruckeri* with known density (Figure 15). The Hom7-685 PCR product standard curve had an application efficiency of 119% and the genomic DNA standard curve 100%. The correlation coefficient (R^2) of the linear regressions were above 0.99. For the highest concentration in the Hom7-685 PCR product standard curve the Ct-value was still lower than expected. If this measurement was removed the efficiency would be 111%. The genomic DNA standard curve had a better amplification efficiency and linearity. However, we also wanted to assess at the accuracy. DNA extracts from *Y. ruckeri* cultured of 2.24 x 10^5 cells/µl was also included in the qPCR assay. Based on the PCR product standard, the genomic standard with quantification based on DNA and with quantification based on cell density the cell density in the sample was estimated to the density in the sample to be 1.77 x 10^5, 2.58 x 10^5, and 7.75 x 10^5 cells/µl, respectively. The genomic standard with quantification based on DNA concentration gave the most accurate measure.

The genomic DNA standard curve had a better amplification efficiency and linearity, with quantification based on DNA concentration giving the most accurate measure. Thus, in further optimization and experiments the genomic DNA standard curve with quantification based on DNA concentration was used.

3.7 Testing of filtration device

For filtration of water samples for DNA extraction a vacuum filtration devise was used. We wanted to verify that our cleaning protocol (Appendix G), was sufficient to avoid cross contamination between sampling days. The filtration setup was contaminated with *Y. ruckeri*. The filtration devise was then cleaned according to our protocol. The following day dH2O (0.2 µm filtered) was filtered true polycarbonate filters (F) or polycarbonate filters in combination with heat sterilizer fiberglass (GF) in the vacuum filtration devise. The filters were subsequently handled equally as polycarbonate filters used for sampling of bacterial communities, and DNA extracted with the powersoil kit. PCR was run for 40 cycles using the 16s rRNA primers 338F and 805R with the DNA extracts as templates. Agarose gel electrophoresis showed no DNA amplification from either F or GF-samples after 40-cycels of PCR amplification (Figure 19). From this we concluded that our cleaning protocol was sufficient to avoid cross contamination between sampling days.

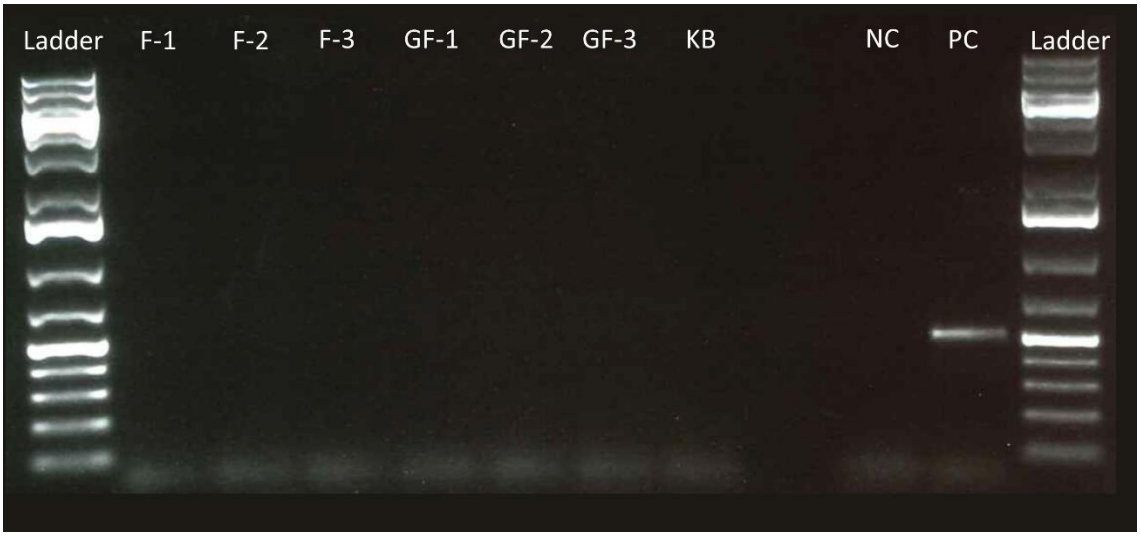

Figure 16: 1,5% agarose gel showing PCR products obtained from dH_2O (0.2 µm filtered) filtered true polycarbonate filters (F) or polycarbonate filters in combination with heat sterilizer fiberglass (GF) in the vacuum filtration devise previously exposed to bacteria and cleaned according to protocol, non-template control (NC), positive control (PC) from *Y. ruckeri* extracted simultaneously with F and GF samples, kit blank (KB) and GeneRuler 1 kb Plus DNA Ladder (Ladder). PCR amplification with 16s rRNA primers 338F and 805R, 40 cycles

3.8 Investigation of flow rate stability

Each bioreactor contained 300 mL of a freshwater bacterial community receiving media by one of two peristaltic pumps. To investigate the flow rate stability the inflow in the reactors were measured at five different time points (Figure 20). This was done by removing the effluent tubing and measuring the change in volume after a known period of time. The two first measurements were performed under experimental conditions (section 2.1.1) while the remaining three measurements were made without aeration while rectors were placed in ice bats to minimize evaporation. Reactors A1, A5 and B1 was excluded du to faulty equipment.

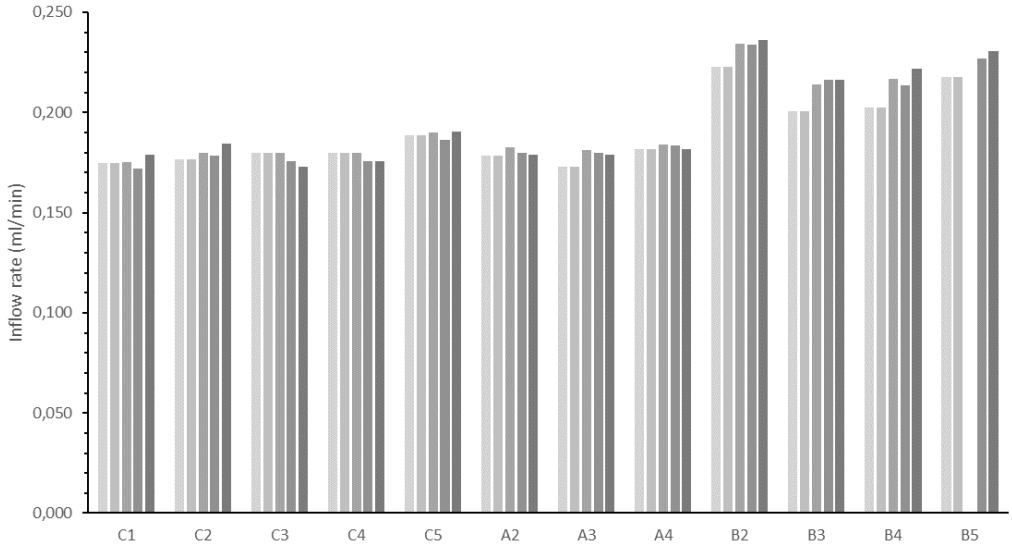

Figure 17: Inflow rate in reactors measured as ml/min by evaluating volume change after a known period of time for five different time periods. The two first measurements were performed under experimental conditions while the remaining three measurements were under conditions minimizing evaporation.

The reactors were divided into two treatment groups, A and C (1) and B (2), connected to two different pumps. The maximum standard deviation in inflow rate between measurement was 0.003 and 0.007 ml/min for the reactors in group 1 and 2, respectively. The average flow rate into each reactor in group 1 was between 0.189 and 0.175 ml/min, while it was between 0.230 and 0.209 ml/min for the reactors in group 2. From this I concluded that the inflow rate between measurement times and between reactors were sufficiently stable for this experiment.

3.9 Investigation of temperature stability

To minimize temperature variation in the cultures, and potential disturbances this would cause, the experimental setup was in a climate-controlled room, holding the temperature at around 14°C. We measured the temperature fluctuation in the room with a wireless smart multi sensor device (MS1, UbiBot). Sensors were placed freestanding in the room (air) and in 300 ml water, logging the temperature every five minuets for 4 days (Fgure 21). The ambient temperature (air) fluctuated between 15.8 and 13.2°C with a mean temperature of 14.4±0.6°C, while the water temperature fluctuated between 14.1 and 13.1°C with a mean temperature of 13.4±0.2°C. From this we concluded that the temperature was sufficiently stable for this experiment.

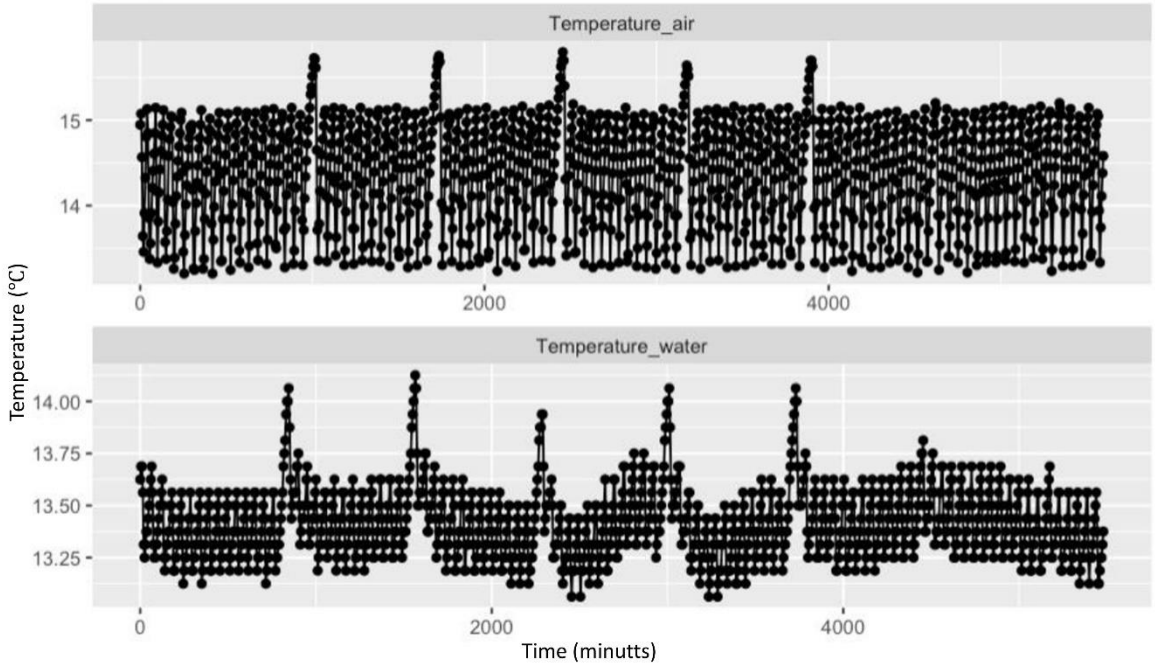

Figure 18: Temperature in a) the air and b) 300 ml water in a climate-controlled room measured every five minutes for 4 days.

4 Results

The aim of this study was to investigate the impact of multiple invasions attempts on the characteristics and invasibility of a planktonic bacterial community in a flow-through system. We cultivated freshwater bacterial communities in lab-scale continuous bioreactors with specific growth medium for carbon limited growth. Treatment group A and B were invaded at 1 and 10% propagule pressure with *Yersinia ruckeri*, four and five times over a 22-day period, respectively. Group C was a control group and was not exposed to any invasion attempts. Invasion success at different propagule pressures was evaluated by quantifying the bacterial density, by flow cytometry, and the abundance of the invader by qPCR in each reactor. For analysis of bacterial community compositions, we used Illumina MiSeq amplicon sequencing of the V3 and V4 region of the 16S ribosomal RNA gene. These results were used to evaluate the success of the invader, the effect of the invasion attempts on the resident community, the temporal stability of the communities and other factors affecting the invasibility of the communities by *Y. ruckeri.*

4.1 *Y. ruckeri* could not invade the communities

Invasion success was evaluated by plotting the quantity of our invader *Y. ruckeri* in the bioreactors versus time (Figure 22a). The plot is semi logarithmic, as we assumed logarithmic growth. I made a linear regression for each community, and the slope equals the relative rate of change (r) of *Y. ruckeri* in the community in question. The relative rate of change indicated whether the invasion was successful or not, where $r \geq 0$ was defined as a successful invasion and $r >$ the dilution rate (D) indicates a positive growth rate. The relative rate of change (r) is shown in Figure 22b.

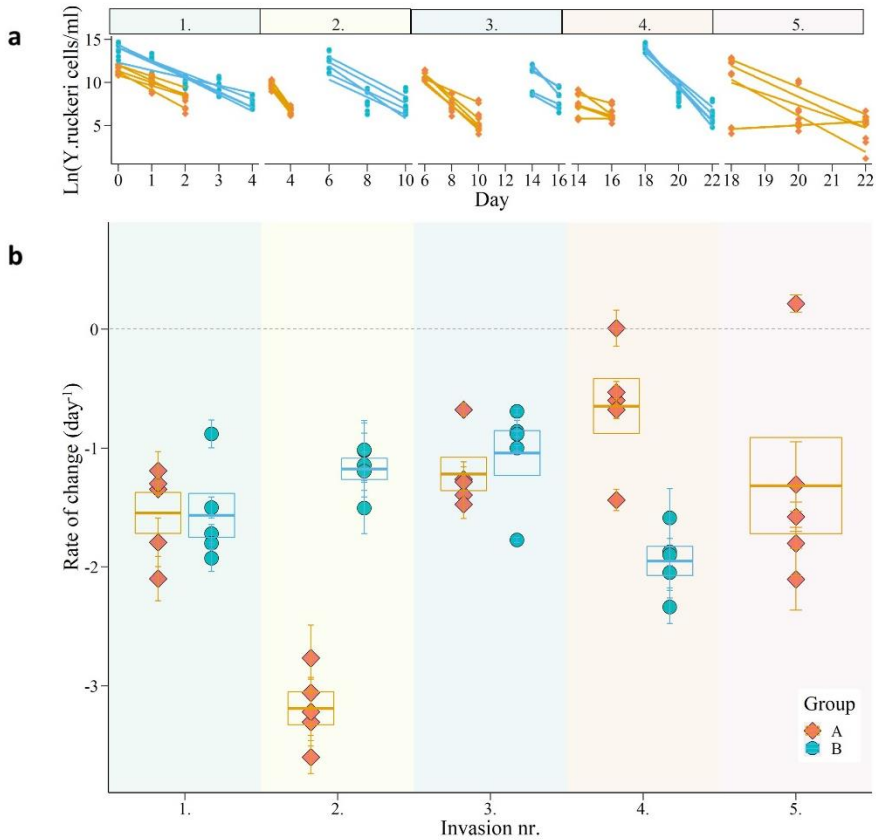

Figure 19: Evaluation of invasion success by *Yersinia ruckeri*. A) The density of *Yersinia ruckeri* on a natural logarithmic scale versus experimental day. Lines are linear regression for each bioreactor and invasion attempt. The plots are split up in the different phases of the experiment first (1.), second (2.), third (3.), fourth (4.), and fifth (5.) invasion attempt. The orange triangles and blue circles represent the bioreactors invaded with 1% and 10% propagule pressure, respectively. B) The net rate of change for *Y. ruckeri* in the reactors for the different phase of the experiment. Average and standard error are indicated for each group (1% and 10%). The boxes with the horizontal line represent interquartile range and group mean.

All invasion attempts were categorized as failures in treatment group B as the relative rate of change was less than 0. In treatment group A two invasion attempts were categorized as successful, reactor 1 at invasion attempt four, and reactor 5 at invasion attempt five. These communities had a relative rate of change for the invader of 0.01 and 0.20 day^{-1}, respectively. However, the invasion success of reactor 1 of the 1% group at invasion attempt four might not be valid as there is only two sampling points and the linear regression has a bad fit (r^2=0.0008). Overall *Y. ruckeri* diapered from the reactors in a matter of days and did not manage to invade the communities.

4.2 The effect of invasion attempts on the composition and diversity of the resident communities

The bacterial composition and the diversity were used to evaluate the impact of the multiple unsuccessful invasions attempts on the resident communities. The raw sequence dataset contained a total of 8 995 449 sequence reads from 159 samples. The samples contained 137 433 to 24 234 reads per sample, with a mean of 56 575± 15 497 reads per sample. A total of 2201 zOTUs (> 8 reads/zOTU) were identified in the dataset. The dataset was estimated with Chao1 to cover 63.7 to 88.1% of the actual zOTU-inventory in the samples with a mean of 78.5% (SD = 4.1%). The dataset was scaled to the 25 quantile with 45 434 sequences per sample. No zOTUs were removed in the normalized dataset.

4.2.1 Taxonomic community composition

The bacterial community composition at the class and family level for all samples at all time points (figure 23) were used to investigate the effect of the invasion attempts. The community composition was generally very similar between treatment groups. Four classes made up most of the taxa present (Figure 23a). *Gamma-proteobacteria* was most abundant, with *Beta-proteobacteria* and an unclassified group from the phylum *Proteobacteria* following. *Cytophagia* was the fourth most abundant class. These four classes made up 71, 15, 10, and 2% of the total reads, respectively. Generally, these taxa were relatively equally represented between samples on any given day. Some exceptions were samples taken from reactors C3, C4, and B2 on day 22. For these communities *Beta-proteobacteria* was more dominating than *Gamma-proteobacteria.*

Ten families made up most of the taxa present (Figure 23b). Pseudomonadaceae and *Moraxellaceae* were the most abundant families, making up 32 and 31% of the total reads, respectively. The family Pseudomonadaceae predominantly consisted of the genera Pseudomonas, while *Acientobacter* was the dominating genera of *Moraxellaceae*. These two families switched between being the dominating families (Figure 24). Pseudomonadaceae dominated all communities from day -1, and had an abundance of 10-14% in the A reactors (day 0). *Moraxellaceae* gradually increased in abundance taking over as the most dominant taxa from day 5. On day 10 the abundance of *Moraxellaceae* was around 14-17% for the A reactors. From day 18 *Pseudomonadaceae* re-established as the dominant taxa. This pattern was recognizable in all communities with no discernable connection to the invasion attempts

Reactors C3 and C4 diverged from the rest of the communities. C4 had more Zoogloeaceae, reaching a peak of 56% of the community on day 5, and *Nevackicea* reached a high relative abundance during the later part of the experiment (49% of the community on day 22). C3 differed by having more *Zoogloeaceae* from day 2 to 5 (20 – 46%) and day 18 onwards (16-22%) compared to the remainder of the reactors (1-13% and 0-11%). C3 also had less *Pseudomonadaceae* making up only 18% of the total reads of C3. From day 6 the community in reactor C3 closely resembled the majority of the other communities, dominated by *Moraxellaceae*. The family Zoogloeaceae predominantly consisted of the genera *Zoogloea*, while *Nevaskia* was the dominating genera of *Nevackicea*.

Overall, the bacterial composition was highly similar between reactors, regardless of invasion attempts. The unsuccessful invasion attempts did not seem to affect the resident community's composition. However, a temporal change in the community's composition occurred across all treatment groups from day 5 to 18.

a)

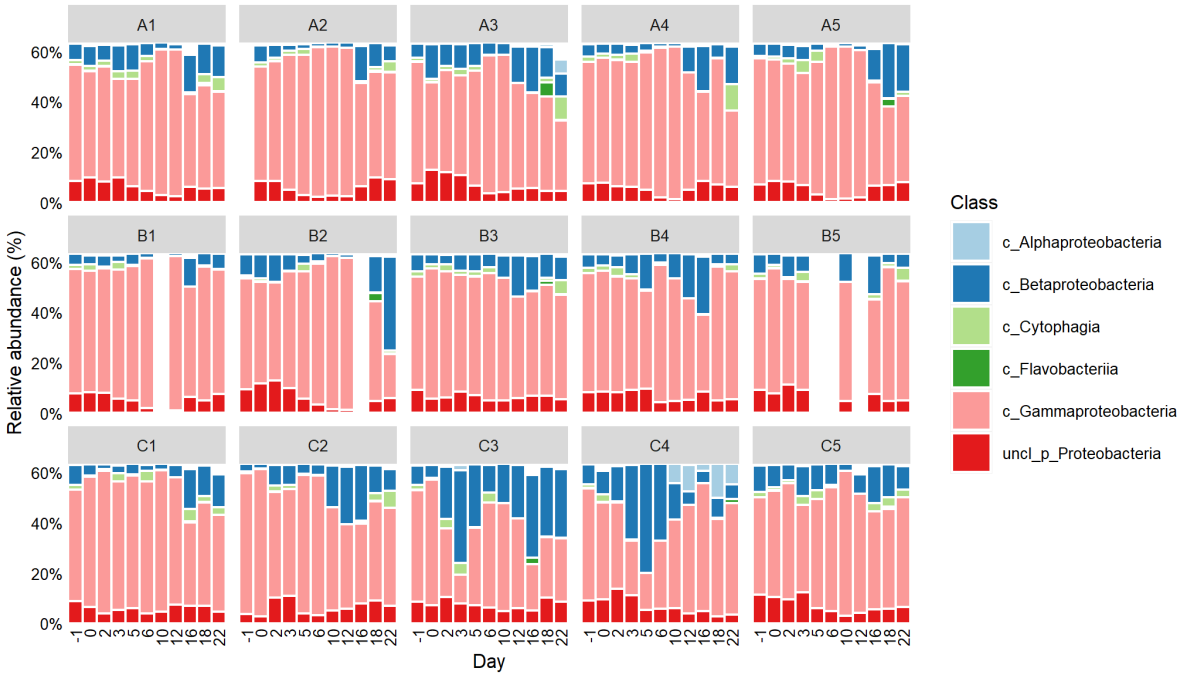

b)

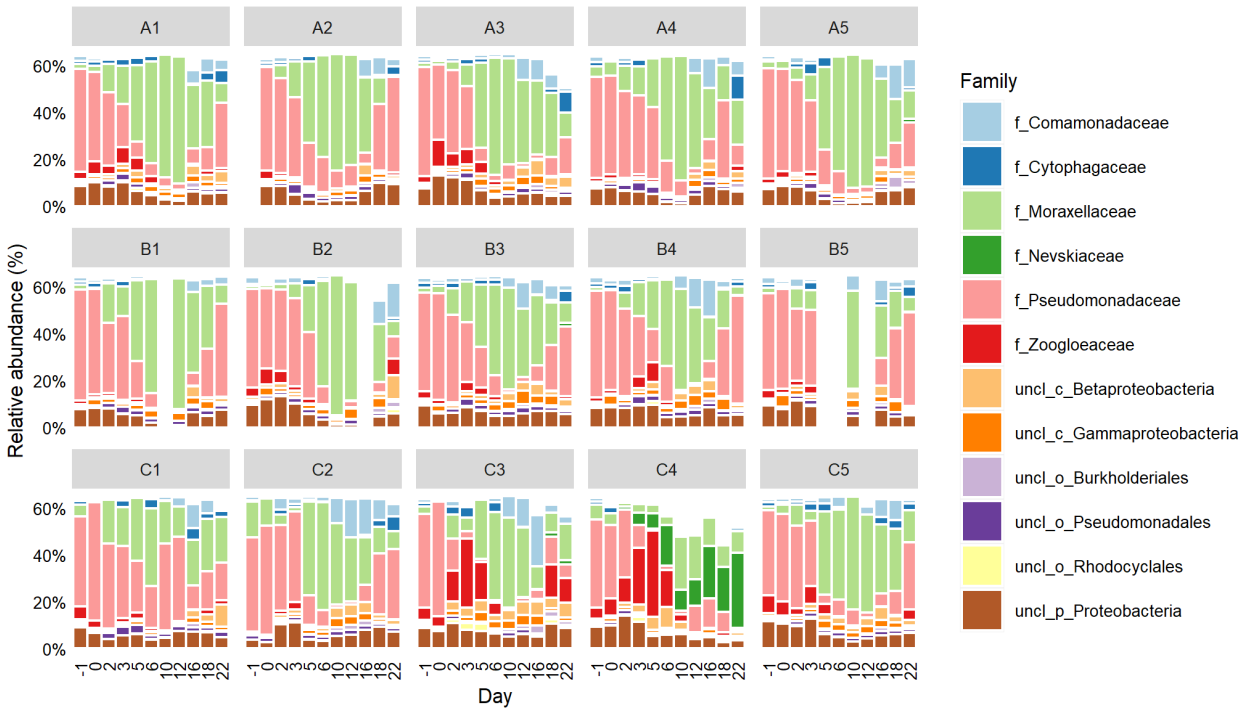

Figure 20: The relative abundance of bacterial a) classes and b) family for each bioreactor over time, starting at one day before the first invasion attempt (day -1). The A and B treatment groups represent the bioreactors invaded with 1% and 10% propagule pressure, respectively. The C group was not invaded. Only the 6 most abundant classes and 12 most abundant genera are presented.

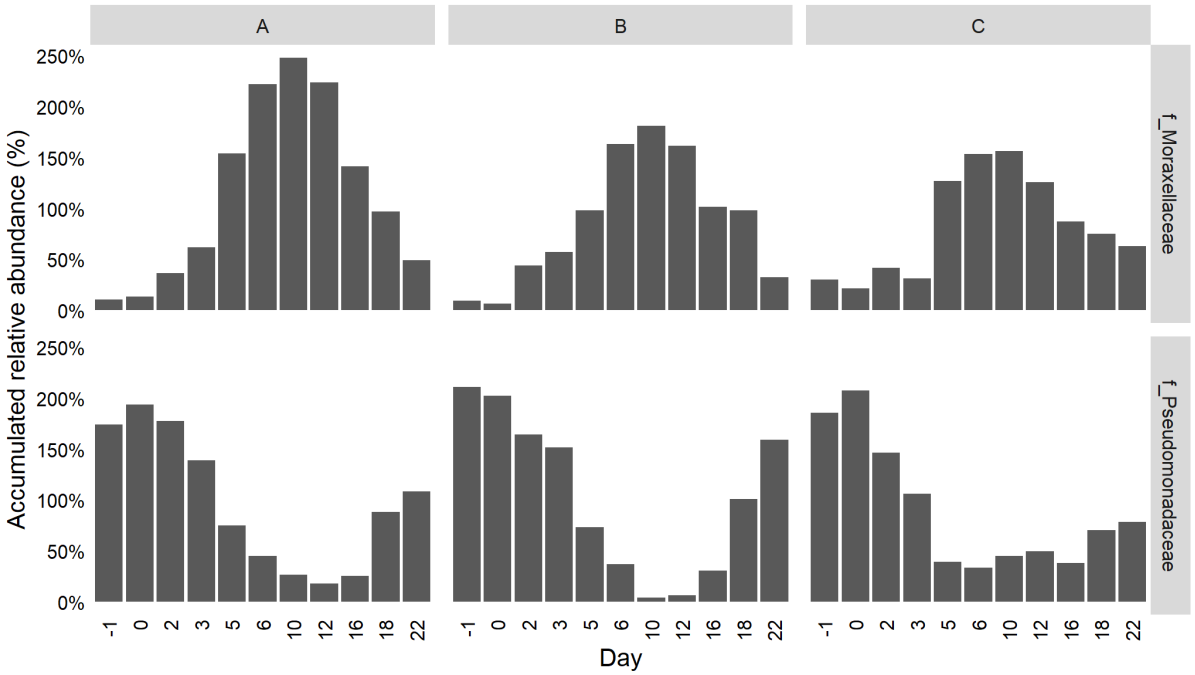

Figure 21: The relative abundance of Moraxellaceae and Pseudomonadaceae for the cultivation regimes A, B and C over time.

4.2.2 Invasion effect on the diversity within the resident communities

The bacterial diversity for each resident community sample was characterized to investigate the effect of the invasion attempts. I used three diversity indices to describe the local diversity (i.e. α-diversity) of the resident communities, i.e. zOTU richness, exp. Shannon diversity, and evenness, equivalent to Hill numbers of order 0, 1, and 1D/0D, respectively (Figure 35).

There was temporal development in the α-diversity of the resident communities. Treating all groups ass one there was a significant difference in zOTU richness, exp. Shannon diversity, and evenness between days of the experiment ($p < 0.05$, Kruskal-Walli's test). zOTU richness started to drop from day 5 with a drastic decrease from day 6 to 10. There was an 66% average reduction in richness from 659 to 433 zOTUs from day 6 to 10 ($p = 6.9 \times 10^{-5}$, Pairwise Wilcoxon test). However, the zOTU ruichness steadily increased again from day 10 ($p < 0.05$, Pairwise Wilcoxon test) to a mean of 789 zOTUs on day 16, the highest zOTU richness of the experiment. The temporal development was similar for all diversity indices, however, exp. Shannon diversity and evenness starts to decrease already from day 3 ($p = 6.9 \times 10^{-5}$, Pairwise Wilcoxon test). From day 3 to 6 exp. Shannon diversity and evenness decreased 64% and 60%, respectively. Exp. Shannon diversity and evenness plateaus from day 6. From day 12 to 16 exp. Shannon diversity and evenness increases back to 9 and 13% higher than before the fall in on day 3. In addition, there was an increase in exp. Shannon diversity and evenness from day -1 to 3. In summary, the communities had a drop in α-diversity from day 3 (exp. Shannon and evenness) evident in zOTU richness from day 5 returning to higher levels on day 16.

The temporal development in α-diversity was similar for all treatment groups. There was no significant difference in zOTU richness between treatment groups on any of the days in the experiment ($p > 0.05$, Kruskal-Wallis test), except for day 5. On day 5 group C had a 20% and 24% lower zOTU richness than treatment group A and B, respectively ($p < 0.05$, Pairwise Wilcox test). However, this was contributed to the outlier C4. Excluding sample from reactor C4 there was no significant difference in zOTU richness on day 5 either ($p > 0.05$, Pairwise Wilcox test). In summary, the zOTU richness was similar for the different treatment groups at any given day of the experiment. I did however find significant differences in exp. Shannon diversity between the treatment groups on day 3, 5 and 6 ($p < 0.05$, Kruskal-Wallis test). Group C had a lowest mean exp. Shannon diversity on day 3 and 5, while it was lowest for treatment group A on day 6. However, a pairwise comparison did not show any significant differences between any of the groups on these days ($p > 0.05$, Pairwise Wilcox test).I also found significant differences in evenness between the treatment groups on day -1, 6 and 12 ($p < 0.05$, Kruskal-Wallis test). Group C starts with 1.4 times higher mean evenness than collective mean of treatment group A and B ($p < 0.05$, Pairwise Wilcox test). On day 6 a pairwise comparison showed no significantly differences between the groups ($p > 0.05$, Pairwise Wilcox test), however mean evenness of group C was still higher than A and B. On day 12 group C had a 2.3 times higher mean evenness than the mean of A ($p < 0.05$, Pairwise Wilcox test). Group C hade higher average evenness than the other treatment groups several days of the experiment, however this was also the case on the first day of the experiment before any invasions had happened. In summary, α-diversity was similar for the different treatment groups at any given day of the experiment. Thus, invasions did not affect the α-diversity.

Overall, the zOTU richnes, exp. Shannon diversity and evenness was highly similar between treatment groups, regardless of invasion attempts. The unsuccessful invasion attempts did not seem to affect the α-diversity. However, there was a transient drop in α-diversity across for all treatment groups from day 3 for exp. Shannon and evennessm and evident in zOTU richness from day 5, until day 16.

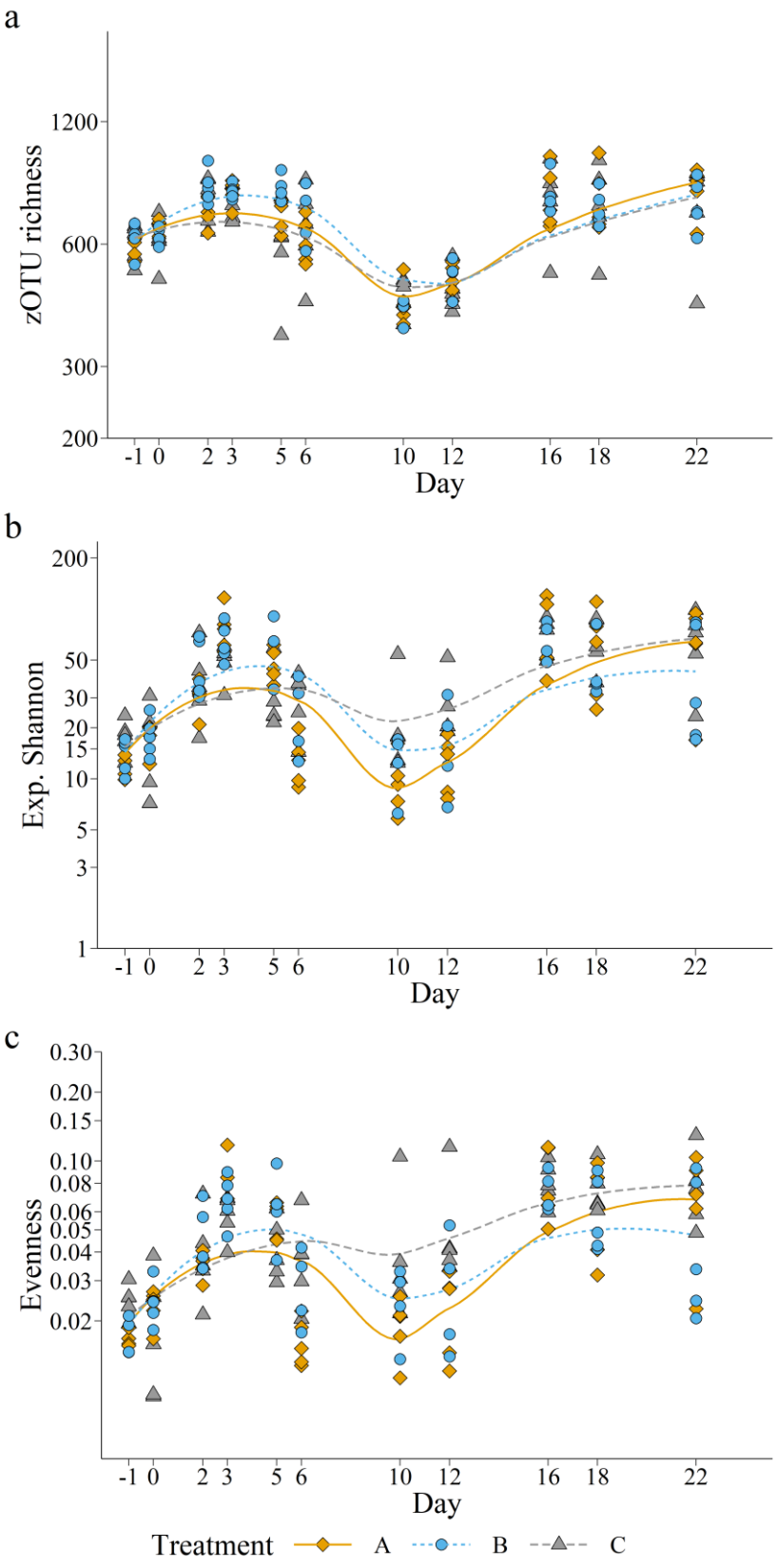

Figure 22: Alpha diversity quantified as richness (a), exp. Shannon (b), and evenness (c) for each treatment group as a function of time for each treatment group, A (orange square), B (blue circle), and C (gray triangle). Note that y-axsis are log scaled.

4.2.3 Invasion effect on differences between communities

To investigate whether invasion attempts affected the composition between the resident communities the Bray-Curtis distance was quantified for all samples at all time points. PcoA analysis based on Bray-Curtis dissimilarity was used to visualize dissimilarity in the bacterial community composition over time (Figure 26). The two first coordinates of the ordination explained 58% (46.2%+11.7%) of the variation in the Bray-Curtis dissimilarity matrix. The variation explained by the first nr. axis's is presented in Figure S1.

All communities clustered tightly for most of the observed time period, with the exception of days 5, 18 and 22. On day 5 the communities were spread out in no discernible pattern. A PERMANOVA analysis revealed no significant difference in the community composition between the three treatment groups on day 5 ($p = 0.425$). The communities clustered tightly again from day 6. However, at the opposite side of the ordination plot compared to the first four days, loading on axis 1 for all communities. The communities increased in dissimilarity from day 16 onwards observed as points became more scattered. From day 16 the loading decreased on axis 1 and points moved towards the ordination space of samples taken the first week. PERMANOVA analysis revealed no significantly difference ($p = 0.15$, 0.091, and 0.275) in the community composition between the three treatment groups on day 16, 18, and 22, respectively.

There was no clear overall difference in the microbiota between the treatment groups, and communities appeared to be similar regardless of the number of unsuccessful invasion attempts the bacterial communities had been subjected to. However, a common successional trajectory of the communities is apparent throughout the experiment. Thus the result indicate a deterministic change in community composition, likely due to a disturbance starting somewhere around day 3 to 5, and the recovery after disturbance starting on day 16.

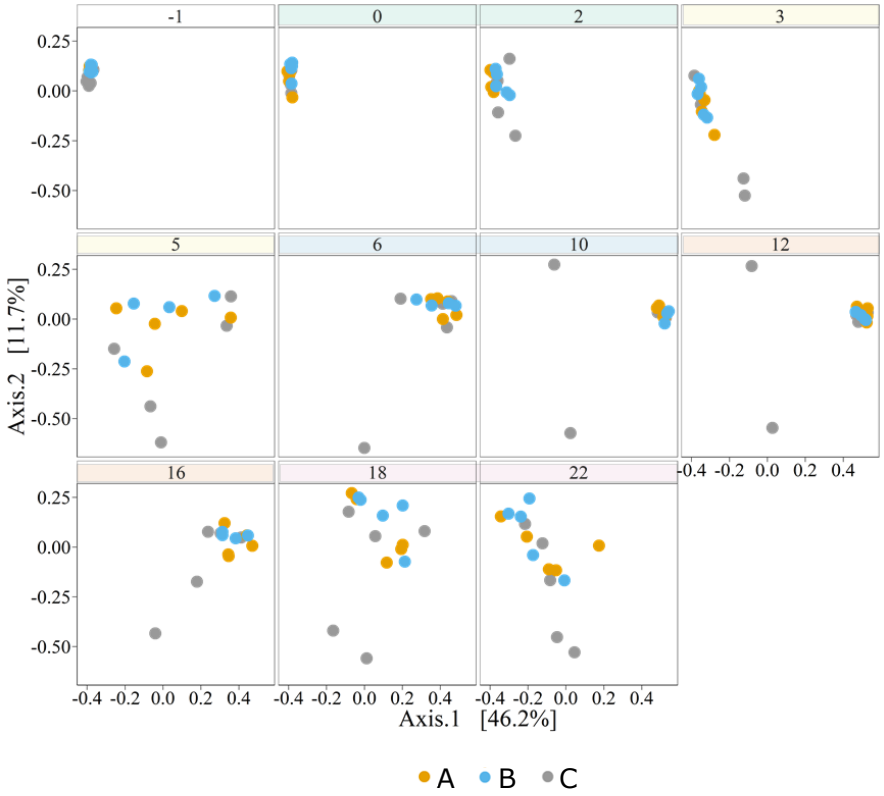

Figure 23: PCoA ordinations based on Bray-Curtis dissimilarity. One ordination was done, but data from the different sampling days are given in individual panels (day indicated on top). A: invaded with 1% propagule pressure. B: invaded with 10% propagule pressure. C: control group, no invasion attempts. Group A was invaded at day 0 (green), 3 (yellow), 6 (blue), 12 (orange) and 17 (pink). Group B at day 0, 6, 12 and 17.

A few communities distinguished themselves from the otherwise similar communities at different times. C3 and C4 separates from the cluster on day 3 creating their own group. C4 had a noticeably different taxonomic composition, as described above, and from day 3 onwards this community was dissimilar to the other communities. On day 6 C3 increased in similarity to the other communities, but changed again on day 18 and 22. C1 differed from the other communities on days 10 and 12 with a higher relative abundance of *Pseudomonadaceae*. These differences did not affect the overall similarity of the microbiota between the treatment groups.

4.2.4 Development in community density

Community density varied throughout the experiment for all groups, (Figure 27). The communities had similar densities regardless of treatment group. Exceptions were on day 6 and 18 when the density variation increased dramatically, but similarly, for all treatment groups. I could not distinguish a consistent trend based on invasion attempts.

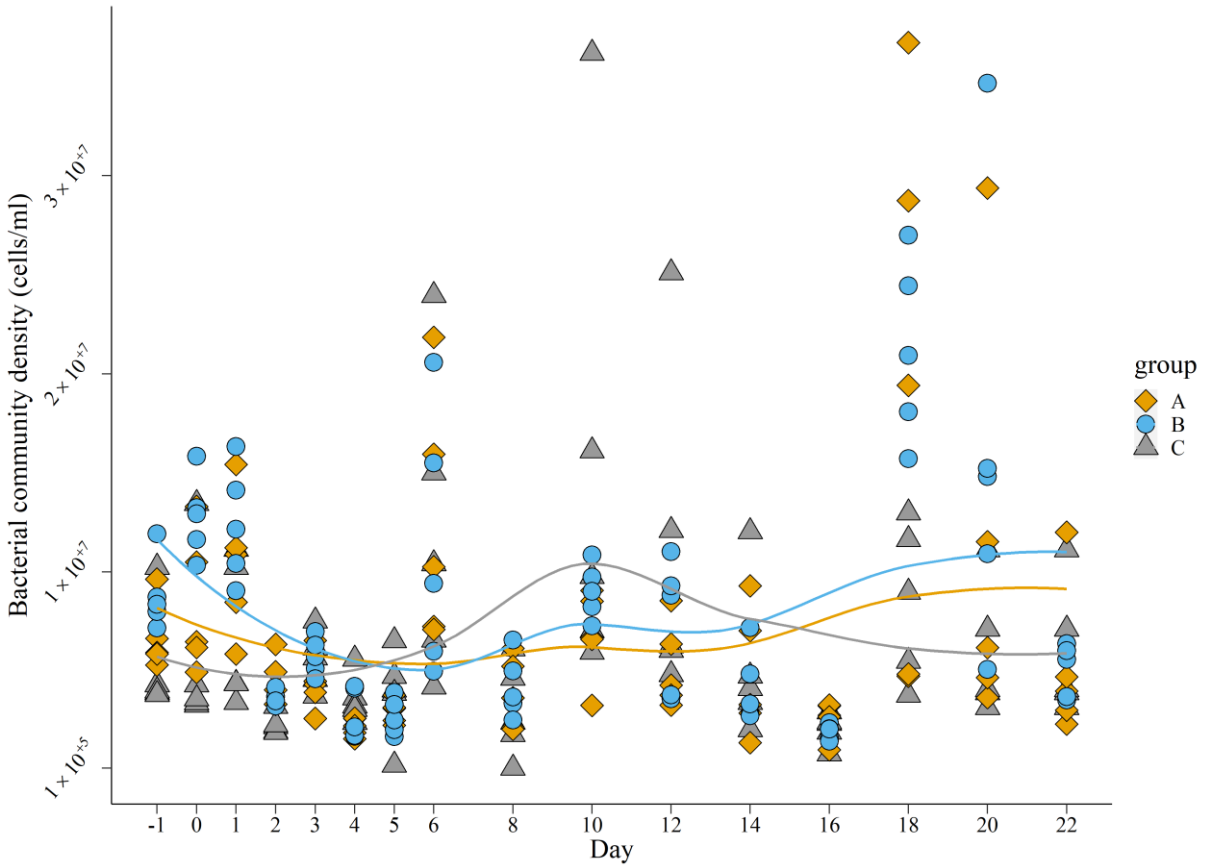

Figure 24: The Bacterial community density (cells/mL) measured for all communities with flow cytometry. A: invaded with 1% propagule pressure. B: invaded with 10% propagule pressure. C: control group, no invasion attempts. Group A was invaded on days 0, 3, 6, 12 and 17. Group B on days 0, 6, 12 and 17.

4.3 What caused the temporal variation in community composition and diversity?

The communities started to change, in regard to composition and diversity, somewhere around day 3 to 5 with recovery starting on day 16. This indicated a deterministic change likely due to a disturbance. This period coincides with an accidental pH-disturbance. The media was phosphate-buffered to pH 7.0. However, on day 11 we discovered that the pH in the reactor effluent was below 5 (Figure 28). The following day we measured the pH in each reactor and found that it varied between 4.3-4.7. On day 15 the pH-buffer was increased from 0.2 to 0.6 mM P-atoms/L. By day 16 the pH had restabilized at pH 6.7-6.9. Interestingly, at day 16 the communities indicated to start recovering from this pH-disturbance, as the community composition and the diversity started to return to the starting conditions. Thus, even though we do not have information on when the pH started to drop, I suspect that it happened somewhere around day 3 to 5 and that it was the cause of the temporal variation in community composition, density, and diversity.

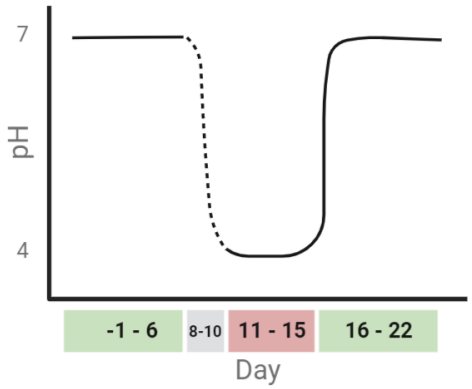

Figure 25: Illustration of temporal pH development in reactors. Created with BioRender.com

4.4 The specific rate of change of the invader

The specific rate of change of the invader in the communities tells us how competitively successful the invader was, and whether changes introduced to the system influenced the competitiveness of the invader. Here I investigate how propagule pressure, previous invasion attempts, the environmental pH and the density of the resident community densities affected the specific rate of change.

4.4.1 The effect of propagule pressure on the specific rate of change of invader

Here I investigate whether invasion of planktonic bacterial communities by *Y. ruckeri* at two different propagule pressures, 1% and 10%, alters the relative rate of change of the invader (r). The bacterial communities belonging to group A and B were invaded on day 0, 6, 12 and 17. Group A was also invaded on day 3 but this was not included in this comperison as there is no comparable data from group B. The average rate of change of *Y. ruckeri* in group A was not significantly different from B ($p > 0.05$, t-test) for any of the invasion attempts, (Figure 29). There was thus no significant difference in the mean specific rate of change of invader due to a tenfold difference in propagule pressure.

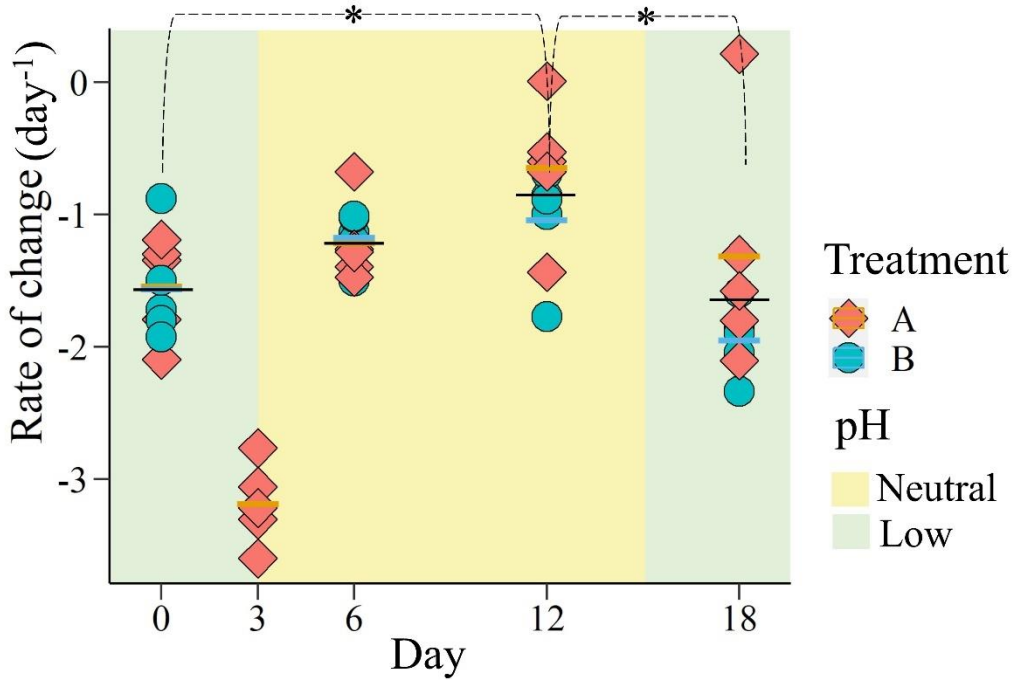

Figure 26: Relative rate of change of invader *Y. ruckeri* added at 1% (A) and 10% (B) propagule pressure to ten planktonic bacterial communities on five (A) and four (B) different days. Mean rate of change of invader is marked with orange (A), blue (B), and black (joint) solid line. There was no significant difference in mean rate of change between treatment groups at any of the days (Students t-test, P > 0.05). Asterisk (*) indicate significant differences in mean rate of joint group between different days (P< 0.005, Tukey's HSD Test), not including day 3.

4.4.2 The effect of number of previous invasion attempts on the specific rate of change of invader

First, I investigate whether there was a correlation between the time of the invasion attempt and the specific rate of change (r) of the invader *Y. ruckeri* for the new invasion attempt. As there was no significant difference in the mean specific rate of change of invader due to a tenfold difference in propagule pressure, I treated the treatment groups A and B as one group in this analysis. A one-way ANOVA analysis revealed significantly difference in the average invader rate of change between the days of the experiment (p = 0.003), indicates that some of the group means are different. To determine which pairs of groups are different the Tukey's HSD Test for multiple pairwise-comparisons was performed. I found that the mean value of invader rate of change was higher from day 0 to 12 (p = 0.01) and lower from day 12 to 18 (p = 0.01-04) (Figure 29). There was no statistically significant difference between the remaining days. In summary, r of *Y. ruckeri* increases from day 0 to 12 and decreases again from day 12 to 18.

To investigate whether the development of r over time was correlated with the number of unsuccessful invasions attempts the bacterial communities had been subjected to previously I plotted r versus the number of invasion attempts the community had been subjected to (Figure 30). Sorting the data like this treatment groups A and B could not be treated as one group. The difference in mean r between A and B was most obvious in the second and fourth invasion attempt. The average invader rate of change for B was 53% higher than A ($p = 6 \times 10\text{-}6$, student-t-test) in the second invasion attempt and 67% larger ($p = 0.002$, Student t-test) in the fourth. These results suggest that the development in r over time was caused by a different factor than the number of unsuccessful invasions the bacterial communities had been subjected to previously.

In summary, I did not find a correlation between the number of unsuccessful invasions the bacterial communities had been subjected to previously, and the specific rate of change of the invader *Y. ruckeri* for the new invasion attempt. However, r changed over time increasing from day 0 to 12 and decreases again from day 12 to 18.

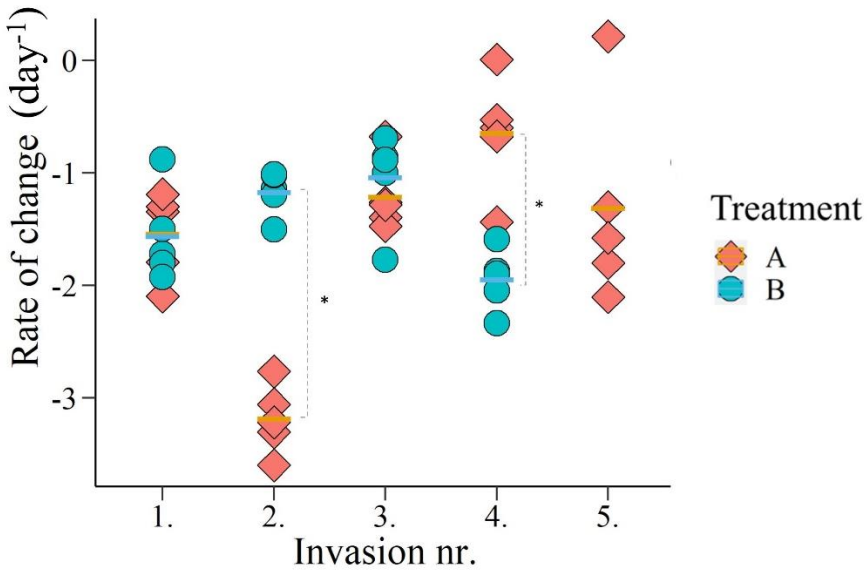

Figure 27: Relative rate of change of invader *Y. ruckeri* added to ten planktonic bacterial communities at five (A) and four (B) different days. Sorted after number of invasion attempts the community had been subjected to. Mean rate of change of invader for each group is marked with solid lines according to group color. Asterisk (*) indicate significant differences in mean rate between groups (Students t-test, $P < 0.005$).

4.4.3 The effect of pH on the specific rate of change of invader

Here I investigate whether there was a correlation between the environmental pH and the specific rate of change of the invader *Y. ruckeri* in the communities. The bacterial communities were invaded two times when the environmental pH was neutral (N) and two times when it was low (L), excluding invasion on day 3 as it was uncertain what the pH was at this time. The average rate of change of *Y. ruckeri* during low pH was, -1.02 day^{-1}, which is 36% higher than during neutral pH (Figure 31) (p = 0.0008, t-test). Average rate of change of *Y. ruckeri* seems to be affected by the pH of the environment. These differences in mean r (Figure 29 and 31) indicate that lower pH appeared to increase *Y. ruckeri*'s ability to grow in the reactors. However, this increased change was not at a faster rate than the dilution rate of the reactors.

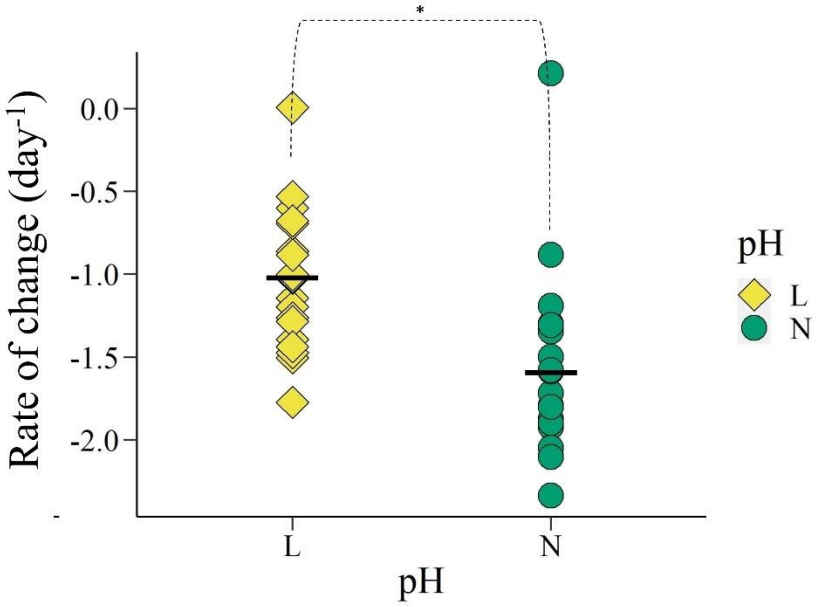

Figure 28: Relative rate of change of invader *Y. ruckeri* added to the bacterial communities two times when the environmental pH was neutral (N) and two times when it was low (L). Mean rate of change of invader for each group is marked with solid black lines. Asterisk (*) indicate significant differences in mean rate between groups (p< 0.05, t-test).

4.4.4 The effect of the bacterial density of the communities on the specific rate of change of invader

Here I investigate whether there was a correlation between the community density and the specific rate of change of the invader *Y. ruckeri* for the invasion attempt (Figure 32). There seemed to be a negative linear correlation between the specific rate of change of the invader *Y. ruckeri* and the community density indicating that communities with higher bacterial density were less invasible. However, R^2 was low indicating a low correlation between the community density and the specific rate of change of the invader *Y. ruckeri*.

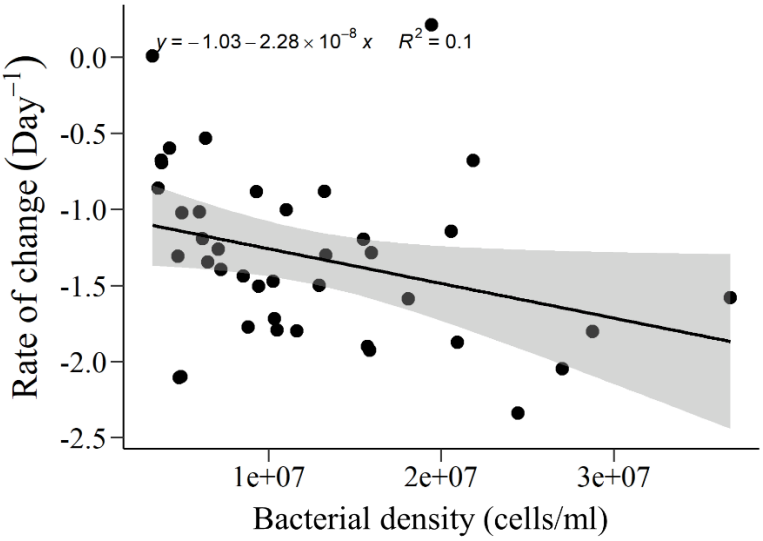

Figure 29: Relative rate of change of the invader *Y. ruckeri* versus the bacterial density of the resident communities.

4.5 Why was the invader disappearing faster than the dilution rate?

The rate of Y.*ruckeri* change was below what we considered the validity area of -1 day-1 for most of the inasion attempts. Considering the specific dilution rate of each reactor I calculated the growth rate and found it to be below 0 for the majority (68%) of the invasion attempts (Figure 33). The invader thus disappeared faster than the dilution rate in these cases. This disappearing indicated that there was a net loss of cells from the reactors due to some other factor than dilution. For the *Y. ruckeri* cells to disappear their DNA must have been released from the cells or broken down in some other way, Due to the nature of our quantification method. Therefore, I conducted several experiments to elucidate why the cells disappeared. I investigated *Y. ruckeri* growth potential at different pHs and whether bacteriophages, osmotic imbalance or lytic enzymes was responsible for the dispersal of *Y. ruckeri*.

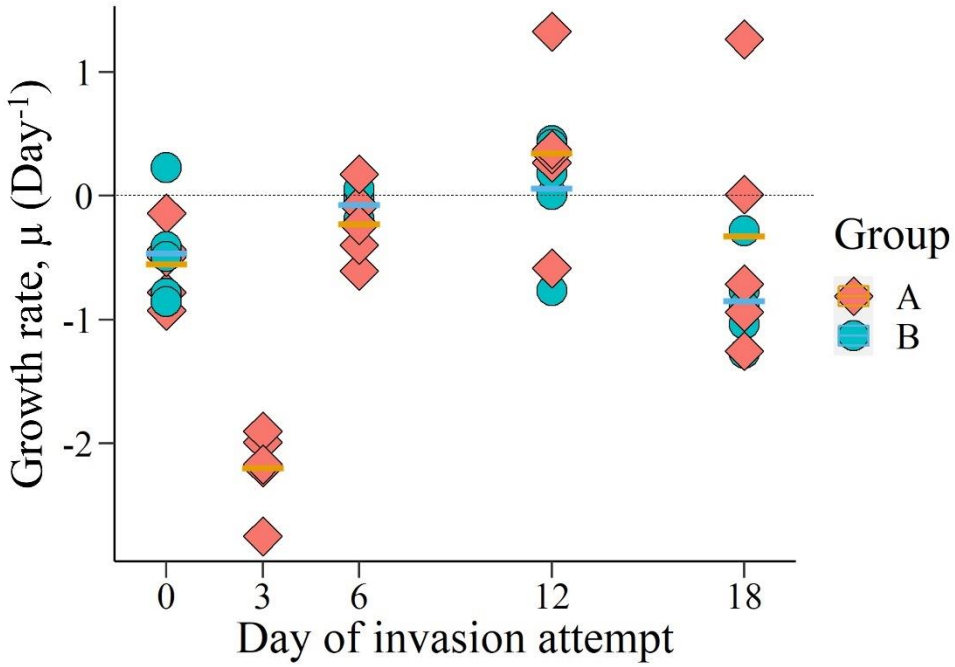

Figure 30: Growth rate (μ) of invader *Y. ruckeri* added to ten planktonic bacterial communities at five (A) and four (B) different days. The mean growth rate of invader for each group is marked with solid lines according to group color. The dotted line marks no growth.

To investigate *Y. ruckeri*s growth potential at neutral and low pH it was inolculated in batch with CD-medium-10 at pH 6.5 and pH 4.5. *Y. ruckeri* was successfully cultivated for four days as batch cultures under both conditions (Figure 34). In low pH environment *Y. ruckeri* had a two- day lag phase before exponential growth started. At neutral pH *Y. ruckeri* seemed to go straight into exponential growth, reaching the stationary phase within two to three days. The growth rate in the exponential phase of *Y. ruckeri* was lower in neutral pH than in low pH. Thus, the pH disturbance did not seem to explain the negative growth rate of *Y. ruckeri* during the main experiment.

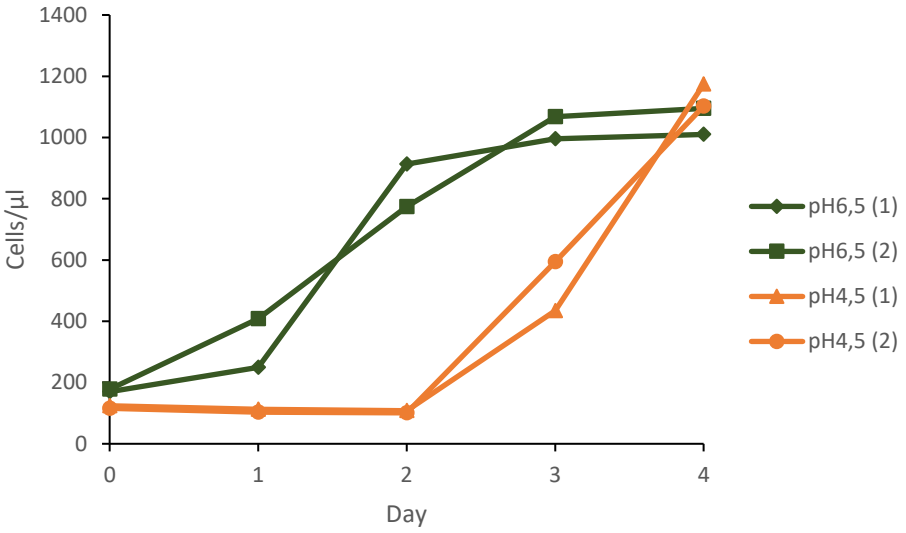

Figure 31: Growth curves for *Yersinia ruckeri* in CD-medium-10 pH 6.5 (green) and pH adjusted media to pH 4.5 (orange), measured over a four-day period. Cell concentration measured as cells per µl by flow cytometry is plotted against time (days). For each pH condition there were two biological replicas.

To determine if *Y. ruckeri* specific bacteriophages were present or if the medium contained smaller lysis-promoting substances I cultivated *Y. ruckeri* in 0.2 um filtered media. Cell density was monitored by measuring optical density (OD) at 600 nm over a three-day period. *Y. ruckeri* was successfully cultivated for three days as batch cultures in the filtrate, (Figure 35). Thus, there does not seem to be any agents <0.2 µm, such as bacteriophages, lytic enzymes or components in the medium causing osmotic imbalance, that could result in lysis of *Y. ruckeri* cells in the reactors.

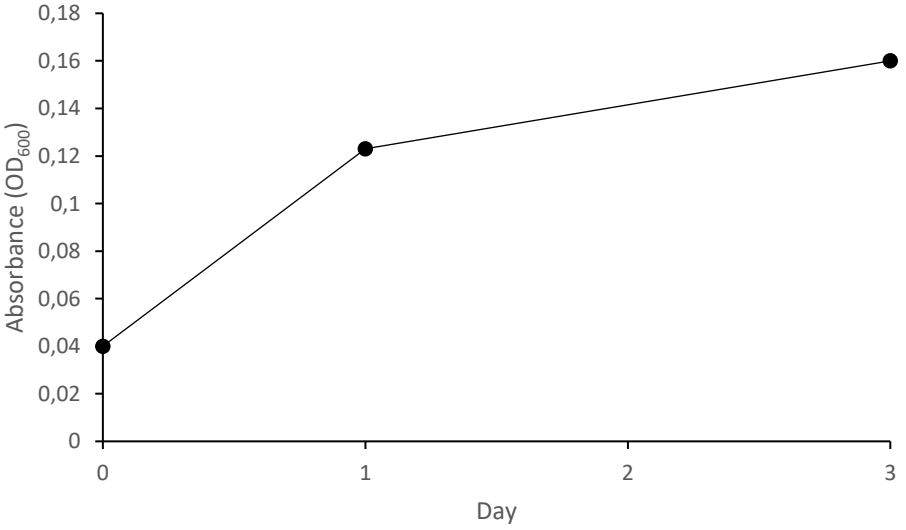

Figure 32: Growth curve for *Yersinia ruckeri* in filtrate (0.2µm) from bio-rectors, measured over a three-day period. Cell density measured as optical density (OD) at 600nm by photospectrometry.

5 Discussion

The aim of this study was to investigate the impact of multiple invasions attempts on the characteristics and invasibility of a planktonic bacterial community in a flow-through system. Here I will discuss what could have caused the net loss of cells from the reactors other than dilution. I will also discuss the research questions of what impact unsuccessful invasions would have on a planktonic bacterial community in a flow-through systems, and whether an unsuccessful invasion would increase the rate of invasion success for subsequent invasions attempts by the same invader. In addition, I will discuss the effect of propagule pressure on the competitiveness of the invader and the effect of a pH drop on the bacterial communities diversity and invasibility.

5.1 Unknown loss factor of *Y. ruckeri*

The specific rate of change (r) of *Y. ruckeri* in the bioreactors indicated whether the invasion was successful or not. $r \geq 0$ indicated that *Y. ruckeri* was maintaining an active population, meaning that the invasion was successful. In contrast, if $r < 0$ the population was decreasing and would eventually disappear completely from the community, meaning that the invasion was unsuccessful. In general, a population can increase due bacterial growth or new cells entering the community, and decrease because of cell death or cells leaving the bioreactor. In our case we can ignore new cells coming entering the community and cell death. There was no addition of *Y. ruckeri* to the system between invasion attempts, and our quantification method cannot distinguish between live and dead cells. Thus, the rate of change of *Y. ruckeri* was a product of bacterial growth and dilution. The dilution rate was approximately 1 day $^{-1}$, we would therefore expect the minimum rate of change to be -1. However, I found the specific rate of change of *Y. ruckeri* in the bioreactors to be less than -1 day^{-1} for most of the invasion attempts. Considering the specific dilution rate of each reactor, I calculated the growth rate to be less than zero for the majority (68%) of the invasion attempts. Meaning that the invader disappeared faster than the dilution rate in these cases. Disregarding methodological errors this indicates that there was a net loss of cells from the reactors due to some other factor than dilution.

Quantification of *Y. ruckeri* happened trough the quantification of a *Y. ruckeri* specific gene region of the Hom7 gene by qPCR. DNA was extracted from 0.2 µm filters used to collect bacterial cells from bioreactor samples. This implies that in order for the *Y. ruckeri* cells not to get quantified their DNA must have been released from the cells or broken down in some other way. Two likely possibilities are that *Y. ruckeri* either was subjected to lysis or was predated. Environmental or biotic factors that could induce lysis are pH changes, osmotic imbalance, bacteriophages or lytic enzymes (Madigan et al., 2015). We suspected that the drop in pH due to poor buffering capacity of the growth medium could have damage the integrity of *Y. ruckeri* cells (Renes et al., 2020). *Y. ruckeri* was, however, successfully cultivated at pH 4.5. Furthermore, after adjusting the buffering capacity negative growth rates were measured in the communities at pH 6.5 as well. The drop in pH could therefore not explain the rapid decline in *Y. ruckeri* in the reactors. Cultivation experiments with filtered media (0.2um) showed growth of Y.*ruckeri*. Thus, it was unlikely that bacteriophages, lytic enzymes or osmotic imbalance was the cause of the rapid decline in *Y. ruckeri* in the reactors. Loss of *Y. ruckeri* from the reactors did not seem to be caused by cell lysis.

Having disregarded lysis, we are left with predation as a possible loss factor for *Y. ruckeri*. Predation is one form of biotic resistance, i.e. when biotic interactions prevent an invasion, called consumptive resistance. The other forms of biotic resistance are competitive resistance and ammensalism (Alofs & Jackson, 2014). Competition would not cause a negative growth rate as it does not cause cell damage. Ammensalism could however have caused cell damage, but as mentioned above *Y. ruckeri* could grow in filtrate from the reactor. Its therefore unlikely that there was an organism secreting a component that could damage *Y. ruckeri.* Consumptive resistance is a more likely explanation. Prior to inoculation of the resident community in the bioreactors the community was filter through a 3.0 µm filter. This filtration should have removed most known predators. The smallest of these are heterotrophic flagellates. Moste heterotrophic flagellates would be removed by a 3.0 µm filter, however some are able to pass true (Arndt et al., 2000). In addition, in a mixed bacteria and flagellate community the bacterial density would typically either or bee oscillating or suppressed below about 2×10^5 ml^{-1} (Pengerud et al., 1987).The bacterial communities had a non-oscillating density, and only three (less than 1.5%) of the samples from the bioreactors had a bacterial density lower than 1×10^6 ml^{-1}. I do therefore not believe that there were predators of bacteria present in the communities.

Methodical errors cannot be completely disregarded. However, I do not believe that it was the cause of the negative growth rates. Firstly, when calculating propagule pressure of *Y. ruckeri* on the first day of the invasion attempts we get the same expected values whether the calculation was based on quantification by qPCR after invasion or density measures of pure culture *Y. ruckeri* by flow cytometry prior to invasion. In addition, sequence data did also confirm that *Y. ruckeri* was present at the expected relative abundance on the first day of each invasion attempt (Figure S2). Indicating that our quantification method does not result in underestimation of *Y. ruckeri*. Regardless, had all the quantification been consistently wrong that would not have resulted in a lowered calculated growth rate. For the relative rate of change, and in turn growth rate, of *Y. ruckeri* to be underestimated the error in quantification would have to get progressively worse for each day following an invasion attempt. Since the growth rate was calculated to less than zero for several separate invasion attempts the error would not have been time dependent. Rather, the possible quantification error would have hade to have been dependent on the concentration of *Y. ruckeri* in the sample. Such that the lower abundance of *Y. ruckeri* in the sample the bigger the error, resulting in an even lower estimated quantification. This is theoretically possible if the quantity in the later samples were lower than the limit of quantification. This is however inconsistent with the quality controls carried out for the qPCR protocol, which show that the quantity in low concentration samples are rather overestimated. In conclusion, there was no apparent methodical error that would have caused the relative rate of change of *Y. ruckeri* to have been underestimated.

In summary, the growth rate of *Y. ruckeri* in the reactors were calculated to be less than zero for the majority of the invasion attempts. This was an unrealistic value as taking all known loss factors in to account the minimum possible growth rate should be zero. I disregarded methodological errors, cell lysis and predation as possible factors. The cause of net negative growth of *Y. ruckeri* is still unknown. Regardless of the rate of which *Y. ruckeri* disappeared from the communities we know that *Y. ruckeri* entered the communities and could not establish, making these unsuccessful invasions. The effect of unsuccessful invasions on the resident community can still be commented on.

5.2 The failed invasions did not affect the diversity and composition of the communities

The intruder *Y. ruckeri* was overall unable to establish in any of the invasion attempts, meaning that the invasion attempts were unsuccessful. Contrary to our hypotheses the unsuccessful invasion attempts did not impact the bacterial composition or diversity of the resident communities. Based on the findings of (Mallon et al., 2018b) I hypothesized that the diversity of the resident community would increase because of an unsuccessful invasion. Mallon et al. observed in 2018 an increase in the diversity and changes in community composition of unsuccessfully invaded soil communities. Lasting effects of unsuccessful invasions on resident communities have also been found in phytoplankton communities (Weithoff et al., 2017), and have also been shown to result in maintained diversity as in contrast to fall in diversity in control communities (Buchberger & Stockenreiter, 2018). However, in our case the bacterial composition, zOTU richness, exp. Shannon diversity and evenness was highly similar between communeties regardless of invasion attempts.

The studies observing lasting effects of unsuccessful invasions all attributed the changes in in community composition to the transient interaction of the invader with the resident community during the invasion process. Mallon et al. suggest that the change in community composition was a product of resource competition between the invader and residents. This implies that the invader in their experiment was active and grew in the soil, even though it was not detected (Mallon et al., 2018b). In our experiment the invader did not merely fail to establish, it disappeared faster than I cud explain. We observed growth rates less than zero for the majority (68%) of the invasion attempts. Given the extreme rate at which *Y. ruckeri* disappeared from our system, it was highly unlikely that our invader was active and competed for resources. In addition, it is important to note that our experiment was conducted under different conditions than Mallon et all's. In our experiment the effect of a transient invader could be lessened by the nature of the environment. In a flow through system an invader will have less time for adaptation as it will be forced to grow at the dilution rate to avoid washout. This further minimized the possible interaction of the invader with the residents. Thus, we cannot rule out the possibility of failed invasions effecting resident communities in flow through systems, given a more competitive invader. To conclude, our results suggest that there was no effect of failed invasions on the diversity and composition of a bacterial community in flow through system. However, based on the extreme rate at which *Y. ruckeri* disappeared from our system and the findings of other studies I sugest that the effect of failed invasions are likely depends on the ability of the invader to interact with the resident community.

5.3 Failed invasion attempts did not increase the competitiveness of the invader for subsequent invasion attempts

The intruder was overall unable to establish in any of the invasion attempts. Only two invasion attempts were categorized as successful, where only one of these were reliable (reactor 5B invasion attempt five). With only one successful invasion there was no measurable change in rate of invasion success. I could not find a correlation between the number of unsuccessful invasions the bacterial communities had been subjected to previously and the specific rate of change of *Y. ruckeri* for the new invasion attempt either. In conclusion, failed invasion attempts did not increase the rate of invasion success or competitiveness of the invader for subsequent invasion attempts in the flow-through systems.

The idea that failed invasions might increase the probability of establishment in subsequent invasion attempts was first addressed by Mallon et al. (Mallon et al., 2018b). They stated that "a second invasion by the same invader can last longer or even result in a unsuccessful invasion" - (Mallon et al., 2018b). This hypothesis was based on the findings of their experiment where unsuccessful invasion created a legacy effect in the form of the resident community shifting its niche structure away from the invader's resources. The proposed model of invasion impacts raised the question of whether this legacy effect would increase the rate of invasion success for subsequent invasion attempts because the nice of the invader would be freed up making for less competition at a secondary invasion attempt.

Our hypothesis was however in accordance with our findings. I thought that the rate of invasion success during subsequent invasions would not increase in a flow-through systems. Mallon et al 2018 experiment was performed with soil microbial community without the influx of new resources. We however preformed our experiment in a flow through system where the resources were continuously supplied. I therefore did not anticipate the possible effect of unsuccessful invasions on the niche structure of resident community to have a lasting impact. Whether the reason for the failed invasion attempts did not increase the rate of invasion success or competitiveness of the invader was due to the invasion effects being transient or not occurring at all was impossible to resolve as we do not have data on the concentrations of available nutrients over the course of the experiment. However, since there was no observed change in community compositions after invasion it is unlikely that a shift in niche structure occurred. To conclude, our results suggest that failed invasion attempts did not increase the rate of invasion success or competitiveness of the invader for subsequent invasion. This was likely due to the prior invasion attempt not effecting the resident communities in the flow through system.

5.4 Propagule pressure did not increase the competitiveness of the invader

Propagule pressure of the invader have been investigated as a determinant of invasion success in many studies (Acosta et al., 2015; Jones et al., 2017). I therefore invaded the bacterial communities at two different propagule pressures, 1% and 10%, to assess whether the strength of the competition in form of the rate of change of the invader in the community would be influenced by cell densities. There was however no significant difference in the mean specific rate of change of invader due to a tenfold difference in propagule pressure. Propagule pressure did not increase the competitiveness of the invader under the conditions of the experiment.

5.5 pH drop lowered bacterial community diversity and increased invasibility

Starting somewhere around day 3 to 5 a temporal change in the community's composition and decrease in exp. Shannon and evenness and zOTU richness occurred across all treatment groups. These results indicate a deterministic change in community the communities, likely due to a disturbance. This period coincides with an accidental pH-disturbance. The change was transient, and all communities returned to equivalent richness, diversity and composition on day 16 after the pH was raised. This suggested that the low pH was the disturbance causing the changes in the communities and that bacterial communities were resilient towards disturbances.

That the zOTU richness, exp. Shannon diversity and evenness decrease in response to the lowered pH. Bacterial community diversity is believed to be strongly influenced by disturbances, such as changes in pH. Disturbances can generally lead to decreases in diversity, and acidification events specifically has been showed to do so (Sjöstedt et al., 2018). Acidification has been shown to decreases bacterial community diversity in seawater (Crummett, 2020) and soil bacterial communities (Wu et al., 2017; Yun et al., 2016). Diversity in bacterioplankton communities in freshwater lakes have also shown positive correlation with pH (Percent Sascha et al., 2008). The changes in the communities in response to the lowered pH was consistent with observations from other studies.

In addition to changes in diversity and community composition, pH seemed to be strongly correlated with the competitiveness of the invader. When the pH the community was low it appeared to increase *Y. ruckeri*'s ability to grow in the reactors. r increasing from day 0 to 12 when the pH fell and decreases again from day 12 to 18 when th pH was raised. This could both be due to the simultaneous reduction in resident community diversity and the growth potential of the invader. In addition to the reduction in diversity the invader *Y. ruckeri* did exhibit a higher growth rate in low pH medium after adaptation. Invasion resistance has been shown to be weaker in bacterial communities with lowered diversity. This is assumed to be due to the fact that communities with lower diversity more likely to have unoccupied niches that can be occupied by invaders (Acosta et al., 2015; Litchman, 2010; Stecher et al., 2010; van Elsas et al., 2012). The increase in *Y. ruckeri*s competitiveness was probably due to a combination of factors initiated by the drop in pH. However, even at low pH with reduced diversity the communities still resisted invasion by *Y. ruckeri*, and one should be careful to read too much into the rate of change of the invader as I still don't know what caused the net negative growth of *Y. ruckeri*.

In conclusion, the pH drop that started somewhere around day 3 to 5 disturbed the communities causing changes in community composition and decrease in the zOTU richness, exp. Shannon diversity and evenness of the communities. It also appeared like the low pH increased *Y. ruckeri*'s ability to grow in the reactors. The bacterial communities were resilient towards the disturbances returning to equivalent zOTU richness, exp. Shannon diversity and evenness after the disturbance had ended.

5.6 Further work

We aimed to answer the following questions: "What is the impact of unsuccessful invasions on a planktonic bacterial community in a flow-through systems?" and "Does an unsuccessful invasion increase the rate of invasion success for subsequent invasions attempts by the same invader?".

From our results we concluded that unsuccessful invasion attempts did not impact the resident community or change the rate of invasion success for subsequent invasion attempts. However, the invader *Y. ruckeri* had a negative growth rate with unexplained loss factor. I suggest, based on the results and other studies, that the impact on the communities, or absence thereof, may be related to how competitive the invader was. In further research, the questions posted in this study should be re-examined with a more competitive intruder. As the change in utilization of different niches in Mallon et all. study in 2018 lay much of the foundation for why these questions were posed in the first place, further research should also look at the impact of invasion attempts on the functionality of bacterial communities.

Should it be shown that unsuccessful invasions can have an impact on a planktonic bacterial community in a flow-through system, an investigation of the connection between the rate of change of the invader and the impact on the community may also be of interest. I would pose the question: Is the impact of unsuccessful invasion enhanced by the time the invader spends in the community or the growth rate of the invader?

Conclusion

This study set out to investigate the impact of repeated bacterial invasion attempts by the same single model invader on a planktonic bacterial community in a flow-through system. To address this, the invader's establishment in the communities was monitored through quantification by qPCR and the bacterial community characteristics were examined using Illumina sequencing and flow cytometry.

Y. ruckeri was not able to invade the communities, and the unsuccessful invasions did not affect the bacterial composition or diversity of the resident communities. The growth rate of *Y. ruckeri* in the reactors were calculated to be less than zero for the majority of the invasion attempts. This was an unrealistic value, as taking all known loss factors in to account the minimum possible growth rate should be zero. I disregarded methodological errors, cell lysis and predation as possible factors. The cause of net negative growth of *Y. ruckeri* is still unknown. Based on the extreme rate at which *Y. ruckeri* disappeared from our system and the findings of other studies I suggest that the effect of failed invasions likely depends on the ability of the invader to interact with the resident community.

The unsuccessful invasion attempts did not change the rate of invasion success or competitiveness of the invader for subsequent invasion attempts. This was likely due to the prior invasion attempt not effecting the resident communities in the flow through system, and thus not freeing up niche space for the invader at the subsequent invasion attempt. A tenfold difference in propagule pressure did not increase the competitiveness of the invader either.

However, a pH drop that started somewhere around day 3 to 5 disturbed the communities, causing changes in community composition and decrease in the zOTU richness, exp. Shannon diversity and evenness of the communities. The changes in the communities in response to the lowered pH was consistent with observations from other studies. The bacterial communities were resilient towards the disturbances, returning to equivalent zOTU richness, exp. Shannon diversity and evenness after the disturbance had ended. It also appeared like the low pH increased *Y. ruckeri*'s ability to grow in the reactors.

References

Acosta, F., Zamor, R. M., Najar, F. Z., Roe, B. A., & Hambright, K. D. (2015). Dynamics of an experimental microbial invasion. *Proceedings of the National Academy of Sciences of the United States of America*, *112*(37), 11594-11599. https://doi.org/10.1073/pnas.1505204112

Adan, A., Alizada, G., Kiraz, Y., Baran, Y., & Nalbant, A. (2017). Flow cytometry: basic principles and applications. *Critical Reviews in Biotechnology*, *37*(2), 163-176. https://doi.org/10.3109/07388551.2015.1128876

Albright, M. B. N., Louca, S., Winkler, D. E., Feeser, K. L., Haig, S.-J., Whiteson, K. L., Emerson, J. B., & Dunbar, J. (2021). Solutions in microbiome engineering: prioritizing barriers to organism establishment. *The ISME Journal*. https://doi.org/10.1038/s41396-021-01088-5

Alofs, K. M., & Jackson, D. A. (2014). Meta-analysis suggests biotic resistance in freshwater environments is driven by consumption rather than competition [https://doi.org/10.1890/14-0060.1]. *Ecology*, *95*(12), 3259-3270. https://doi.org/https://doi.org/10.1890/14-0060.1

Ames, N. J., Ranucci, A., Moriyama, B., & Wallen, G. R. (2017). The Human Microbiome and Understanding the 16S rRNA Gene in Translational Nursing Science. *Nursing research*, *66*(2), 184-197. https://doi.org/10.1097/NNR.0000000000000212

Arndt, H., Dietrich, D., Auer, B., Cleven, E.-J., Grafenhan, T., Weitere, M., & Mylnikov, A. P. (2000). Functional diversity of heterotrophic flagellates in aquatic ecosystems. *Systematics association Special volume*, *59*, 240-268.

Barb, J. J., Oler, A. J., Kim, H.-S., Chalmers, N., Wallen, G. R., Cashion, A., Munson, P. J., & Ames, N. J. (2016). Development of an Analysis Pipeline Characterizing Multiple Hypervariable Regions of 16S rRNA Using Mock Samples. *PLoS One*, *11*(2), e0148047-e0148047. https://doi.org/10.1371/journal.pone.0148047

BD Accuri™ C6 Plus System User's Guide. (2016). BD Biosciences. https://static.bdbiosciences.com/documents/BD-Accuri-C6-Plus-Users-Guide.pdf

Blackburn, T. M., Pyšek, P., Bacher, S., Carlton, J. T., Duncan, R. P., Jarošík, V., Wilson, J. R. U., & Richardson, D. M. (2011). A proposed unified framework for biological invasions. *Trends in Ecology & Evolution*, *26*(7), 333-339. https://doi.org/https://doi.org/10.1016/j.tree.2011.03.023

Bonnevier, J., Hammerbeck, C., & Goetz, C. (2018). Flow Cytometry: Definition, History, and Uses in Biological Research. In C. Goetz, C. Hammerbeck, & J. Bonnevier (Eds.), *Flow Cytometry Basics for the Non-Expert* (pp. 1-11). Springer International Publishing. https://doi.org/10.1007/978-3-319-98071-3_1

Brankatschk, R., Bodenhausen, N., Zeyer, J., & Bürgmann, H. (2012). Simple absolute quantification method correcting for quantitative PCR efficiency variations for microbial community samples. *Applied and environmental microbiology*, *78*(12), 4481-4489. https://doi.org/10.1128/AEM.07878-11

Buchberger, F., & Stockenreiter, M. (2018). Unsuccessful invaders structure a natural freshwater phytoplankton community [https://doi.org/10.1002/ecs2.2158]. *Ecosphere*, *9*(3), e02158. https://doi.org/https://doi.org/10.1002/ecs2.2158

Callahan, B. J., Sankaran, K., Fukuyama, J. A., McMurdie, a. J., & Holmes, S. P. (2017). Workflow for Microbiome Data Analysis: from raw reads to community analyses. http://web.stanford.edu/class/bios221/MicrobiomeWorkflowII.html#abstract

Crummett, L. T. (2020). Acidification decreases microbial community diversity in the Salish Sea, a region with naturally high pCO2. *PloS one*, *15*(10), e0241183-e0241183. https://doi.org/10.1371/journal.pone.0241183

Curtis, T. P., & Sloan, W. T. (2005). Microbiology. Exploring microbial diversity--a vast below. *Science*, *309*(5739), 1331-1333. https://doi.org/10.1126/science.1118176

Davey, H. M., & Kell, D. B. (1996). Flow cytometry and cell sorting of heterogeneous microbial populations: the importance of single-cell analyses. *Microbiol Rev*, *60*(4), 641-696. https://doi.org/10.1128/mr.60.4.641-696.1996

Di Bella, J. M., Bao, Y., Gloor, G. B., Burton, J. P., & Reid, G. (2013). High throughput sequencing methods and analysis for microbiome research. *Journal of Microbiological Methods*, *95*(3), 401-414. https://doi.org/https://doi.org/10.1016/j.mimet.2013.08.011

diCenzo George, C., & Finan Turlough, M. The Divided Bacterial Genome: Structure, Function, and Evolution. *Microbiology and Molecular Biology Reviews*, *81*(3), e00019-00017. https://doi.org/10.1128/MMBR.00019-17

Drågen, M. K. R. (2020). *Immersion Challenge of Atlantic Salmon (Salmo salar) yolk sac fry with Yersinia ruckeri* Norwegian University of Science and Technology].

Eisenhauer, N., Schulz, W., Scheu, S., & Jousset, A. (2013). Niche dimensionality links biodiversity and invasibility of microbial communities. *Functional Ecology*, *27*(1), 282-288. https://doi.org/10.1111/j.1365-2435.2012.02060.x

Gao, C. H., Zhang, M., Wu, Y., Huang, Q., & Cai, P. (2019). Divergent Influence to a Pathogen Invader by Resident Bacteria with Different Social Interactions. *Microb Ecol*, *77*(1), 76-86. https://doi.org/10.1007/s00248-018-1207-z

Goodwin, S., McPherson, J. D., & McCombie, W. R. (2016). Coming of age: ten years of next-generation sequencing technologies. *Nature Reviews Genetics*, *17*(6), 333-351. https://doi.org/10.1038/nrg.2016.49

Heid, C. A., Stevens, J., Livak, K. J., & Williams, P. M. (1996). Real time quantitative PCR. *Genome Res*, *6*(10), 986-994. https://doi.org/10.1101/gr.6.10.986

Hu, T., Chitnis, N., Monos, D., & Dinh, A. (2021). Next-generation sequencing technologies: An overview. *Human Immunology*, *82*(11), 801-811. https://doi.org/https://doi.org/10.1016/j.humimm.2021.02.012

Illumina Sequencing Technology. (2010). Illumina. https://www.illumina.com/documents/products/techspotlights/techspotlight_sequencing.pdf

Jachimowicz, L. (2017). *Enhancing Bacterial Research Using Flow Cytometry*. Retrieved 2022, March 16. from https://www.biocompare.com/Bench-Tips/339240-Enhancing-Bacterial-Research-Using-Flow-Cytometry/

Janda, J. M., & Abbott, S. L. (2007). 16S rRNA gene sequencing for bacterial identification in the diagnostic laboratory: pluses, perils, and pitfalls. *Journal of clinical microbiology*, *45*(9), 2761-2764. https://doi.org/10.1128/JCM.01228-07

Jones, M. L., Ramoneda, J., Rivett, D. W., & Bell, T. (2017). Biotic resistance shapes the influence of propagule pressure on invasion success in bacterial communities. *Ecology*, *98*(7), 1743-1749. https://doi.org/10.1002/ecy.1852

Kinnunen, M., Dechesne, A., Proctor, C., Hammes, F., Johnson, D., Quintela-Baluja, M., Graham, D., Daffonchio, D., Fodelianakis, S., Hahn, N., Boon, N., & Smets, B. F. (2016). A conceptual framework for invasion in microbial communities. *The ISME Journal*, *10*(12), 2773-2779. https://doi.org/10.1038/ismej.2016.75

Konopka, A. (2009). What is microbial community ecology? *Isme j*, *3*(11), 1223-1230. https://doi.org/10.1038/ismej.2009.88

Krebs, C. J. (1985). A General Theory [The Ecological Web, H. G. Andrewartha, L. C. Birch]. *Science*, *228*(4701), 873-874. http://www.jstor.org/stable/1694693

Kumar, G., Menanteau-Ledouble, S., Saleh, M., & El-Matbouli, M. (2015). Yersinia ruckeri, the causative agent of enteric redmouth disease in fish. *Veterinary Research*, *46*(1), 103. https://doi.org/10.1186/s13567-015-0238-4

Li, S.-p., Tan, J., Yang, X., Ma, C., & Jiang, L. (2019). Niche and fitness differences determine invasion success and impact in laboratory bacterial communities. *The ISME Journal*, *13*(2), 402-412. https://doi.org/10.1038/s41396-018-0283-x

Litchman, E. (2010). Invisible invaders: non-pathogenic invasive microbes in aquatic and terrestrial ecosystems. *Ecology Letters*, *13*(12), 1560-1572. https://doi.org/https://doi.org/10.1111/j.1461-0248.2010.01544.x

Lourenco, K. S., Suleiman, A. K. A., Pijl, A., van Veen, J. A., Cantarella, H., & Kuramae, E. E. (2018). Resilience of the resident soil microbiome to organic and inorganic amendment disturbances and to temporary bacterial invasion. *Microbiome*, *6*(1), 142. https://doi.org/10.1186/s40168-018-0525-1

Ma, C., Liu, M., Wang, H., Chen, C., Fan, W., Griffiths, B., & Li, H. (2015). Resource utilization capability of bacteria predicts their invasion potential in soil. *Soil Biology and Biochemistry*, *81*, 287-290. https://doi.org/https://doi.org/10.1016/j.soilbio.2014.11.025

Macey, M. G. (2007). Principles of Flow Cytometry. In M. G. Macey (Ed.), *Flow Cytometry: Principles and Applications* (pp. 1-15). Humana Press. https://doi.org/10.1007/978-1-59745-451-3_1

Madigan, M. T., Martinko, J. M., Bender, K. S., Buckley, D. H., Stahl, D. A., & Brock, T. D. (2015). *Brock biology of microorganisms* (Global edition, fourteenth edition. ed.). Pearson.

Mallon, C. A., Elsas, J. D. v., & Salles, J. F. (2015). Microbial Invasions: The Process, Patterns, and Mechanisms. *Trends in Microbiology*, *23*(11), 719-729. https://doi.org/https://doi.org/10.1016/j.tim.2015.07.013

Mallon, C. A., Le Roux, X., van Doorn, G. S., Dini-Andreote, F., Poly, F., & Salles, J. F. (2018a). The impact of failure: unsuccessful bacterial invasions steer the soil microbial community away from the invader's niche. *Isme j*, *12*(3), 728-741. https://doi.org/10.1038/s41396-017-0003-y

Mallon, C. A., Le Roux, X., van Doorn, G. S., Dini-Andreote, F., Poly, F., & Salles, J. F. (2018b). The impact of failure: unsuccessful bacterial invasions steer the soil microbial community away from the invader's niche. *The ISME Journal*, *12*(3), 728-741. https://doi.org/10.1038/s41396-017-0003-y

Martiny, J. B. H., Bohannan, B. J. M., Brown, J. H., Colwell, R. K., Fuhrman, J. A., Green, J. L., Horner-Devine, M. C., Kane, M., Krumins, J. A., Kuske, C. R., Morin, P. J., Naeem, S., Øvreås, L., Reysenbach, A.-L., Smith, V. H., & Staley, J. T. (2006). Microbial biogeography: putting microorganisms on the map. *Nature Reviews Microbiology*, *4*(2), 102-112. https://doi.org/10.1038/nrmicro1341

Nemergut, D. R., Schmidt, S. K., Fukami, T., O'Neill, S. P., Bilinski, T. M., Stanish, L. F., Knelman, J. E., Darcy, J. L., Lynch, R. C., Wickey, P., & Ferrenberg, S. (2013). Patterns and Processes of Microbial Community Assembly. *Microbiology and Molecular Biology Reviews*, *77*(3), 342-356. https://doi.org/doi:10.1128/MMBR.00051-12

Pabinger, S., Rödiger, S., Kriegner, A., Vierlinger, K., & Weinhäusel, A. (2014). A survey of tools for the analysis of quantitative PCR (qPCR) data. *Biomolecular Detection and Quantification*, *1*(1), 23-33. https://doi.org/https://doi.org/10.1016/j.bdq.2014.08.002

Pearson, D. E., Ortega, Y. K., Eren, Ö., & Hierro, J. L. (2018). Community Assembly Theory as a Framework for Biological Invasions. *Trends in Ecology & Evolution*, *33*(5), 313-325. https://doi.org/https://doi.org/10.1016/j.tree.2018.03.002

Pengerud, B., Skjoldal, E. F., & Thingstad, T. F. (1987). The reciprocal interaction between degradation of glucose and ecosystem structure—studies in mixed chemostat cultures of marine-bacteria, algae, and bacterivorous nanoflagellates. *Mar. Ecol. Prog. Ser*, *35*, 111-117.

Percent Sascha, F., Frischer Marc, E., Vescio Paul, A., Duffy Ellen, B., Milano, V., McLellan, M., Stevens Brett, M., Boylen Charles, W., & Nierzwicki-Bauer Sandra, A. (2008). Bacterial Community Structure of Acid-Impacted Lakes: What Controls Diversity? *Applied and environmental microbiology*, *74*(6), 1856-1868. https://doi.org/10.1128/AEM.01719-07

Poretsky, R., Rodriguez, R. L., Luo, C., Tsementzi, D., & Konstantinidis, K. T. (2014). Strengths and limitations of 16S rRNA gene amplicon sequencing in revealing temporal microbial community dynamics. *PLoS One*, *9*(4), e93827. https://doi.org/10.1371/journal.pone.0093827

Props, R., Monsieurs, P., Mysara, M., Clement, L., & Boon, N. (2016). Measuring the biodiversity of microbial communities by flow cytometry. *Methods in Ecology and Evolution*, *7*(11), 1376-1385. https://doi.org/https://doi.org/10.1111/2041-210X.12607

Prosser, J. I., Bohannan, B. J. M., Curtis, T. P., Ellis, R. J., Firestone, M. K., Freckleton, R. P., Green, J. L., Green, L. E., Killham, K., Lennon, J. J., Osborn, A. M., Solan, M., van der Gast, C. J., & Young, J. P. W. (2007). The role of ecological theory in microbial ecology. *Nature Reviews Microbiology*, *5*(5), 384-392. https://doi.org/10.1038/nrmicro1643

Qin, Z., Baker, A. T., Raab, A., Huang, S., Wang, T., Yu, Y., Jaspars, M., Secombes, C. J., & Deng, H. (2013). The Fish Pathogen Yersinia ruckeri Produces Holomycin and Uses an RNA Methyltransferase for Self-resistance. *Journal of Biological Chemistry*, *288*(21), 14688-14697. https://doi.org/https://doi.org/10.1074/jbc.M112.448415

Qin, Z., Huang, S., Yu, Y., & Deng, H. (2013). Dithiolopyrrolone natural products: isolation, synthesis and biosynthesis. *Marine drugs*, *11*(10), 3970-3997. https://doi.org/10.3390/md11103970

Quantification of Bacteria by Flow Cytometry. University of Konstanz. https://www.biologie.uni-konstanz.de/typo3temp/secure_downloads/85186/0/d56e6f8532395ac8607e0e7a322ee9557ef9ecdd/Quantification_of_bacteria_by_flow_cytometry_neu.pdf

Rausch, P., Rühlemann, M., Hermes, B. M., Doms, S., Dagan, T., Dierking, K., Domin, H., Fraune, S., von Frieling, J., Hentschel, U., Heinsen, F.-A., Höppner, M., Jahn, M. T., Jaspers, C., Kissoyan, K. A. B., Langfeldt, D., Rehman, A., Reusch, T. B. H., Roeder, T., . . . Baines, J. F. (2019). Comparative analysis of amplicon and metagenomic sequencing methods reveals key features in the evolution of animal metaorganisms. *Microbiome*, *7*(1), 133. https://doi.org/10.1186/s40168-019-0743-1

Renes, S. E., Sjöstedt, J., Fetzer, I., & Langenheder, S. (2020). Disturbance history can increase functional stability in the face of both repeated disturbances of the same type and novel disturbances. *Scientific Reports*, *10*(1), 11333. https://doi.org/10.1038/s41598-020-68104-0

Rosselli, R., Romoli, O., Vitulo, N., Vezzi, A., Campanaro, S., de Pascale, F., Schiavon, R., Tiarca, M., Poletto, F., Concheri, G., Valle, G., & Squartini, A. (2016). Direct 16S rRNA-seq from bacterial communities: a PCR-independent approach to simultaneously assess microbial diversity and functional activity potential of each taxon [Article]. *Scientific Reports*, *6*, 32165. https://doi.org/10.1038/srep32165

https://www.nature.com/articles/srep32165#supplementary-information

Schwarz, A., & Jax, K. (2011). Etymology and Original Sources of the Term "Ecology". In A. Schwarz & K. Jax (Eds.), *Ecology Revisited: Reflecting on Concepts, Advancing Science* (pp. 145-147). Springer Netherlands. https://doi.org/10.1007/978-90-481-9744-6_9

Shapiro, H. M. (2003). *Practical flow cytometry* (4th ed. ed.). Wiley-Liss.
Sjöstedt, J., Langenheder, S., Kritzberg, E., Karlsson, C. M. G., & Lindström, E. S. (2018). Repeated disturbances affect functional but not compositional resistance and resilience in an aquatic bacterioplankton community [https://doi.org/10.1111/1758-2229.12656]. *Environmental Microbiology Reports*, *10*(4), 493-500. https://doi.org/https://doi.org/10.1111/1758-2229.12656
Slatko, B. E., Gardner, A. F., & Ausubel, F. M. (2018). Overview of Next-Generation Sequencing Technologies. *Current protocols in molecular biology*, *122*(1), e59-e59. https://doi.org/10.1002/cpmb.59
Smith, C. J., & Osborn, A. M. (2009). Advantages and limitations of quantitative PCR (Q-PCR)-based approaches in microbial ecology. *FEMS Microbiology Ecology*, *67*(1), 6-20. https://doi.org/10.1111/j.1574-6941.2008.00629.x
Stecher, B., Chaffron, S., Käppeli, R., Hapfelmeier, S., Freedrich, S., Weber, T. C., Kirundi, J., Suar, M., McCoy, K. D., von Mering, C., Macpherson, A. J., & Hardt, W.-D. (2010). Like Will to Like: Abundances of Closely Related Species Can Predict Susceptibility to Intestinal Colonization by Pathogenic and Commensal Bacteria. *PLOS Pathogens*, *6*(1), e1000711. https://doi.org/10.1371/journal.ppat.1000711
SYBR® Green II RNA Gel Stain. (2001). Molecular Probes. https://assets.thermofisher.com/TFS-Assets/LSG/manuals/mp07568.pdf
van Elsas, J. D., Chiurazzi, M., Mallon, C. A., Elhottova, D., Kristufek, V., & Salles, J. F. (2012). Microbial diversity determines the invasion of soil by a bacterial pathogen. *Proceedings of the National Academy of Sciences of the United States of America*, *109*(4), 1159-1164. https://doi.org/10.1073/pnas.1109326109
Vellend, M. (2010). Conceptual synthesis in community ecology. *Q Rev Biol*, *85*(2), 183-206.
Verstraete, W., Wittebolle, L., Heylen, K., Vanparys, B., de Vos, P., van de Wiele, T., & Boon, N. (2007). Microbial Resource Management: The Road To Go for Environmental Biotechnology. *Engineering in Life Sciences*, *7*(2), 117-126. https://doi.org/https://doi.org/10.1002/elsc.200620176
Vila, J. C. C., Jones, M. L., Patel, M., Bell, T., & Rosindell, J. (2019). Uncovering the rules of microbial community invasions. *Nat Ecol Evol*, *3*(8), 1162-1171. https://doi.org/10.1038/s41559-019-0952-9
Vitousek, P. M., apos, Antonio, C. M., Loope, L. L., & Westbrooks, R. (1996). Biological invasions as global environmental change [Article]. *American Scientist*, *84*, 468+. https://link.gale.com/apps/doc/A18667286/AONE?u=anon~c357cf8b&sid=googleScholar&xid=e4cd91e8
Weithoff, G., Taube, A., & Bolius, S. (2017). The invasion success of the cyanobacterium Cylindrospermopsis raciborskii in experimental mesocosms. *Aquatic Invasions*, *12*, 333-341. https://publishup.uni-potsdam.de/frontdoor/index/index/docId/53550
Wrobel, A., Ottoni, C., Leo, J. C., Gulla, S., & Linke, D. (2018). The repeat structure of two paralogous genes, Yersinia ruckeri invasin (yrInv) and a "Y. ruckeri invasin-like molecule", (yrIlm) sheds light on the evolution of adhesive capacities of a fish pathogen. *Journal of Structural Biology*, *201*(2), 171-183. https://doi.org/https://doi.org/10.1016/j.jsb.2017.08.008
Wu, Y., Zeng, J., Zhu, Q., Zhang, Z., & Lin, X. (2017). pH is the primary determinant of the bacterial community structure in agricultural soils impacted by polycyclic aromatic hydrocarbon pollution. *Scientific Reports*, *7*(1), 40093. https://doi.org/10.1038/srep40093
Yun, Y., Wang, H., Man, B., Xiang, X., Zhou, J., Qiu, X., Duan, Y., & Engel, A. S. (2016). The Relationship between pH and Bacterial Communities in a Single Karst Ecosystem and Its Implication for Soil Acidification. *Frontiers in Microbiology*, *7*, 1955-1955. https://doi.org/10.3389/fmicb.2016.01955

List of appendices

APPENDIX A: Carbon Defined Medium

This medium contains 28 C-sources each adjusted to be of equally molarity with regards to their C-atoms (1,12 µM carbon per component). These C-sources are meant to select for different bacterial populations.

To make 1 L of the medium

1. Mix the following components from stock solutions

Stock	Stock concentrated	Volume	Concentration (mol/L) in medium
Carbon sources (nr 1-3, 5-9, 11-13, 15, 17-19)	100 000	10 µL x 15	31.4 µM C-atoms (total)
Carbon sources (nr 21-31)	200 000	5 µL x 11	
Carbon sources (nr.10 and 14)	22 573	40 µL x 2	
Ammonium chloride (N-source)	1000	1 mL	170 µM N-atoms
Phosphate source (+ buffer)	10 000	100 µL	0.2 mM P-atoms
Sodium chloride	100	10 mL	13 mM
Magnesium sulphate	100	10 mL	0,8 mM
Potassium + Calcium	500	2 mL	1.6 mM
Trace elements	1000	1 mL	39 µM
Iron	1000	1 mL	20 µM
Vitamins	2500	400 µL	2.55 µM

2. Sterile filter mixture at 0.2 µm
3. Under sterile conditions add sterile filtered mixture to 800 mL autoclaved MQ water
4. Bring final volume to 1 L
5. Mix well
6. Take a sample of approx. 2 mL, measure pH (the pH should be 6.8 - 7.5).

Stock solutions

Mixed carbon source stock – 1000 x

Suggested mixed carbon stock: to prepare a 0.8L = 800 mL mixed carbon stock measure 565 mL MQ-water, then add each carbon stock to the mixed carbon stock as indicated in the table below. Sterile filter (0.2 µm) with Vacuum filtration units, Rapid-Flow™ filters MF 75, Nalgene®, 1000 mL and store in room temp.

Stock	Stock concentrated	New stock	Volume stock	mL to add from conc. Stock to new stock
Carbon sources (nr 1-3, 5-9, 11-13, 15, 17-19)	100 000	1000	0.8 L	8 mL
Carbon sources (nr 21-31)	200 000	1000		4 mL
Carbon sources (nr.10 and 14)	22 573	1000		35.4 mL

Carbon sources – 100 000 or 200 000x

Dissolve each component in 45 mL of MQ water in a sterile 50 mL centrifuge tubes to make 100 000 x or 200 000x stock solutions. Sterile filter the solutions to a new sterile 50 mL centrifuge tube. Store at room temperature.

	100 000 x	Concentration g/L	amount to add in stock (g)
1	Methyl alpha-D-glucopyranoside	3,1	0,140
2	D-ribose	3,4	0,152
3	L-arginine	3,3	0,147
5	D-Xylose	3,4	0,152
6	D-(+)-Galacturonic acid monohydrate	4,0	0,179
7	L-Asparagine monohydrat	4,2	0,190
8	Tween 20	2,3	0,102
9	i-Erythritol	3,4	0,154
11	L-Phenylalanine	2,1	0,093
12	Tween 80	2,1	0,095
13	D-Mannitol	3,4	0,153
15	L-Serine	3,9	0,177
17	N-Acetyl-D-Glucosamine	3,1	0,140
18	gamma-Amino Butyric Acid	2,9	0,130
19	L-Threonine	3,3	0,150

	200 000 x	Concentration g/L	amount to add in stock (g)
21	Glycerol	3,4	0,155
22	Itaconic Acid	2,9	0,131
23	Gelatin	2,7	0,121
24	D-Cellobiose	3,2	0,144
25	D-(+)-glucose	3,4	0,152
26	alpha-Keto Butyric Acid	2,9	0,129
27	Phenylethylamine	1,7	0,077
28	alpha-D-Lactose monohydrat	3,4	0,152
29	Methyl pyruvate	2,9	0,129
30	D-Malic Acid	3,8	0,169
31	Putrescine	2,5	0,111

Carbon sources – 22 573x

Dissolve each component in 200 mL of MQ water to make 22 573x stock solutions. Sterile filter the solutions to four sterile 50 mL centrifuge tubes. Store at room temperature.

		Concentration g/L	amount to add in stock (g)
10	2-Hydroxy Benzoic Acid	0,5	0,100
14	4-Hydroxy Benzoic Acid	0,5	0,100

Nitrogen stock – 1000 x

Dissolve the salt in 500 mL of MQ water and autoclave. Store at room temperature.

		Concentration g/L	amount to add in stock (g)
N	Ammonium chloride	9,1	4,55

Phosphorus stock – 10 000 x

Dissolve the salt in 40 mL of MQ water in a sterile 50 mL centrifuge tube. Adjust pH to 7.5 and add water to a final volume of 45 mL. Sterile filter solution at 0.2 µm. Store at room temperature.

		Concentration mol/L	amount to add in stock (g)
P	Potassium dihydrogen phosphate	0,161	0,99
	Disodium phosphate	1,814	11,59

Sodium chloride stock – 100 x

Dissolve the salt in 800 mL of MQ water. Autoclave and store at room temperature.

		Concentration g/L	amount to add in stock (g)
S	Sodium chloride	80	64

Magnesium sulfate heptahydrate – 100 x

Dissolve the salt in 200 mL of MQ water and autoclave. Store at room temperature.

		Concentration g/L	amount to add in stock (g)
Mg	Magnesium sulfate heptahydrate	20	4

Potassium and Calcium stock – 500 x

Dissolve the salts in 800 mL of MQ water and adjust pH to 7.5. Autoclave and store at room temperature.

		Concentration g/L	amount to add in stock (g)
KCl	Potassium chloride	50	40
Ca	Calcium dichloride dihydrate	20	16

Trace metal stock – 1000 x

Dissolve the salts one by one in 45 mL MQ water (=270 mL). Do not adjust pH. Mix all components together and bring the volume to a final of 400 mL. Sterile filter the solution over a 0.22-µm filter into an autoclaved bottle and store at room temperature.

		Concentration g/L	amount to add in stock (g)
TM	Manganese(II) chloride tetrahydrate	5	2,00
	Cobalt dichloride hexahydrate	1	0,400
	Zinc chloride	1	0,400
	Copper(II) chloride dihydrate	0,1	0,040
	Nickel dichloride hexahydrate	0,01	0,004
	Sodium molybdate dihydrate	0,1	0,040

Iron stock – 1000 x

Dissolve EDTA in 350 mL MQ water a bit at a time and let stir for 20 minutes. Gradually increase the pH of the EDTA solution to pH 7. Gradually add the FeCl2

and Iron(II) chloride tetrahydrate in 350 ml MQ water. Bring the volume up to a final volume of 400 mL. Sterilize the solution over a 0.22-µm filter into an autoclaved bottle, cover in aluminum foil and store at room temperature.

		Concentration g/L	amount to add in stock (g)
Fe	Iron(II) chloride tetrahydrate	4	1,60
	EDTA	5	2

Vitamin stock – 2500 x

Dissolve the vitamins one by one in MQ water. Bring the volume to a final of 400 mL. Sterile filter the solution into sterile 50 mL centrifuge tubes.

		Concentration g/L	amount to add in stock (g)
Vit	Pyridoxine hydrochloride	0,25	0,1
	Thiamine hydrochloride	0,13	0,05
	Riboflavin	0,13	0,05
	Calcium D-pantothenate	0,13	0,05
	Thioctic acid	0,13	0,05
	4-Aminobenzoic acid	0,13	0,05
	Nicotinic acid	0,13	0,05
	Cyanocobalamin	0,13	0,05
	2-Mercaptoethanesulfonic acid	0,13	0,05
	biotin	0,13	0,05
	Folic acid	0,13	0,05

APPENDIX B: Qiagen PowerSoil DNEasy kit

Quick-Start Protocol June 2016

DNeasy® PowerSoil® Kit

The DNeasy PowerSoil Kit can be stored at room temperature (15–25°C) until the expiry date printed on the box label.

Further information

- Safety Data Sheets: **www.qiagen.com/safety**
- Technical assistance: **support.qiagen.com**

Notes before starting

- Perform all centrifugation steps at room temperature (15–25°C).
- If Solution C1 has precipitated, heat at 60°C until precipitate dissolves.
- 2 ml collection tubes are provided.

1. Add 0.25 g of soil sample to the PowerBead Tube provided. Gently vortex to mix.
2. Add 60 µl of Solution C1 and invert several times or vortex briefly.
   Note: Solution C1 may be added to the PowerBead tube before adding soil sample
3. Secure PowerBead Tubes horizontally using a Vortex Adapter tube holder (cat. no. 13000-V1-24).
4. Vortex at maximum speed for 10 min.
   Note: If using the 24-place Vortex Adapter for more than 12 preps, increase the vortex time by 5–10 min.
5. Centrifuge tubes at 10,000 x *g* for 30 s.
6. Transfer the supernatant to a clean 2 ml collection tube.
   Note: Expect between 400–500 µl of supernatant. Supernatant may still contain some soil particles.
7. Add 250 µl of Solution C2 and vortex for 5 s. Incubate at 2–8°C for 5 min.

Sample to Insight

Note: You can skip the 5 min incubation. However, if you have already validated the DNeasy PowerSoil extractions with this incubation we recommend you retain the step.

8. Centrifuge the tubes for 1 min at 10,000 x *g*.
9. Avoiding the pellet, transfer up to 600 µl of supernatant to a clean 2 ml collection tube.
10. Add 200 µl of Solution C3 and vortex briefly. Incubate at 2–8°C for 5 min.

    Note: You can skip the 5 min incubation. However, if you have already validated the PowerSoil extractions with this incubation we recommend you retain the step.
11. Centrifuge the tubes for 1 min at 10,000 x *g*.
12. Avoiding the pellet, transfer up to 750 µl of supernatant to a clean 2 ml collection tube.
13. Shake to mix Solution C4 and add 1200 µl to the supernatant. Vortex for 5 s.
14. Load 675 µl onto an MB Spin Column and centrifuge at 10,000 x *g* for 1 min. Discard flow through.
15. Repeat step 14 twice, until all of the sample has been processed.
16. Add 500 µl of Solution C5. Centrifuge for 30 s at 10,000 x *g*.
17. Discard the flow through. Centrifuge again for 1 min at 10,000 x *g*.
18. Carefully place the MB Spin Column into a clean 2 ml collection tube. Avoid splashing any Solution C5 onto the column.
19. Add 100 µl of Solution C6 to the center of the white filter membrane. Alternatively, you can use sterile DNA-Free PCR Grade Water for this step (cat. no. 17000–10).
20. Centrifuge at room temperature for 30 s at 10,000 x *g*. Discard the MB Spin Column. The DNA is now ready for downstream applications.

    Note: Solution C6 is 10 mM Tris-HCl, pH 8.5. We recommend storing DNA frozen (–20° to –80°C) as Solution C6 does not contain EDTA. To concentrate DNA see the Hints & Troubleshooting Guide.

APPENDIX C: SequalPrep Normalization Plate (96) Kit (Invitrogen)

invitrogen™

SequalPrep™ Normalization Plate (96) Kit

Catalog no: A10510-01 **Store at room temperature (15–30°C)**

Contents and Storage

The components included with the SequalPrep™ Normalization Plate (96) Kit are listed in the table below. Sufficient reagents are included to perform 10 × 96 purification/normalization reactions. Upon receipt, **store all components at room temperature (15–30°C)**. Store plates for up to 6 months.

Components	Quantity
SequalPrep™ Normalization Plate (96)	2 bags of 5 plates each
SequalPrep™ Normalization Binding Buffer	40 ml
SequalPrep™ Normalization Wash Buffer	50 ml
SequalPrep™ Normalization Elution Buffer (10 mM Tris-HCl, pH 8.5)	40 ml

Description

The SequalPrep™ Normalization Plate Kit allows simple, one-step, high-throughput amplicon purification and normalization of PCR product concentration (2–3 fold range) via a limited binding capacity solid phase. Each well of the SequalPrep™ Normalization Plate can bind and elute ~25 ng of PCR amplicon. Eluted PCR amplicon can be subsequently pooled and subjected to a variety of massively parallel sequencing analyses. The SequalPrep™ Normalization Plate is compatible with any automated liquid handling workstations without the need for shakers, magnets, or vacuum. The SequalPrep™ Normalization Plate Kit when used with SequalPrep™ Long PCR Kit provides a complete PCR enrichment and amplicon normalization system that is designed to complement amplicon sequencing workflows such as next-generation sequencing.

The conventional next generation sequencing workflows require laborious sample prep methods consisting of amplicon purification, quantitation, and manual normalization to adjust amplicon concentration. The SequalPrep™ Normalization Plate Kit eliminates the tedious amplicon quantitation and manual normalization steps.

SequalPrep™ Normalization Plate Kits utilize ChargeSwitch® Technology that provides a switchable surface charge depending on the pH of the surrounding buffer to facilitate nucleic acid purification. Under low pH conditions, the positive surface charge of the ChargeSwitch® coating binds the negatively charged nucleic acid backbone. Proteins and other contaminants (such as short oligonucleotide primers) are not bound and are simply washed away.

System Overview

The SequalPrep™ Normalization Plate Kit is a solid phase, high-throughput amplicon purification and normalization system in a 96-well plate format. PCR products (5–25 µl) are added to a SequalPrep™ Normalization Plate well and mixed with the Binding Buffer. DNA binding to the plate is performed at room temperature for 1 hour. The wells are washed with Wash Buffer to efficiently remove contaminants. Purified PCR products are eluted using 20 µl Elution Buffer at normalized concentrations.

System Specifications

Starting Material:	At least 250 ng PCR product (amplicon) per well
DNA Fragment Size:	100 bp to 20 kb
Elution Volume:	20 µl
DNA Yield:	Up to 25 ng per well
Normalization Range:	2–3-fold
Plate Dimensions:	Standard SBS (Society for Biomolecular Screening) footprint, semi-skirted 96-well plate
Plate Capacity:	0.2 ml

Accessory Products

The following products may be used with the SequalPrep™ Normalization Plate Kit. For details, visit www.invitrogen.com.

Product	Quantity	Catalog no.
SequalPrep™ Normalization Wash Buffer	4 × 50 ml	A10510-03
SequalPrep™ Long PCR Kit with dNTPs	1,000 units	A10498
Platinum® PCR Supermix	100 reactions	11306-016
Platinum® PCR Supermix High Fidelity	100 reactions	12532-016
Quant-iT™ PicoGreen® dsDNA Assay Kit	1 kit	P7589
PureLink™ Foil Tape	50 tapes	12261-012
E-Gel® 96 gels 1% (or 2%)	8 gels	G7008-01 (G7008-02)

Part no: 100003531 Rev. date: 5 May 2008

For technical support, email tech_support@invitrogen.com. For country-specific contact information, visit ***www.invitrogen.com***.

General Guidelines

- Wear a laboratory coat, disposable gloves, and eye protection when handling reagents and plate.
- Always use proper aseptic techniques when working with DNA and use only sterile, DNase-free tips to prevent DNase contamination.
- If you are using only part of the plate for DNA purification, cover unused wells with the Plate Seal and leave them attached while purifying DNA in the other wells. The plates can be stored at room temperature for up to 6 months.
- The SequalPrep™ Normalization Plates are compatible for use with automated liquid handling workstation; the workstation must be capable of handling and manipulating 96-well plates.
- If you are using automated liquid handling workstations for purification, you may need additional Wash Buffer depending on your type of workstation. See previous page for Wash Buffer ordering information.

Generating PCR Amplicon

You can generate the PCR amplicon using a method of choice. General recommendations for generating PCR amplicons are listed below:

- To obtain the best results, we recommend using the SequalPrep™ Long PCR Kit with dNTPs (page 1) which provides a robust system for long-range, high-fidelity PCR for use in next-generation sequencing applications.
- Other commercially available PCR supermixes and enzymes such as Platinum® PCR Supermix (page 1), Platinum® PCR Supermix High Fidelity (page 1), or equivalent are suitable for use.
- Perform PCR in a separate plate. **Do not** use the SequalPrep™ Normalization Plate to perform PCR.
- You need at least 250 ng amplicon per well to use with the SequalPrep™ Normalization Plate (see below).

Sample Amount

To achieve robust normalization, we recommend adding at least 250 ng/well of amplicon. This input amount is easily achieved using only a fraction of most PCR amplification reactions. An average efficiency PCR (20 µl reaction volume) produces product in the range of 25–100 ng/µl, allowing you to purify 5–10 µl using the SequalPrep™ system.

Elution Options

Depending on the nature of the downstream application and target nucleic acid concentrations desired, the SequalPrep™ kit offers the flexibility to elute purified DNA in a variety of options.

The **standard elution** method described in the protocol below is designed to elute purified DNA from each well using 20 µl elution volume to obtain each amplicon at a concentration of 1–2 ng/µl.

The **optional sequential elution** method is designed to sequentially elute multiple rows or columns using the same 20 µl of elution buffer to obtain higher amplicon concentrations. The amplicon concentrations will be additive as sequential wells are eluted. For example, dispense 20 µl of elution buffer into the first column (A1–H1), mix well, and incubate for 5 minutes at room temperature. Then, simply move this column of elution buffer to the next column (A2–H2), and again incubate for 5 minutes. Continue this step to obtain your specific elution needs for the downstream application of choice.

Materials Needed

- PCR reactions containing amplicons of the desired length (see **Generating PCR Amplicon**, above)
- DNase-free, aerosol barrier pipette tips
- *Optional:* automated liquid handling workstation capable of handling and manipulating 96-well plates
- *Optional:* PureLink™ Foil Tape (see previous page)

Binding Step

1. Transfer the desired volume of PCR product (5–25 µl PCR reaction mix, at least 250 ng amplicon/well) from the PCR plate into the wells of the SequalPrep™ Normalization plate.
2. Add an equivalent volume of SequalPrep™ Normalization Binding Buffer.

   For example: To purify 10 µl of PCR product, add 10 µl SequalPrep™ Normalization Binding Buffer.
3. Mix completely by pipetting up and down, or seal the plate with PureLink™ Foil Tape (page 1), vortex to mix, and briefly centrifuge the plate.
4. Incubate the plate for 1 hour at room temperature to allow binding of DNA to the plate surface. Mixing is not necessary at this stage.

   Note: Incubations longer than 60 minutes do not improve results. However, depending on your workflow you may perform overnight incubation at room temperature for the binding step.
5. **Optional:** If >25 ng DNA/well yield is desired, transfer the amplicon/Binding Buffer mixture from Step 4 to another, fresh well/plate to sequentially bind more DNA. Perform DNA binding at room temperature for 1 hour.

   Note: After binding is complete, you can remove the amplicon/Binding Buffer mixture from the well and store at –20°C for up to 30 days to perform additional purifications at a later time.
6. Proceed to **Washing Step**, next page.

Washing Step

1. Aspirate the liquid from wells. Be sure not to scrape the well sides during aspiration.

   Note: If you wish to store the amplicon/Binding Buffer mixture for additional purifications at a later time, aspirate the liquid from wells into another plate and store at –20°C for up to 30 days.

2. Add 50 µl SequalPrep™ Normalization Wash Buffer to the wells. Mix by pipetting up and down twice to improve removal of contaminants.

3. Completely aspirate the buffer from wells and discard.

   To ensure complete removal of wash buffer and maximize elution efficiency, you may need to invert and tap the plate on paper towels depending on the pipetting technique or instrument used. A small amount of residual Wash Buffer (1–3 µl) is typical and does not affect the subsequent elution or downstream applications.

4. Proceed to **Elution Step**, below.

Elution Step

Review **Elution Options** (previous page).

1. Add 20 µl SequalPrep™ Normalization Elution Buffer to each well of the plate.

   Note: Do not use water for elution. If you need to elute in any other buffer, be sure to use a buffer of pH 8.5–9.0. If the pH of the buffer is <8.5, the DNA will not elute efficiently.

2. Mix by pipetting up and down 5 times or seal the plate with PureLink™ Foil Tape (page 1), vortex to mix, and briefly centrifuge the plate. Ensure that the buffer contacts the entire plate coating (up to 20 µl level).

3. Incubate at room temperature for 5 minutes.

4. Transfer and pool the purified DNA as desired or store the eluted DNA at 4°C (short-term storage) or –20°C (long-term storage) until further use.

Expected Yield and Concentration

The expected DNA concentration is 1–2 ng/µl when using 20 µl elution volume. The expected DNA yield is ~25 ng/well normalized.

Optional: DNA Quantitation

The SequalPrep™ Normalization Plate Kit is designed to eliminate the quantitation and manual dilution steps typically performed for normalization in next-generation sequencing workflows. You can pool the eluted amplicon and use the pooled amplicons directly for your downstream applications without DNA quantitation.

However, if your downstream application requires DNA quantitation, you may determine the yield of the eluted amplicon using Quant-iT™ PicoGreen® dsDNA Assay Kit (page 1). We **do not** recommend using UV spectrophotometric measurements (A_{260}/A_{280} nm), as this method is inaccurate for low DNA concentrations.

Downstream Applications

The SequalPrep™ Normalization Plate Kit is designed to produce purified PCR products with normalized concentrations and substantially free of salts and contaminating primers. PCR amplicons purified from this system can be used individually or pooled in any downstream application for which normalization is an important sample preparation criterion such as next generation sequencing applications.

Pooled amplicons purified using the SequalPrep™ Normalization Plate Kit have produced successful data from massively parallel sequencing-by-synthesis on the Illumina/Solexa Genome Analyzer indicating that the amplicon purity is suitable for other next-generation sequencing platforms (Roche/454 FLX, Applied Biosystems SOLiD™ system). For detailed sample preparation guidelines, refer to the instrument manufacturer's recommendations.

APPENDIX D: Supplementary figures and tables

Table S1: Reference genomes of *Y. ruckeri* retrieved from the JGI IMG/M database with their respective IMG submission IDs.

Strain	IMG submission ID
Y. ruckeri ATCC29473	60758
Y. ruckeri Big Creek 74	74047
Y. ruckeri YRB	75967
Y. ruckeri SC09	226377
Y. ruckeri NHV-3758	2211721
Y. ruckeri QMA0440	211682

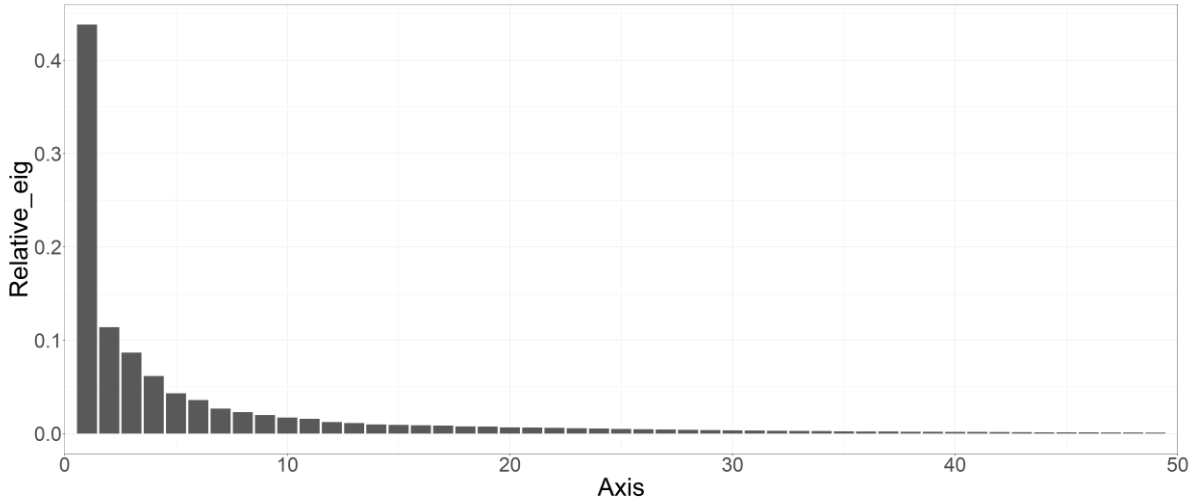

Figure S1: Scree plot of the first 50 axis of the PCoA ordination of the Bray-Curtis matrix

Table S2: Dilution series of Hom7 PCR product for qPCR standard curve. DNA diluted with PCR grade water. Standard samples in bold were included in the standard curve.

Standard name	DNA conc. (ng/ul)	Molecules/µl	Log copy number
S-org	2.14 ng/ul	3.1*10^10	10.5
S-8	69.03 pg/ul	1*10^9	9
S-7	**6.903 pg/ul**	**1*10^8**	**8**
S-6	**0.6903 pg/ul**	**1*10^7**	**7**
S-5	**0.13806 pg/ul**	**2*10^8**	**6,3**
S-4	**0.02761 pg/ul**	**400 000**	**5,6**
S-3	**5.52 fg/ul**	**80 000**	**4,9**
S-2	**0.00110 pg/ul**	**16 000**	**4.2**

Table S3: Dilution series of genomic DNA of *Y. ruckeri* isolate NVI-10705 for qPCR standard curve. DNA diluted with PCR grade water. DNA diluted with PCR grade water. Standard samples in bold were included in the standard curve.

Standard name	Cell conc. (celler/ul)	DNA conc. (ng/ul)
Y-org	3.4*10^7	48,01 ng/ul
Y-7	**1*10^7**	**14.12 ng/ul**
Y-6	**1*10^6**	**1.41 ng/ul**
Y-5	**2*10^5**	**0.28200 ng/ul = 282 pg/ul**
Y-4	**40 000**	**56.4 pg/ul**
Y-3	**8000**	**11.28 pg/ul**
Y-2	**1600**	**2.256 pg/ul**
Y-1	**160**	**0.22560 pg/ul**
Y-0	**16**	**22.56 fg/ul**
Y-wow	**1.6**	**2.256 fg/ul**

..

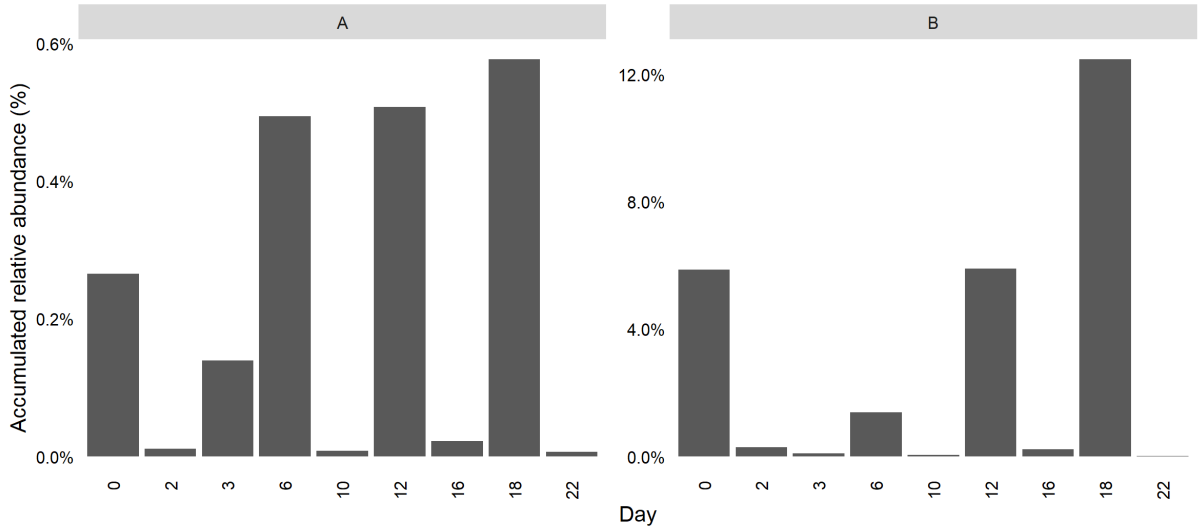

Figure S1: Relative abundance of Y. ruckeri for the cultivation regimes A and B over time.

Protocol: QIAquick PCR Purification using a Microcentrifuge

This protocol is designed to purify single- or double-stranded DNA fragments from PCR and other enzymatic reactions using the QIAquick PCR Purification Kit or the QIAquick PCR & Gel Cleanup Kit. For cleanup of other enzymatic reactions, follow the protocol as described for PCR samples or use the MinElute Reaction Cleanup Kit. Fragments ranging from 100 bp to 10 kb can be purified from primers, nucleotides, polymerases and salts using QIAquick spin columns in a microcentrifuge.

Important points before starting

- Add ethanol (96–100%) to Buffer PE before use (see bottle label for volume).
- All centrifugation steps are carried out at 17,900 x *g* (13,000 rpm) in a conventional tabletop microcentrifuge at room temperature (15–25°C).
- Add 1:250 volume pH Indicator I to Buffer PB (i.e., add 120 µl pH Indicator I to 30 ml Buffer PB or add 600 µl pH Indicator I to 150 ml Buffer PB). The yellow color of Buffer PB with pH Indicator I indicates a pH ≤7.5.
- Add pH Indicator I to entire buffer contents. Do not add pH Indicator I to buffer aliquots.
- If the purified PCR product is to be used in sensitive microarray applications, it may be beneficial to use Buffer PB without the addition of pH Indicator I.

Procedure

1. Add 5 volumes of Buffer PB to 1 volume of the PCR sample, and then mix. It is not necessary to remove mineral oil or kerosene.

   For example, add 500 µl of Buffer PB to 100 µl PCR sample (not including oil).
2. If pH Indicator I has been added to Buffer PB, check that the mixture's color is yellow.

   If the color of the mixture is orange or violet, add 10 µl of 3 M sodium acetate, pH 5.0, and mix. The color of the mixture will turn yellow.

3. Place a QIAquick spin column in a provided 2 ml collection tube.
4. To bind DNA, apply the sample to the QIAquick column and centrifuge for 30–60 s.
5. Discard flow-through. Place the QIAquick column back into the same tube.

   Collection tubes are reused to reduce plastic waste.
6. To wash, add 0.75 ml Buffer PE to the QIAquick column and centrifuge for 30–60 s.
7. Discard flow-through and place the QIAquick column back into the same tube. Centrifuge the column for an additional 1 min.

   IMPORTANT: Residual ethanol from Buffer PE will not be completely removed unless the flow-through is discarded before this additional centrifugation.
8. Place QIAquick column in a clean 1.5 ml microcentrifuge tube.
9. To elute DNA, add 50 µl Buffer EB (10 mM Tris·Cl, pH 8.5) or water (pH 7.0–8.5) to the center of the QIAquick membrane and centrifuge the column for 1 min. Alternatively, for increased DNA concentration, add 30 µl elution buffer to the center of the QIAquick membrane, let the column stand for 1 min, and then centrifuge.

   IMPORTANT: Ensure that the elution buffer is dispensed directly onto the QIAquick membrane for complete elution of bound DNA. The average eluate volumes are 48 µl from 50 µl elution buffer volume and 28 µl from 30 µl elution buffer.

   Elution efficiency is dependent on pH. Maximum elution efficiency is achieved between pH 7.0 and 8.5. When using water, make sure that the pH value is within this range, and store DNA at –30°C to –15°C because DNA may degrade in the absence of a buffering agent. The purified DNA can also be eluted in TE buffer (10 mM Tris·Cl, 1 mM EDTA, pH 8.0), but the EDTA may inhibit subsequent enzymatic reactions.
10. If the purified DNA is to be analyzed on a gel, add 1 volume Loading Dye to 5 volumes of purified DNA. Mix the solution by pipetting it up and down before loading the gel.

    Loading Dye contains 3 marker dyes – bromophenol blue, xylene cyanol and orange G – that facilitate estimation of DNA-migration distance and optimization of the agarose gel run time. Refer to Table 2 (page 17) to identify the dyes according to migration distance and agarose gel percentage and type.

APPENDIX F: Qubit 4 Fluorometer (Invitrogen)

invitrogen

QUICK REFERENCE

Qubit™ Assays

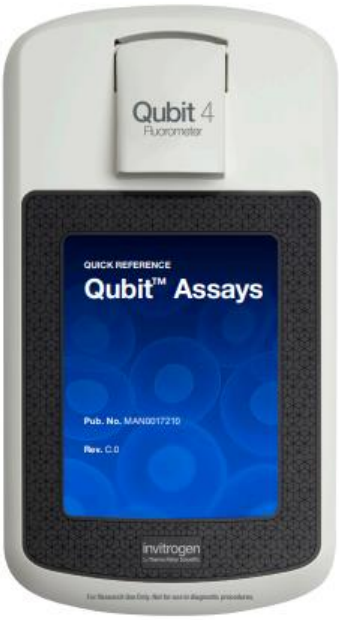

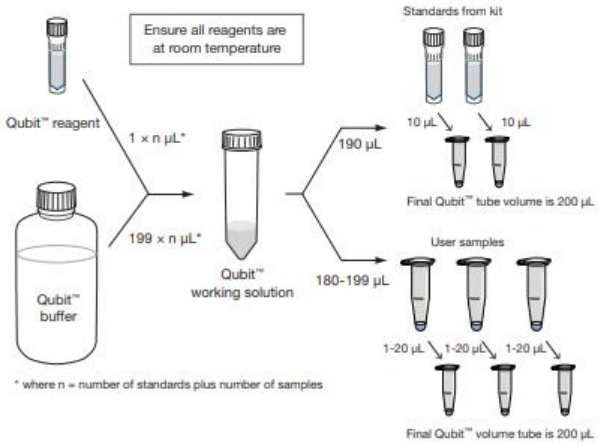

General Qubit Assay Protocol

1. Set up two assay tubes for the standards (three for the protein or RNA IQ assay) and one assay tube for each sample.
2. Prepare the Qubit™ working solution by diluting the Qubit™ reagent 1:200 in Qubit™ buffer. Prepare 200 µL of working solution for each standard and sample.†
3. Prepare the assay tubes* according to the table below.
4. Vortex all tubes for 2–3 seconds.
5. Incubate the tubes for 2 minutes at room temperature (15 minutes for the Qubit™ protein assay).
6. Insert the tubes in the Qubit™ Fluorometer and take readings. For detailed instructions, refer to the Qubit™ Fluorometer manual.

	Standard assay tubes	User sample assay tubes
Working solution† (from step 2)	190 µL	180–199 µL
Standard (from kit)	10 µL	–
User sample	–	1–20 µL
Total Volume in each assay tube	200 µL	200 µL

† Qubit 1X dsDNA assays (Cat. Nos. Q33230, Q33231, Q33265, Q33266) are supplied with a ready-to-use working solution, and do not require preparation.
* Use only thin-wall, clear 0.5 mL PCR tubes. Acceptable tubes include Qubit™ assay tubes (set of 500, Cat. No. Q32856).

ThermoFisher SCIENTIFIC

invitrogen

For Qubit Protein BR Assay only

1. Set up two assay tubes for the standards, one assay tube for a buffer blank and one assay tube for each sample.
2. Prepare assay tubes according to the table below. Adding solutions in the following order to the assay tubes: (1) Standards/Sample/Sample Buffer, (2) Protein BR Assay Buffer, (3) Protein BR Assay Reagent.
3. Vortex for 5-7 seconds immediately after addition of Protein BR Assay Reagent.
4. Incubate tubes for 10 minutes at room temperature.
5. Insert the tubes in the Qubit™ Fluorometer and take readings. For detailed instructions, refer to the Qubit™ Fluorometer manual.

	Standard assay tubes	Buffer blank	User sample assay tubes
Standard (from kit)	20 µL	-	-
User sample buffer	-	10 or 20 µL	-
User sample	-	-	10 or 20 µL
Protein BR Assay Buffer	150 µL	150 or 160 µL	150 or 160 µL
Protein BR Assay Reagent	30 µL	30 µL	30 µL
Total volume in each assay tube	200 µL	200 µL	200 µL

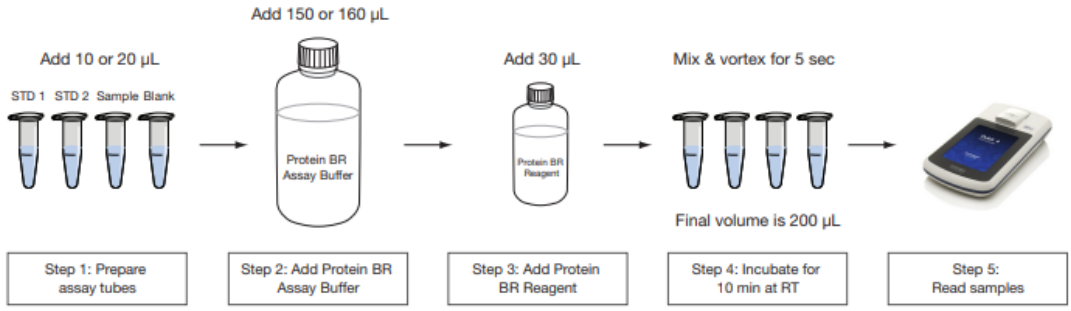

Find out more at **thermofisher.com/qubit**

ThermoFisher SCIENTIFIC

APPENDIX G: Protocol for cleaning of filter devise

1. Disassemble filter devise and soak in warm water
2. Clean all parts thoroughly with dish soap and warm water, scrubbing with a stiff brush
3. Rins all parts with distilled water
4. Coat in 70% ethanol, and let evaporate

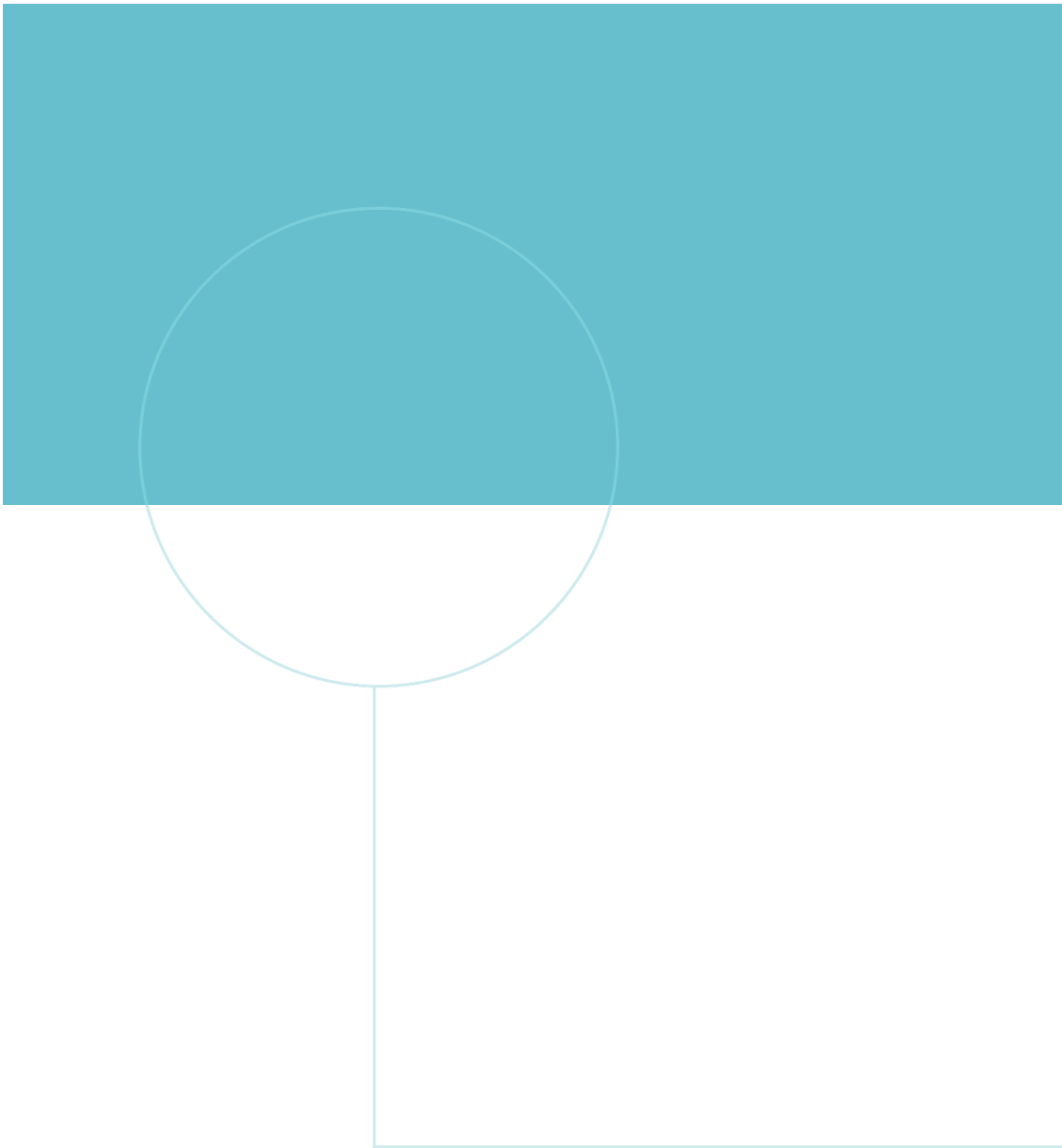

NTNU

Kunnskap for en bedre verden